Insights Towards Optimizing Palladium-Catalyzed Bioorthogonal Reactions

by

Krystyn Irena Dubicki

A thesis submitted in partial fulfillment of the requirements for the degree of

Master of Science

Department of Chemistry
University of Alberta

Abstract

Despite large amounts of research investigating the mechanism and kinetics of the Suzuki-Miyaura reaction in organic solvent, very little research has been completed to investigate this mechanism or kinetic properties in aqueous solvent. Due to properties of the Suzuki-Miyaura reaction which are favourable to bioorthogonal reaction, I first investigated a method to study the kinetics of the Suzuki-Miyaura in water using NHC/Pd complexes that had been designed to facilitate cross-coupling in aqueous environments. I also designed a prototype assay for testing these catalysts that could be adapted for high-throughput screening. Synthesis towards a fluorescent probe for a high-throughput screen was also started. I determined that UV-Vis spectroscopy was not suitable for studying the Suzuki-Miyaura reaction in aqueous conditions, and that studying this reaction with fluorescent probes looks more promising.

Examining Committee

Dr. Florence Williams, Assistant Professor, University of Iowa

Dr. Matthew Macauley, Assistant Professor, University of Alberta

Dr. Ran Zhao, Assistant Professor, University of Alberta

Dedication

To Mom, Dad, Adam, and Smudge

Acknowledgements

They really meant it when they said, “It takes a village”. My journey through graduate school was by no means easy and each of the people below had some part in helping me get to the end.

First, I would like to thank my supervisor, Dr. Florence Williams. No amount of thanks can encompass the gratitude I have for your continuous support (in and out of the lab), patience, insightful conversations, and level of perseverance to strive towards. I would also to like to extend my gratitude to my initial supervisor, Dr. Robert Campbell, who helped me realize what my research interests truly where and gave me his blessing to pursue a different path through graduate school.

At the University of Alberta, I would like to thank: Andreas Dorian, Khyati Gohil, Zain Kazmi, Nam Truong, Alex Predy, Princey Raju, Luca Maiorana, Yifan Yang, Caley Craven, Emily Rodrigues, Brittany Reib, Rochelin Dalangin, Jessica Amorim, Jasper Woodard, Jonah Curl, Dr. Ryan McKay, Mark Miskolzie, Karlene Lynch, Bela Reiz, Wayne Moffat, Dr. Edan Foley, Dr. Meagan Oakley and Dr. Sorina Chiorean.

At the University of Iowa, I would like to thank: Dr. Ben Hale, Ashely Schneider, Piyumi Wijesirigunawardana, Megan Polz, Theodora Leventis, Andrej Corkovic, Hannah Sunderman, Hannah Nennig, Parijat Tripathi, Cameron Chiste, Cassie Moeller, Dr. George Crull, Peter Franke, Hoang Dang, Bill Weigel, Cory Ludwig, Dr. Dave Martin, Maddie Parker and Dr. Mersad Raeisi.

Outside of these universities, I would like to thank: Dr. Emma Davy, Dr. Amanda Whiting, Dr. Robin Kopelman, Monica Schmidt, Dr. Sarah Hodgson, Ethon Burns, Skyler Lamb, Sarah Harkness, Matt Hrvol, Kelly Clark, Caitlan Vinkle, Val Kerr, Erika Wall, Dr. Ellen Busby, Alex Pollock, Emily Nantel, Natalia Buendia Calvillo, Troy Hasanen, Sharla Becker, Alyssa Shear, Krista Zeleke, and Marie-France Bérubé.

Additionally, I would like to thank the Twitch.tv communities of the following streamers: SpecsNStats, SkurryPls, Zant, Linkus7, MajinPhil, and DorkTales. Thank you for always giving me a welcoming place to unwind, vent, think about other things, and introducing me to the speedrunning and GamesDoneQuick community.

Table of Contents

List of Figures

List of Tables

List of Abbreviations

Ab	antibody
ABP	activity-based probe
ABPP	activity-based protein profiling
Ac	acetyl
Ac_4ManNAz	peracetylated *N*-azidoacetylmannosamine
AF488	AlexaFluor 488
AF555	AlexaFluor 555
BODIPY	boron dipyrromethene
Bz	benzoyl
CD_3CN	deuterated acetonitrile
$CDCl_3$	deuterated chloroform
CuAAC	copper-catalyzed azide-alkyne cycloaddition
D_2O	deuterated water
DCM	dichloromethane
DCVC	dry-column vacuum chromatography
DDQ	2,3-dichloro-5,6-dicyano-1,4-benzoquinone
DIEA	*N,N*-diisopropylethylamine
DIFO	difluorocyclooctyne
DIPEA	*N,N*-diisopropylethylamine
DMA	dimethylacetamide
DMF	dimethylformamide
DMSO	dimethylsulfoxide
DNA	deoxyribonucleic acid
EtOAc	ethyl acetate
EtOH	ethanol
FBS	fetal bovine serum
Fmoc	fluorenylmethyloxycarbonyl
Gly	glycine

GO	glucose oxidase
H_2O	water
HBSS	Hanks' Balanced Salt Solution
HK	hexokinase
HOMO	highest occupied molecular orbital
hpf	hours post-fertilization
HPLC	high pressure/preformance liquid chromatography
HTS	high throughput screening
iEDDA	inverse electron demand Diels-Alder
LUMO	lowest unoccupied molecular orbital
ManNAz	*N*-azidomannosamine
Me	methyl
MeOD	deuterated methanol
NADH	nicotinamide adenine dinucleotide (reduced)
NHC	*N*-heterocyclic carbene
nm	nanometers
NMR	nuclear magnetic resonance
OTf-	triflate
PBS	phosphate buffered saline
PEG	polyethylene glycol
Ph	phenyl
Phe	phenylalanine
PhMe	toluene
PNP	*p*-nitrophenol
PTM	post-translational modification
RBF	round-bottom flask
RNA	ribonucleic acid
SDS-PAGE	sodium dodecyl sulfate polyacrylamide gel electrophoresis
SiaNAz	azido sialic acid
SMCC	Suzuki-Miyaura Cross Coupling

SPAAC	strain-promoted azide-alkyne cycloaddition
TBAF	tetrabutylammonium fluoride
TBDMS	*tert*-butyldimethylsilyl
^{t}BuOH	*tert*-butanol
THF	tetrahydrofuran
TMR	tetramethylrhodamine
Trx	thioredoxin
UV-Vis	ultraviolet-visible spectroscopy

A Note on Numbering

Compounds listed in this thesis are either numbered (e.g., **2.1**) or lettered (e.g., **2a**). Compounds that are numbered were synthesized by the author, whereas compounds that are lettered were either purchased commercially or synthesized by others.

Chapter 1: Perspectives on designing catalysts for metal-catalyzed bioorthogonal reactions

1.1 Introduction to Bioorthogonal Reactions

Bioconjugate chemistry is a sub-field of chemistry that focuses on forming covalent bonds between two molecules, where one of those molecules is a biomolecule. The non-biological component is typically a probe, tag, sensor, dye, or polymer and the biological component can be a peptide, protein, antibody, lipid, carbohydrates, DNA or RNA.

A subset of bioconjugate reactions are bioorthogonal reactions. These reactions occur on a cellular surface, inside a cell or *in vitro* and can be defined by their lack of cross-reactivity with cellular components and their specific reactivity with each other. As their name suggests, bioorthogonal reactions (ideally) do not interfere with the main functionality of the cell. Chemists do this by using orthogonal functionality in their reaction – using unnatural or biologically inert functional groups to form covalent bonds. In addition, another feature of bioorthogonal reactions is that they can be performed in neutral aqueous conditions.

In general, bioorthogonal conjugations have a few important properties to make them useful for chemical applications. First, bioconjugate reactions need be "fast" (ex: k_2 = 50 – 2.8 x10^6 $M^{-1}s^{-1}$). [1] This is out of necessity – the researcher does not want the reaction to take several hours to occur because cellular processes, like degradation of the reagents/targets being conjugated complicate investigatory assays. Second, the reagents being used *should* only react with each other and not be promiscuous to other reactive groups in the cell. Therefore, the reagents need to be inert to groups such as amines (e.g., *N*-terminus of proteins), free thiols (cysteine side-chains), and carbonyl groups (free carboxylic acids, esters, and ketones) to name some examples. As one can imagine, this presents a significant challenge in reaction design. Third, the conjugation product should be stable for the time period required (e.g., in an example presented later in this chapter, the linkage needed to be stable for 76 hours). Linkages that are readily degraded by cellular enzymes are not always useful to a researcher. The general design idea behind bioorthogonal

reactions is that such reactions produce a linkage that is "foreign" to the cell, so that the cell does not have any innate machinery to react/degrade/digest with the reaction product. This ensures that the product will last long enough to get a readout (i.e., measuring fluorescence, absorbance, etc). The following examples are types of reactions that can currently be found in a chemist's "bioorthogonal toolkit".[1]

1.1.1 Staudinger ligation

First described in 1919 under non-biological conditions, the Staudinger ligation (named after Hermann Staudinger) involves the reaction of an azide (a popular functional group in this space due to its high reactive potential) and a triphenylphosphine.[2] The product is an iminophosphorane intermediate, which under aqueous conditions is further hydrolyzed to produce an amine and a triphenylphosphine oxide.[2] About 80 years later, Bertozzi and colleagues first described using this reaction as a *"chemoselective ligation"* (the term *"bioorthogonal reaction"* hadn't been coined yet) between a biotinylated phosphine and an azido-modified sialic acid bound to the cell surface.[3] Bertozzi and colleagues showed that their Staudinger ligation was both selective (orthogonal) and their reaction partners did not negatively affect the growth rate of the cells (tolerance). Shortly after this initial entry, the groups of Raines and Bertozzi have further developed this reaction resulting in a "traceless" ligation, citing similar reaction rates to the non-traceless ligation. [4a, b] (Non-traceless 2nd order rate constant = 0.83-3.8 x 10^{-3} $M^{-1}s^{-1}$; traceless 2nd order rate constant = 0.12-7.7 x 10^{-3} $M^{-1}s^{-1}$) [4c, d] (*See Figure 1.1)*

1.1.2 Copper-catalyzed Azide-Alkyne Cycloaddition (CuAAC) & Strain-promoted Azide-Alkyne Cycloaddition (SPAAC)

The copper-catalyzed azide-alkyne cycloaddition was first reported independently by two groups, that of Meldal [5] and Sharpless [6] in 2002. This reaction was based off the Huisgen cycloaddition, first described by Huisgen in 1960.[7] Meldal, Sharpless and co-workers found that the addition of a copper catalyst (Cu(I)) to Huisgen 1,3-dipolar cycloadditions greatly improved the yield (usually greater than 85%, and more than 95% purity) and were able to be completed in aqueous solvent mixtures (e.g., H_2O/^{t}BuOH) at ambient temperatures (25 °C). While these "click" reactions (as coined by Sharpless) were perfectly suitable for ligations on biological molecules (e.g., modification of virions, protein profiling) [8], copper is toxic to both bacterial and mammalian

(a) Initial Staudinger Reaction (1919)

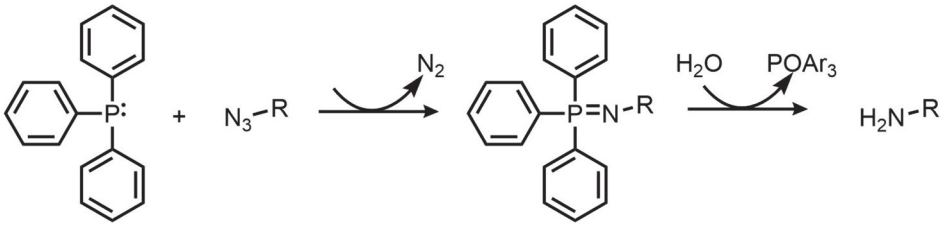

(b) Staudinger-Bertozzi Ligation (2000)

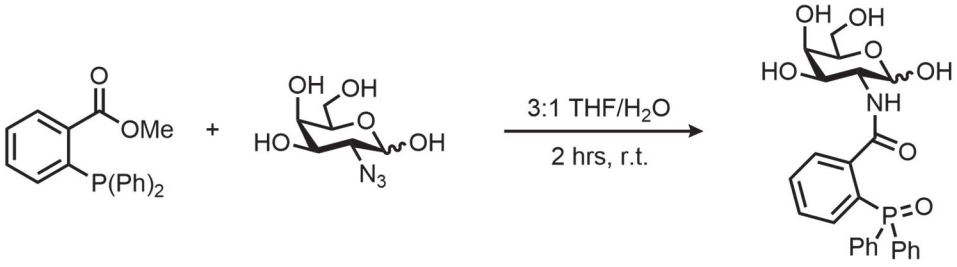

(c) Traceless Staudinger-Raines Ligation (2000)

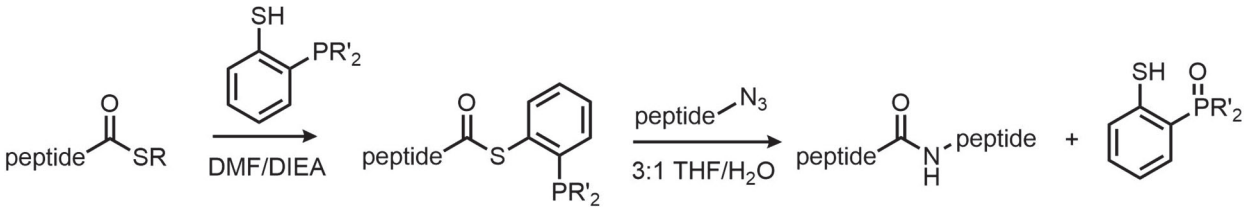

(d) Traceless Staudinger-Bertozzi Ligation (2000)

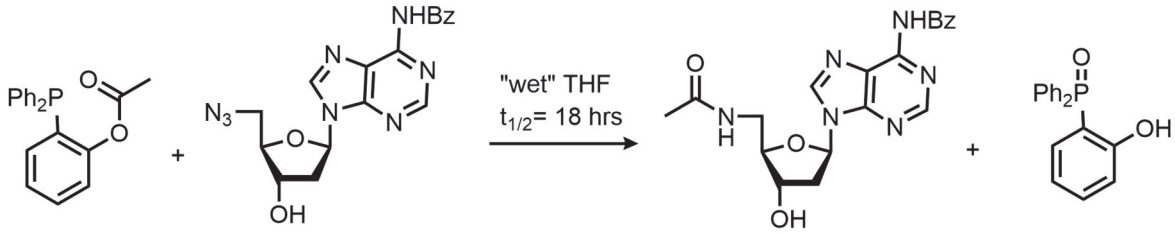

Figure 1.1 Examples of the development of the Staudinger reaction to Staudinger Ligation and traceless modifications.

cells – therefore, these click reactions cannot be used for *in vivo* modifications. In 2004, Bertozzi sought to look for alternative means to activate the alkyne partner without a catalyst. Taking

inspiration from Wittig and Krebs' account of reactions between neat cyclooctyne and phenyl azide [9] Bertozzi and co-workers synthesized a versatile substituted cyclooctyne probe that was further modified with a biotin tag. The alkyne tethered in a cyclooctyne ring results in a large amount of "ring strain", which accounts for 18 kcal/mol of stored energy.[9] Bertozzi and co-workers therefore can use this stored energy to allow for the cycloaddition reaction to proceed without needed a copper catalyst. Using a similar approach to their work on the Staudinger ligation using azide-modified cell-surface sialic acids, Bertozzi and co-workers noted that their strain-promoted reaction did not cause any "apparent physiological harm" [9] to living cells. The SPAAC reaction is slightly faster than the previously developed Staudinger ligation (k_2 (SPAAC) = 0.0012-0.14 $M^{-1}s^{-1}$).[1] (*See Figure 1.2)*

1.1.3 Inverse Electron Demand Diels-Alder: Tetrazine Ligation

Reported independently from each other in 2008, the groups of Hilderbrand [10] and Fox [11] both developed methods of employing an inverse electron demand Diels-Alder reaction using substituted tetrazines and strained dienophiles (e.g., norbornene and *trans*-cyclooctene). The Diels-Alder reaction was already poised to be compatible for bioorthogonal reactions as it can be done in aqueous conditions [11], however the reaction sequence of the diene and the dienophile is inverted (i.e., the diene is electron-deficient [lowers the LUMO] and the dienophile is electron-rich [raises the HOMO] to allow for a stabilizing HOMO-LUMO interaction). These tetrazine ligations are irreversible due to the loss of one equivalent of nitrogen which differ from traditional from Diels-Alder reactions which are reversible. [12, 13]

For Fox and co-workers, the inspiration to pursue bioorthogonal reactions came from their previous work on a practical synthesis of *trans*-cyclooctenes.[14] Looking for a reaction space that benefited from fast reactions, they turned to the development of bioorthogonal ligations using tetrazines. The prototypical tetrazine ligation with *trans*-cyclooctene has an impressive rate of k = 2000 $M^{-1}s^{-1}$; more development into this reaction has resulted in substrates that can perform at a rate of $k = 2.8 \times 10^6$ $M^{-1}s^{-1}$ which is 6 orders of magnitude faster than the next fastest bioorthogonal ligation, a 1,3-dipolar cycloaddition involving oxanorbornadiene.[1] Tetrazine ligations overall have broad functional group tolerance and proceed in high yields independent of

(a) Husigen Cycloaddition (1961)

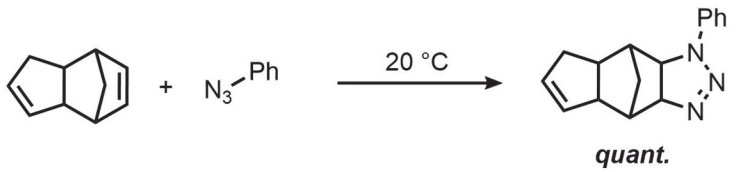

(b) Meldal: Copper-catalyzed 1,3-dipolar cycloaddition (2002)

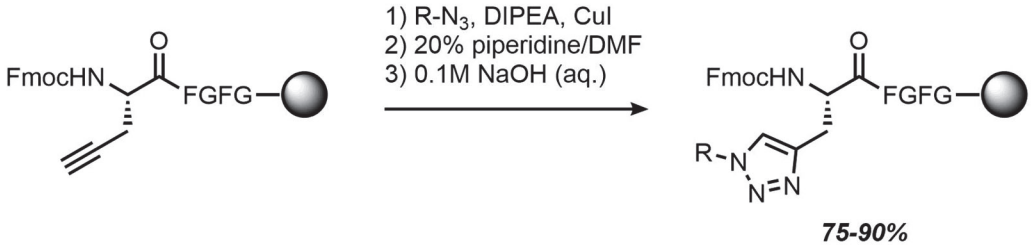

(c) Sharpless: Copper-catalyzed 1,3-dipolar cycloaddition (2002)

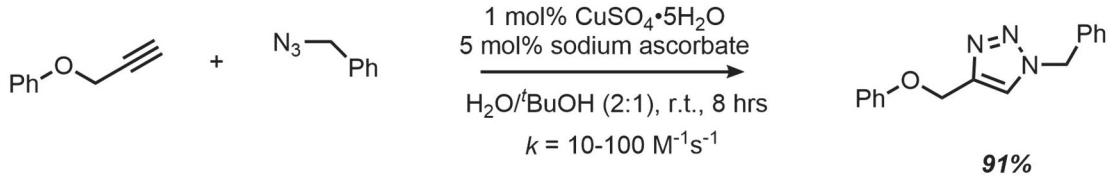

(d) Bertozzi: Strain-promoted azide-alkyne cycloaddition (2004)

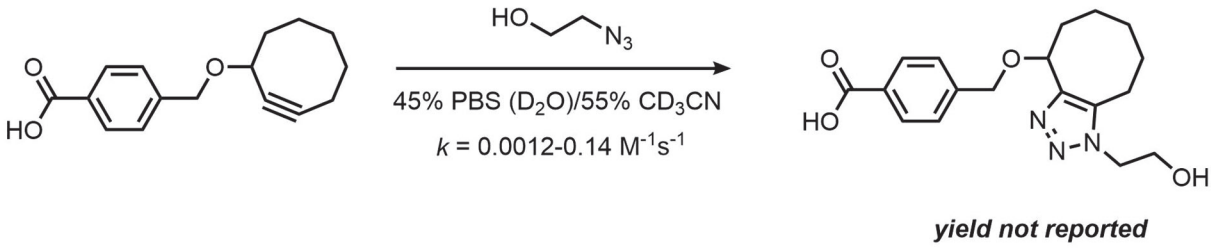

Figure 1.2 Examples of the development of 1,3-dipolar cycloadditions over time. (a) Huisgen cycloaddition described by Husigen at a Centenary Lecture at the University of Munich, Germany in 1961.[15] (b) Copper-catalyzed cycloaddition on a propargyl peptide side-chain as described by Meldal and co-workers [5] in 2002. FGFG = Phe-Gly-Phe-Gly; attached to a $PEGA_{800}$ resin. (c) Copper-catalyzed cycloaddition as described by Sharpless and co-worker [6], also in 2002. (d) Modification to the azide-alkyne cycloaddition as described by Bertozzi and co-worker [9] using bond-strain to provide the necessary energetics for the reactions to occur without the addition of a copper catalyst.

(a) Tetrazine cycloaddition described by Fox et al. (September 2018)

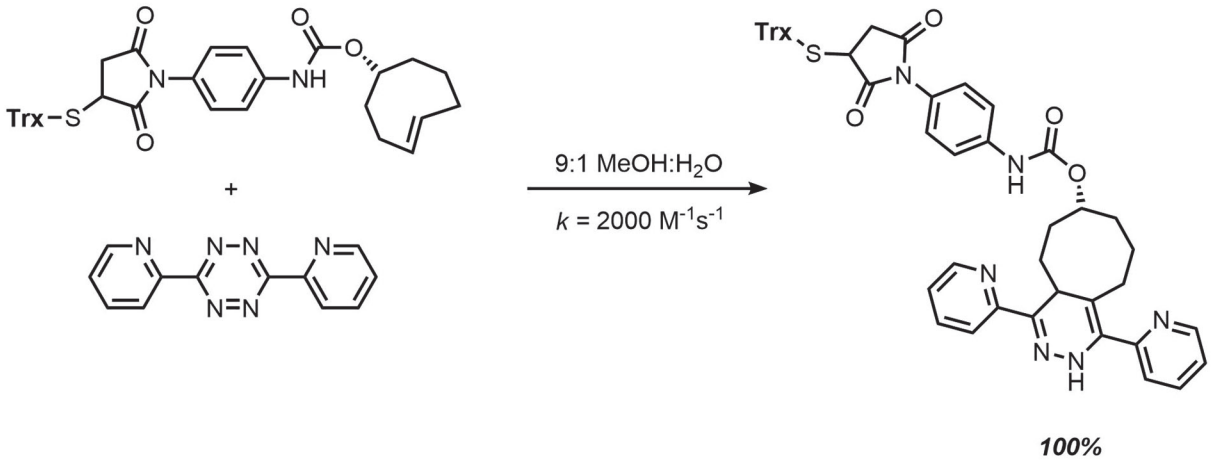

(b) Tetrazine cycloaddition described by Hilderbrand et al. (October 2018)

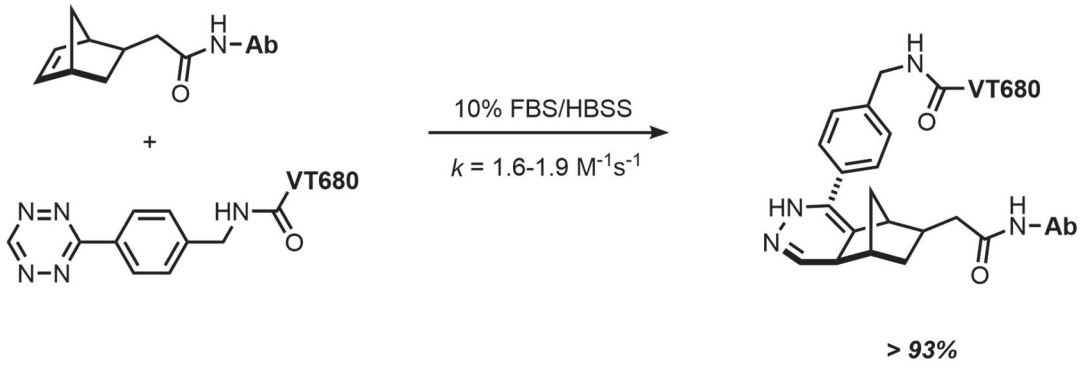

Figure 1.3 First described tetrazine ligations by Hilderbrand [10] and Fox [11], published one month apart. (a) Example of a tetrazine ligation using a trans-*cyclooctene functionalized thioredoxin (**Trx**) with a bipyridyl-tetrazine as described by Fox and co-workers.[11] (b) Example of using tetrazine ligations to functionalize biological molecules (e.x.: antibodies, **Ab**). In Hilderbrand et al.'s [10] work, they conjugated norborene functionalized antibodies with tetrazine-functionalized fluorescence probes (**VT680**).*

solvent. Their fast reaction kinetics makes them also suited to one of the "requirements" of bioorthogonal reactions, in that they can proceed at dilute concentrations – further increasing their tolerance *in vivo*. The by-products of this reaction are diatomic nitrogen (N_2) released from the tetrazine during ligation, as well as the leftover pyridazine ring where the ligation took place.

Overall, since their introduction, the tetrazine ligation has been the gold-standard "reaction-to-beat" in terms of its kinetics and *in vivo* tolerance. *(See Figure 1.3)*

1.1.4 The Pictet-Spengler Ligation

A more recent addition to the toolkit of bioconjugate reactions is an adaptation of the Pictet-Spengler reaction. The original reaction was discovered in 1911 by Pictet and Spengler and involves the cycloaddition of an amine and an aldehyde through an oxime intermediate. [16, 17] In 2013, Bertozzi and co-workers wanted to capitalize on the oxime intermediate of this reaction, as the reaction had potential to be bioorthogonal. Testing this reaction (now called the Pictet-Spengler ligation; *Figure 1.4(b)*) in the modification of biomolecules such as purified proteins and antibodies, Bertozzi and cowokers found that their Pictet-Spengler ligation was 4-5 orders of magnitude faster in aqueous media than the traditional reaction (k = 1.39-2.74 x 10^{-7} $M{\cdot}s^{-1}$ v.s. k = 0.26-10.57 $M^{-1}s^{-1}$) and that the oxacarboline formed in the process was substantially more stable than a traditional oxime linkage. [17] In 2020, Bertozzi and colleagues further utilized a variation of this chemistry (a hydrazine-*iso*-Pictet-Spengler [HIPS] reaction) in synthesizing an antibody-enzyme conjugate, which was previously shown to be susceptible to oxime hydrolysis, to be sufficiently stable for the length of time required for their assay. [18] *(See Figure 1.4(c))*

1.2 Applications of Bioorthogonal Reactions

There are several reasons why researchers use bioorthogonal reactions. In broadest terms, these reactions are used to probe and complete our understanding of cellular/organismal biology. Researchers use these reactions to track molecules such as glycans and lipids and better understand and unravel the mysteries of how biology functions. These reactions are also used when researchers are unable to incorporate a "tag" genetically. Two literature examples that use bioorthogonal chemistry to answer important biological questions, that truly show just how much information can be garnered from these types of investigations are explained below.

(a) The Pictet-Spengler Reaction (1911)

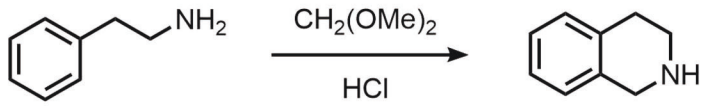

(b) Pictet-Spengler ligation developed by Bertozzi and co-workers (2013)

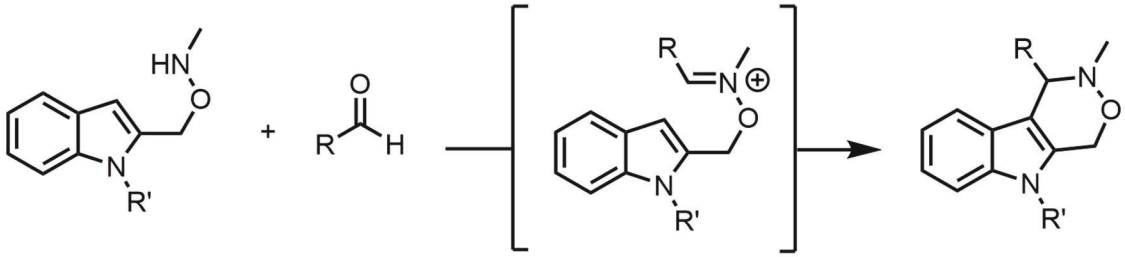

(c) Pictet-Spengler ligation used by Bertozzi and co-workers (2020)

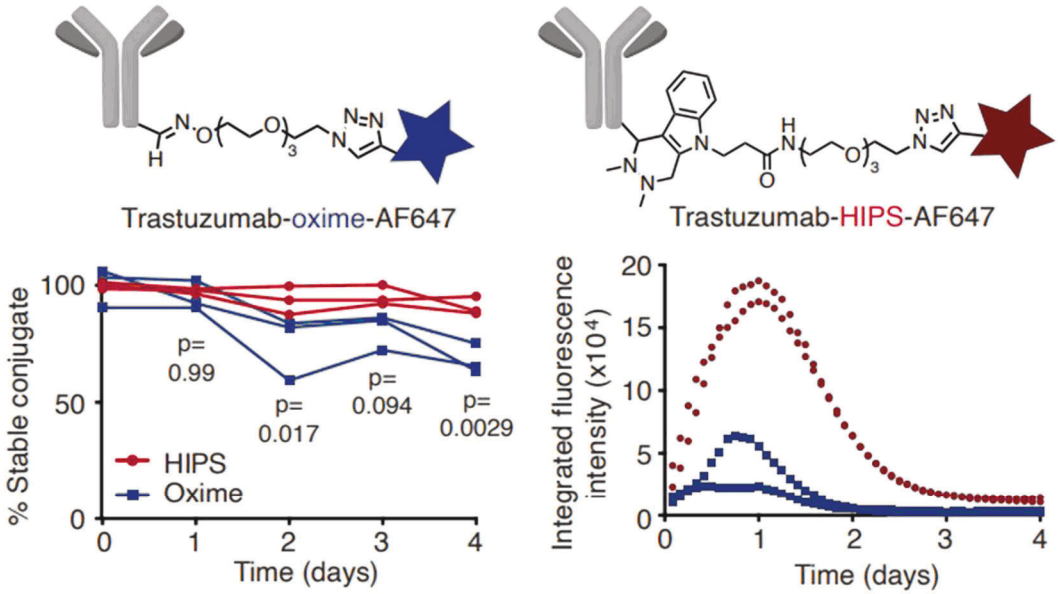

Figure 1.4 (a) The original Pictet-Spengler reaction discovered by Pictet and Spengler in 1911. (b) Adaptation by Bertozzi and co-workers of the Pictet-Spengler reactions to include an oxime intermediate. (c) Utilization of a variation of the Pictet-Spengler reaction, the HIPS reaction, to yield a stable antibody conjugate. Images taken from [18].

1.2.1 Using bioorthogonal reactions to determine the temporal localization of sialic acids during embryonic development

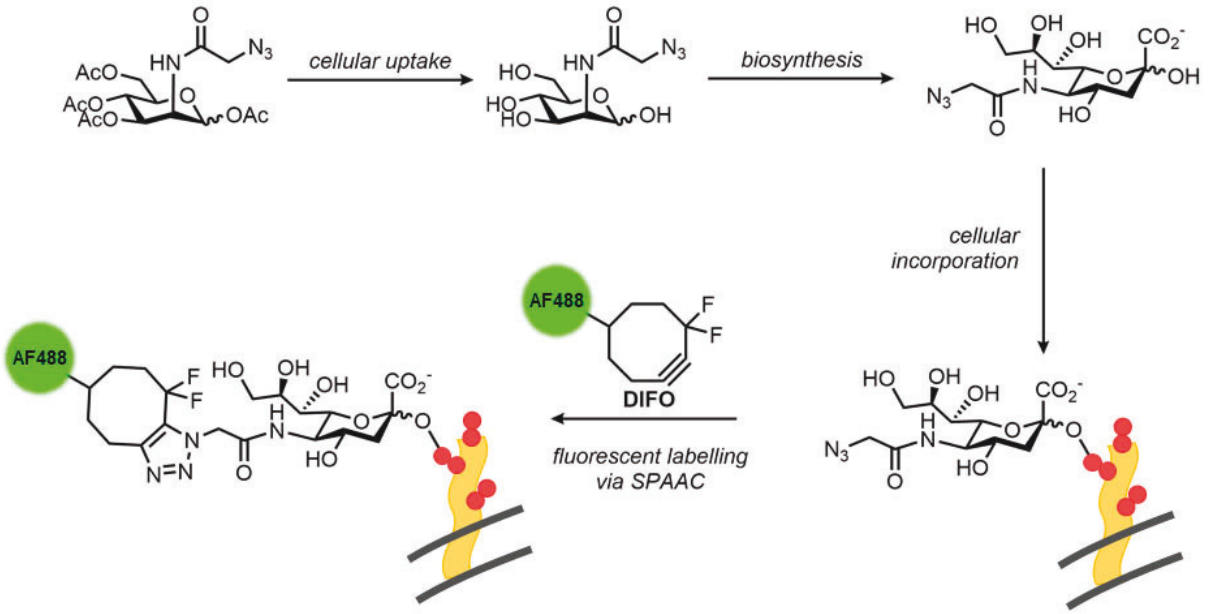

Figure 1.5 First part of the work done by Bertozzi and co-workers to temporally locate sialic acids during embryonic development.[19] Ac_4ManNAz is taken up by cells and deacetylated to ManNAz which undergoes further biosynthetic transformations to SiaNAz. SiaNAz is then incorporated into cell surface proteins (grey = cellular membrane, yellow = cell surface protein, red = glycosylated moieties of the

The year was 2012 – up to that point, methods to determine sialic acid functionality were few and far between. The issue was that cells have several (to the point of redundancy) sialic acid transferases, and there was a lack of tools to probe sialic acids directly. Studying sialic acids and their functions was and still is important, due to their presence on cell surface proteins. Sialylated glycoproteins function as recognition sites, post-translational modifications (PTMs), and mediate cell-cell interactions and migration in the brain and during neuronal development. Knock out experiments with rodents were observed to cause premature death during embryonic development. Enter the strain-promoted azide-alkyne cycloaddition and Bertozzi *et al.* [19] In this seminal work, Bertozzi and co-workers first started by showing how their reaction would work. First, they fed cells a functionalized sialic acid precursor: peracetylated *N*-azidoacetylmannosamine (abbreviated as Ac_4ManNAz). This sugar is cell-permeable and enters the cell's biosynthetic pathways where

it is converted first to *N*-azidomannosamine (ManNAz) then to an azido sialic acid (SiaNAz). These modified sialic acids are then presented on cell surface glycoproteins, identically to their non-azido modified counterparts. Bertozzi and co-workers, already having developed *two* methods to tag azide handles, then tagged these azido-modified with AlexaFluor 488 pre-conjugated to a difluorinated cyclooctyne (DIFO*) (Figure 1.5).*

Next, Bertozzi and co-workers applied their system *in vivo*. Zebrafish embryos (which are conveniently translucent) where fed Ac_4ManNAz which was incorporated into the cell surface proteins of the growing embryo. During hours 4-72 of growth post-fertilization (hpf) DIFO-AF488 probe was added to the growth media to label the sialic acids incorporated onto the cell surface at this time. At hour 72, the remaining DIFO-AF488 was washed away, then DIFO-AF555 (same reaction as the DIFO-AF488 probe, but with a different fluorescent output) was added during 73-76 hpf. The result, once imaged under a fluorescence microscope, was a coloured "map" of which

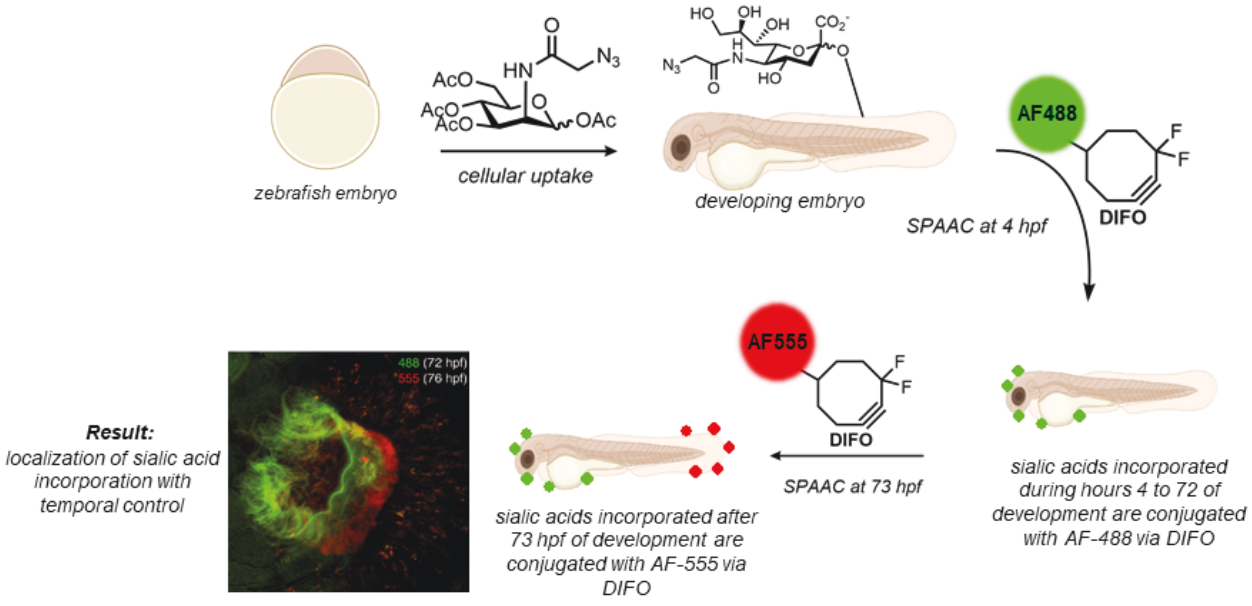

Figure 1.6 In vivo *experiment showing temporal localization of sialic acid incorporation on cell surface proteins during embryonic development of a zebrafish. Fluoresence image is the Z-projection of the zebrafish olfactory organ; green indicating sialic acid were incorporated during the first 72 hrs of development, and red indicating sialic acids incorporated after. Zebrafish images from biorender.com and [19].*

areas of the zebrafish embryo incorporated sialic acid onto their cell surface at different stages of development. *(Figure 1.6)* This remarkable feat of temporal localization would be exceptionally difficult to accomplish without the use of bioorthogonal chemistry.

1.2.2 Using bioorthogonal chemistry to simultaneously label three different enzyme-active sites during activity-based protein profiling

Developed in 1999 by Ben Cravatt and co-workers, activity-based protein profiling (ABPP) is a proteomic technique to elucidate information about enzymes present in a cell lysate. ABPP uses a designed chemical probe ("warhead") that will react covalently with the active site of enzymes the researcher is interested in. [20] The chemical probe usually has a tag as part of its structure which can be used to visualize or purify the targeted proteins. Examples of commonly used tags include radioisotopes (analyzed by electrophoresis and autoradiography), affinity tags (e.g., biotin/streptavidin pairs), and fluorophores (analyzed by laser scanning after SDS-PAGE). [20] Utilizing bioorthogonal reactions to conjugate fluorophores or affinity tags onto these activity-based probes (ABPs) is a more recent strategy which removes the obstacles of ABPs that have poor cell permeability, limiting their usage with *in situ* and *in vivo* applications.[20] Instead, the reactive group (warhead) with a bioorthogonal handle is added to the cell culture, and then after the cells are lysed the proteins can be picked out via a subsequent bioconjugation allowing further purification and/or visualization. Therefore, bioorthogonal chemistry widens the applications of ABPP, allowing the researcher to probe the cell in its native unperturbed state, and perform characterization and analysis after lysis.

In biological systems, if a researcher is interested in studying a particular biological process, it is important to consider a myriad of possible interactions inside the cell. For instance, a target may be regulated by other enzymes or by the availability of coenzymes/metabolites, it may act as part of larger protein complexes, or may have multiple areas of localization. Therefore, single-target labeling (e.x. only labeling one target without these considerations for multiple interactions) and study often results in an incorrect and not clear picture of the whole story. Multi-labeling is often difficult to do, as several probes/tags have cross-reactivity. Here bioorthogonal reactions become useful again. In 2012, Overkleeft and co-workers [22] strategized a way to use *three* different bioorthogonal pairs allowing for tri-colour labeling (i.e., three orthogonal reactions)

of a single lysate sample. Overkleeft *et al*. decided to build their proof-of-concept system around the human 20S proteosome. This large protein complex (composed of two "caps" of seven α-subunits, and two "cores" of seven β-subunits) contains three catalytically active subunits: β1, β2 and β5. Since the 20S is well characterized, there exist β-specific inhibitors for the different subunits. *(Figure 1.7(a))*

Overkleef and co-workers then ligated different orthogonal handles onto 3 previously discovered β-specific probes. The authors found that the tetrazine ligation (iEDDA) between the β5-specific probe and tetrazine-BODIPY-TMR tag was incompatible with the CuAAC reaction between β2- specific probe and azide-BODIPY tag due non-specific fluorescence from one of the

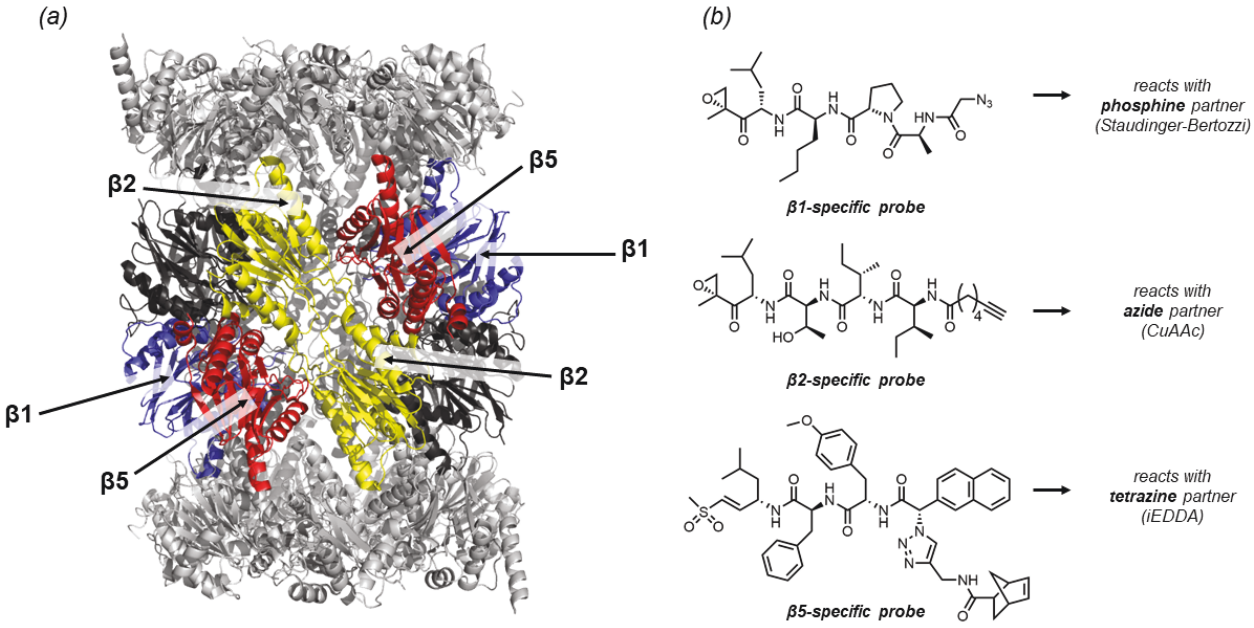

Figure 1.7 (a) PyMol rendering of the human 20S proteosome (PDB: 6RGQ).[23] The α-subunits are coloured in light grey, the non-catalytically active β-subunits are coloured in dark grey, the β1 subunits are coloured in blue, the β2 subunits are coloured in yellow and the β5 subunits are coloured in red. (b) ABPs used to specifically target the separate catalytically active subunits of the 20S proteosome. β1-specific probe was reacted with a phosphine-conjugated to a biotin tag, and β5-specific probe was reacted with tetrazine conjugated BODIPY-TMR tag. The β1-specific probe and β5-specific probe reactions occurred simultaneously in the same reaction vessel. Reaction with the β2-specific probe and an azide conjugated BODIPY tag were reacted subsequently. Proteins were separated by SDS-PAGE and then visualized by Western blot (biotin tag, β1), and in-gel fluorescence (BODIPY, β2; BODIPY-TMR, β5).

fluorophores in the presence of copper sulfate required for the CuAAC reaction.[22] Therefore, to succeed in their triple-labeling experiment, reactions specific to β1 and β5 occurred first (simultaneously), followed by the reaction to β2. Therefore, by using bioorthogonal reactions, Overkleef *et al*. were able to chemically modify three different activity sites on a single protein in a cell lysate, almost concurrently. Concurrent labeling also reveals a more complete picture of the large number of interactions within the cell.

I believe that these two literature examples really highlight the applicability of bioorthogonal reactions and show why expanding the availability of orthogonal bioorthogonal reactions would be of benefit to the field.

1.3 A Case for Metal-Catalyzed Bioorthogonal Reactions

When most non-biologically inclined chemists think of fast, stable and selective reactions, their mind would likely go to a metal-catalyzed cross-coupling reaction. Traditionally, this large family of reactions (e.g., Suzuki-Miyaura, Heck, Sonogashira, Buchwald-Hartwig, Hiyama-Denmark, Fukuyama, Olefin Metathesis…) offer decent reactions rate, stable linkages (carbon-carbon bonds), and utilize reactive groups not typically found in a biological context.

Therefore, the original goal of this thesis was to rationally adapt the Suzuki-Miyaura cross-coupling reaction so that it could be used in a bioorthogonal context. Adapting metal-catalyzed cross coupling reactions for biological contexts was not a completely new idea – select reports of such reactions were published prior to my work described in this thesis. Some notable efforts include work from Lin and co-workers [25] involving a copper-free Sonogashira cross-coupling in *E.coli*. Another example was reported from Bradley and Unciti-Broceta [26] showing Suzuki-Miyaura reactions *in cellulo* with mammalian cell lines (HeLa) and minimal toxicity and observed perturbation to the cell. However, all previous attempts to include metal-catalyzed cross-coupling reactions in the "bioorthogonal toolkit" have been missing pieces of the full puzzle. Most research in this area has under-explored the requirement that bioorthogonal reactions need fast kinetics and limited mechanistic and kinetic investigations have occurred in this space. Additionally, rational

Reaction	Coupling Partner A	Coupling Partner B	Metal Catalyst	Product Linkage
Suzuki-Miyaura	R_1–$B(Y)_2$	R_2–X	Pd	R_1–R_2
Heck		R_2–X	Pd	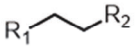
Sonogashira	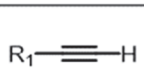	R_2–X	Pd or Cu	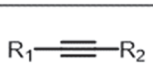
Buchwald-Hartwig	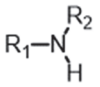	R_3–X	Pd	
Hiyama-Denmark	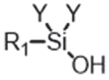	R_2–X	Pd	R_1–R_2
Fukuyama	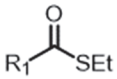	R_2–Zn–I	Pd or Ni	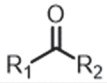
Olefin Metathesis			Ru, Ta, Mo (e.g. Grubbs, Schrock)	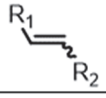

Table 1.1 Summary of a selected group of metal-catalyzed cross-coupling reactions. Here, "X" is noted to be a halide or halide equivalent. "Y" is to note a variable group such as a hydroxyl, pinacol ester or methyl group. "R" is to note the group of interest for coupling, typically an aryl group of a more complex molecule. [24]

design of the palladium ligand has not occurred, with researchers opting instead to recycle readily accessible ligands and attempt their usage in aqueous media.

In 2018, I began the Williams Group development from this starting point. Based on previous research,[27] the Williams group had rationally designed palladium-ligand complexes with the intent on using them for catalysis in aqueous media. I therefore wanted to start by examining the kinetics of the Suzuki-Miyaura reaction in an aqueous environment, to fully understand where our new catalysts would need to perform optimally. From there, my goal was to develop a high-throughput method of testing our palladium complexes on a variety of "challenging" substrates – those like what you would find in a biological context. Last, I wanted to take our primed reaction, and apply it to a bioorthogonal Suzuki-Miyaura reaction.

Chapter 2: Towards a Simple Assay to Investigate the Mechanism of Suzuki-Miyaura Catalysis in Aqueous Media

2.1 Introduction

Introduced in 1981 by N. Miyaura, T. Yanagi, and A. Suzuki, the Suzuki-Miyaura cross-coupling reaction has become one of the most widely used and efficient methods to build substituted aromatic molecules.[28] The reaction involves an aryl halide (or halide equivalent), an aryl boronic acid or ester and a palladium catalyst to aid in stitching together a carbon-carbon bond where the halide and boron components once stood.

This Nobel Prize winning reaction has a catalytic cycle that shares many features with other metal-catalyzed cross-coupling reactions. First, the palladium catalyst undergoes oxidative addition with the aryl halide or aryl halide equivalent (e.g., OTf-). The palladium center is oxidized ($Pd^0 \rightarrow Pd^2$) and is inserted between the aryl group and the halide atom. The next step, transmetalation, has been the subject of intense study in the last two decades.[29] Two potential pathways for transmetalation exist, either going through a nucleophilic boronate species (Figure 2.1, Pathway A) or four-centered palladium hydroxo complex (Figure 2.1, Pathway B). The specifics of this step are discussed in further detail below. The third step of the catalytic cycle, reductive elimination, results in the elimination of the palladium complex, reducing the metal center back to Pd^0 and stitching the two aryl groups together. The proposed and accepted catalytic cycle is shown in Figure 2.1.

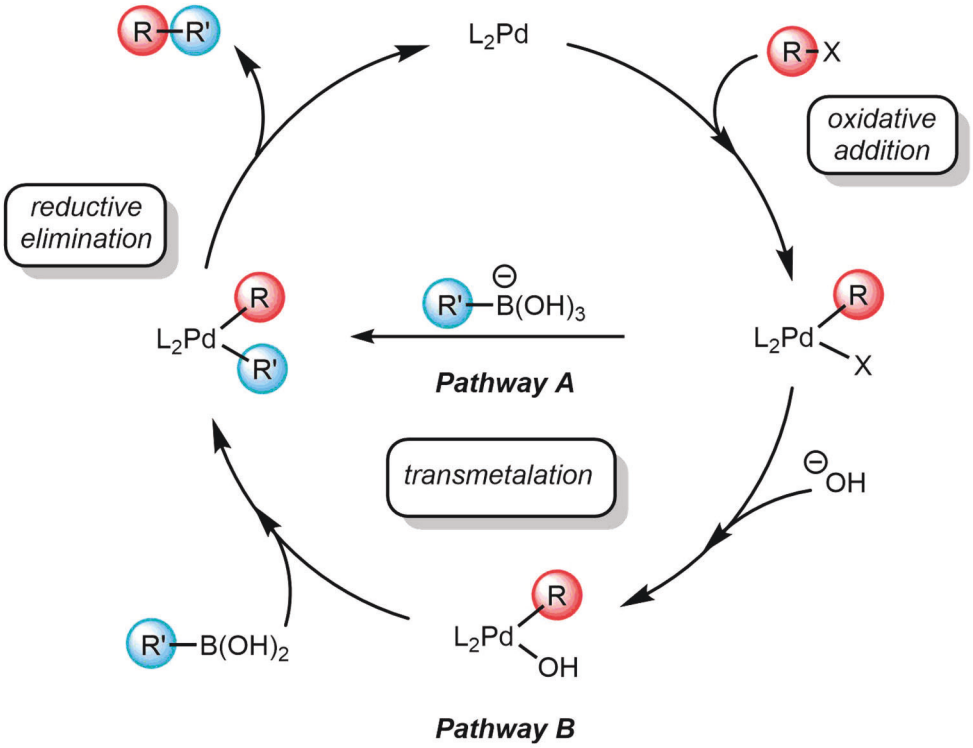

Figure 2.1 Proposed and accepted catalytic cycle of the Suzuki-Miyaura cross-coupling reaction. The palladium complex undergoes oxidative addition with an aryl halide (red, R), followed by transmetalation (two pathways available) with the boron-containing coupling partner (blue, R'), and lastly reductive elimination, which covalently bonds the two partners together through a carbon-carbon linkage. Figure reproduced from Ortuño et al. [30]

As mentioned above, the transmetalation step of the Suzuki-Miyaura cross-coupling (SMCC) reaction has been the subject of concentrated study and academic debate over the last 40 years, especially regarding the role of base. As early as 1979, Miyaura, Suzuki and Yamada concluded that base was required for transmetalation to occur since under neutral conditions the organoboron reagent was not sufficiently nucleophilic.[31] When Suzuki and Miyaura published their work, they postulated that the addition of sodium ethoxide or sodium hydroxide converted the organoboron reagent to the four-coordinate boronate, which is nucleophilic enough to undergo transmetalation.[31] Six years later, conflicting evidence arose when Miyaura and co-workers published more detailed mechanistic work related to alkenyl-alkenyl couplings, which suggested

the formation of an alkoxo-palladium species. (Figure 2.2) [32] So, which pathway is correct, and why is this important?

Research published by Hartwig[33], Denmark[29], Amatore[34], Schmidt[32] and Soderquist[36] (note that this is not an exhaustive list of researchers investigating this step) has concluded that under specific conditions (i.e. coupling partners must be an aryl boronic acid or ester, and an aryl halide, in wet DMF or acetone or THF and with a carbonate base) that Pathway B (the hydroxo-palladium species) is the pathway occurring *in situ*.[31] The large amount of research in this area has also concluded that when transmetalation is the rate-determining step, it is the most sensitive to the environmental conditions of the reaction.[33] Therefore, for my research in the Williams Group, it is important to understand which pathway Suzuki-Miyaura reactions take under relevant biological conditions (e.g. neutral aqueous protic media) so that we can better design our palladium-complexes to facilitate efficient reaction rates. I found that full mechanistic and kinetics data on SMCC in aqueous/green solvents was lacking – therefore, we sought to design an assay that could be used to test SMCC catalysts that had been designed for optimal performance in water, so that we could elucidate mechanistic and kinetic details on how the reaction functions under our conditions.

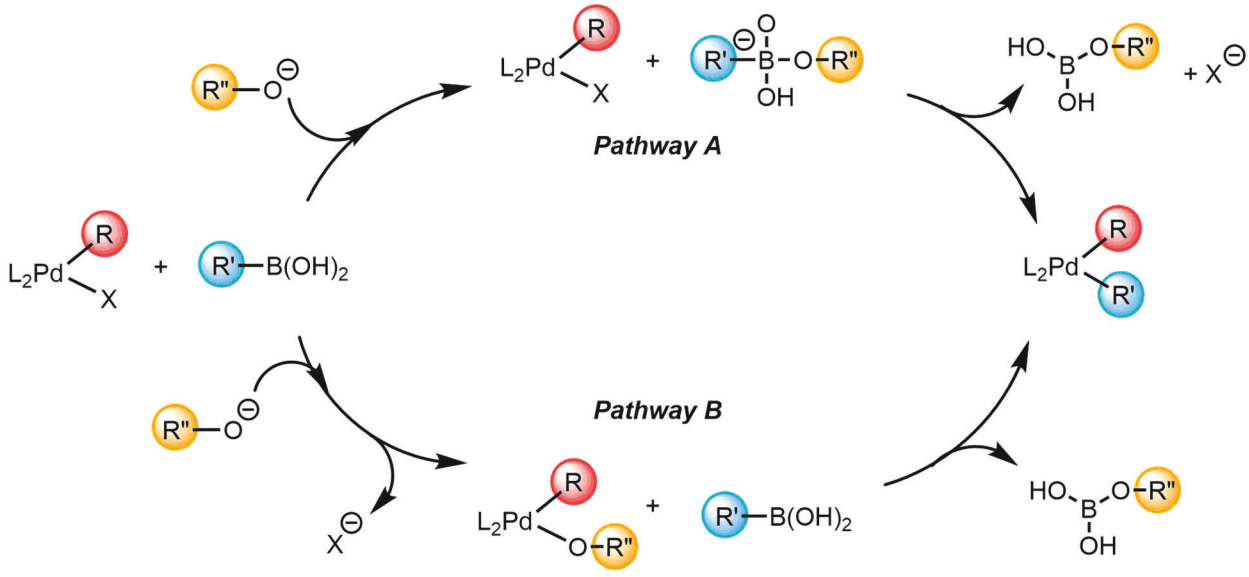

Figure 2.2 Detailed look at the two possible pathways of transmetalation between the palladium catalyst and the organoboron compound. In pathway A, a four-coordinate boronate is formed, whereas in pathway B an alkoxy-palladium complex is formed instead. Figure reproduced from Maseras et al. [37]

2.2 *N*-Heterocyclic Carbenes as Ligands and Ligand Design

Introduced in the early 1990's as phosphine ligand mimics, *N*-heterocyclic carbenes (NHCs) have become popular ligands for palladium chemistry.[38] Similar to phosphine ligands, the NHC is a strong sigma (σ) donor via its L → M bond.[38] Unlike phosphine ligands, the pendant groups (groups bonded to the central imidazole ring at the nitrogen centers) are situated in the coordination sphere. [38] This structure allows a chemist to tune the properties and reactivity of the ligand side chains to facilitate a particular need. Another bonus is that NHC-Pd complexes are easily synthesized by several methods – the Williams Group has taken the approach of using transmetalation from the corresponding Ag complexes.

When designing a ligand for palladium catalysis in water, there are several considerations that must be considered. Traditionally, the reaction requires an electronically rich metal center to facilitate the first step of the cycle – oxidative addition. In addition, the reaction also requires exogenous strong base to activate the boronyl coupling partner, so that transmetalation can occur.[34] While these traditional conditions in organic media often result in high reaction efficiencies, they occur in organic solvents, and require high temperatures and long reaction times. Therefore, when transferring the reaction into aqueous solution or for biological applications we need to consider these requirements and compensate for them.

The Williams Lab has designed and synthesized (by Alex Predy)[1] several NHC ligands for palladium mediated catalysis that are designed to address the requirements listed above. Our ligands have three key attributes to their design. First, NHC-electron donation to the palladium center allows the metal to undergo oxidative addition at ambient temperatures (20°C). Second, the ligands contain at least one Lewis basic group which will activate the boryl arene by coordinating to the boron center and introducing negative charge character. This is typically the role of exogenous base.[29] Third, a pendant hemilabile group positioned on the opposite side of the palladium center. This group can readily dissociate, allowing for sterically and coordinatively

[1] Alex Predy was an undergraduate research student in the Williams Group from 2016 to 2019. All Pd-NHC complexes in this chapter were synthesized by her as part of her independent research project.

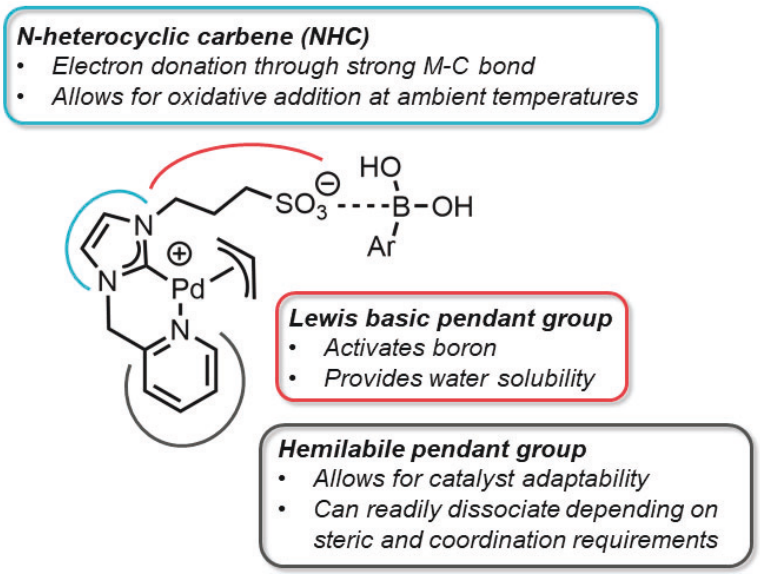

Figure 2.3 Catalyst design of palladium complexes synthesized by Alex Predy. Features of the pendant groups are highlighted in grey and red, and the features of the NHC are highlighted in blue. Figure reproduced from and with permission from Alex Predy. [39]

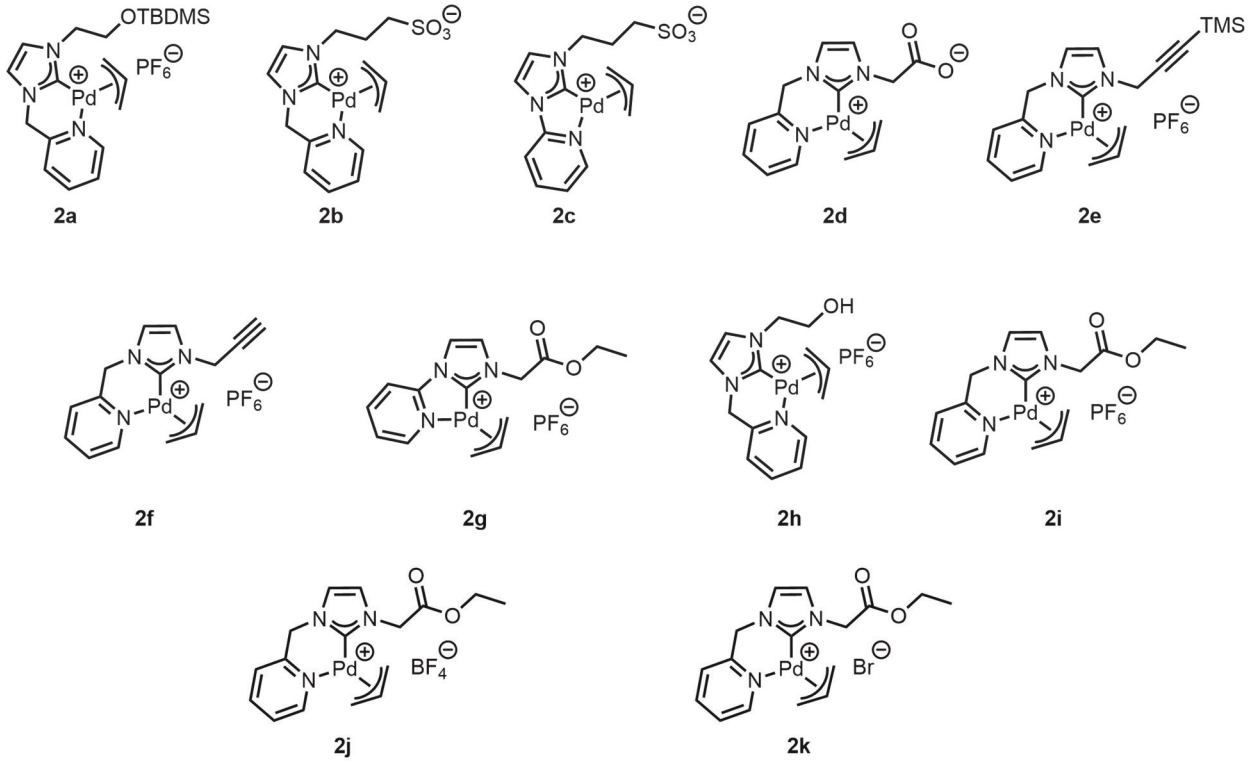

Figure 2.4 The collection of Pd-complexes synthesized by Alex Predy and used in this chapter.

demanding steps in addition to tolerance of reaction-problematic functional groups (e.g., nucleophiles present in a cellular environment). (See Figure 2.3)

2.3 Assay Rationale and Design

To better understand the differences in reaction mechanism between a Suzuki-Miyaura reaction occurring in organic solvent versus in aqueous media, we sought to design an assay that would allow tracking of reaction kinetics. Ideally, this assay would be facile to perform to allow rapid testing of multiple different catalysts.

When designing this assay, we had a few requirements; first, we wanted to utilize UV-Vis spectroscopy for this assay due to the relative ease of collecting data. Therefore, the components of our reaction (the reactants, catalyst and product(s)) needed to have unique UV-Vis spectrum characteristics, where the absorbance maxima of one reagent did not have significant overlap with the absorbance of other reaction components. Second, we wanted the reaction components to be soluble in aqueous media to produce a homogenous solution to allow for monitoring in a standard 1 cm path length quartz cuvette with no stirring. Lastly, we wanted to be able to tune the rate of the reaction so that it could be observed on a time scale measurable by UV-Vis spectroscopy. Once this assay was developed, we hoped to further miniaturize the protocol to use HPLC to test several catalysts using high throughput screening.

We also wanted to use starting materials that were similar to biological molecules since the eventual purpose of these catalysts would be to use them for bioorthogonal reactions. Therefore, thinking about biologically relevant functional groups that have unique UV-Vis signatures, we decided to pursue synthesizing an indole-based probe as one of the assay coupling partners.

2.4 Indole-based probe strategies

Wanting to keep the mechanistic probe simple, we opted to pursue a literature compound (**2.3**) for initial testing. Starting with indole (**2.1**), the 3-position was iodinated (by electrophilic aromatic substitution) with elemental iodine, and Et_3N in DMF.[40] Since this compound (**2.2**) is

known to be unstable [40], the crude was carried forward quickly and stabilized by methylation of the indole using NaH and CH_3I. [40] Extraction from 1:1 EtOAc:Hexanes led to isolation of the product in good yield (86%).

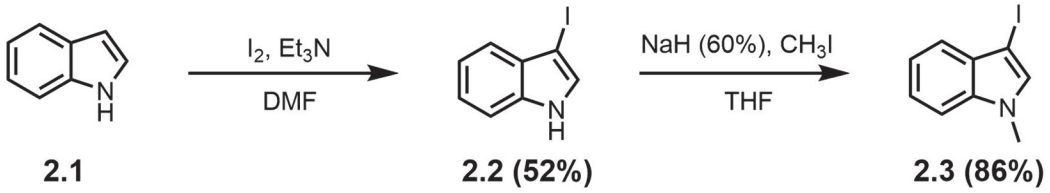

Figure 2.5 Synthesis towards a simple indole-based probe with a coupling handle place on the 3-position of the ring.

This probe was then tested with simple aromatic molecules by using Suzuki-Miyaura coupling. Unfortunately, when coupled with simple aromatic coupling partners, the difference in absorbance maxima between the starting materials and the crude product was not different enough for easy testing.

Thinking that any aromatic system conjugated to the indole probe would preferentially lie perpendicular to the aromatic ring due to steric hindrance (and therefore be out of conjugation which would limit UV-Vis absorbance shifts), we sought to synthesize a coupling partner based on a different organic structure that had fluorescence properties so that both the indole and coupling component could be tracked more easily and independently. (See Figure 2.6)

2.5 Alternative coupling partners

When deciding what other small molecule to use as a coupling partner to our indole probe, we came up with several ideas. The first was to use a boron-dipyrromethene (BODIPY) probe due to the intense fluorescence properties and known synthetic access to variants of the BODIPY scaffold.

Following a procedure from DiCesare et al. [41], I protected the boronic acid **2.4** with 2,2-dimethylpropane-1,3-diol to make the boronic ester (89% yield). I then attempted DiCesare and coworkers' one-pot synthesis of the BODIPY by first condensing 2,4-dimethylpyrrole onto the

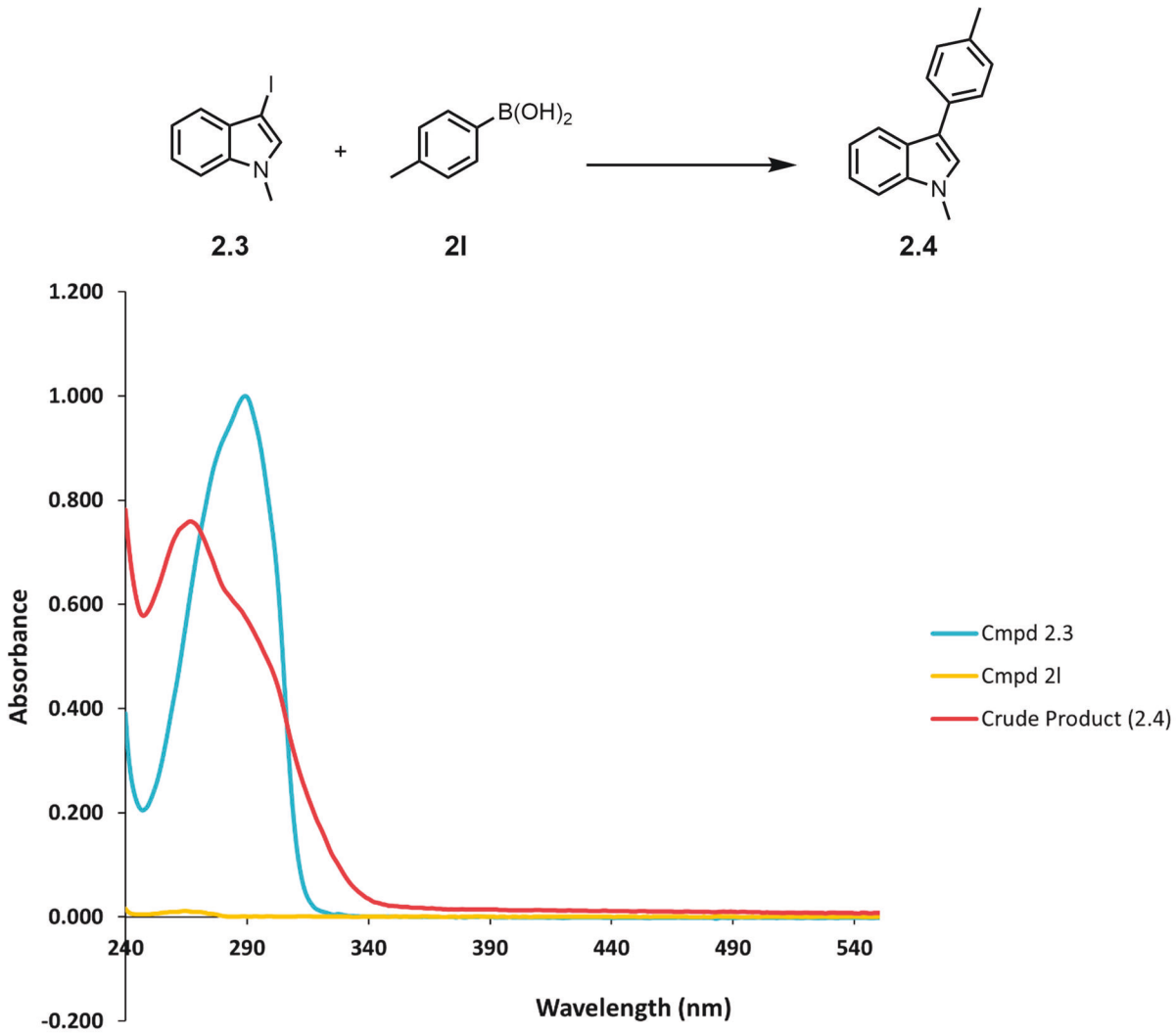

*Figure 2.6 UV-Vis spectral overlay of compounds **2.3, 2l**, and their crude coupling product (**2.4**). Instrument was blanked with PhMe, and compounds were read in PhMe at ~1 mg/mL concentrations. Peaks have been normalized to the absorbance maximum of **2.3** at its lambda max at 289 nm.*

aldehyde, followed by oxidation by DDQ. Last, complexation with boron trifluoride diethyl etherate was performed. **2.6** was supposed to have an absorption maximum at 495nm.[41] We believed that this peak would be decently separated from the indole peak at 289 nm. This one-pot synthesis proved to lead to a complex mixture of crude products that I found impossible to isolate or even separate by extraction. Since this sort of probe was not found to be commercially available and the purification was difficult, we abandoned this route.

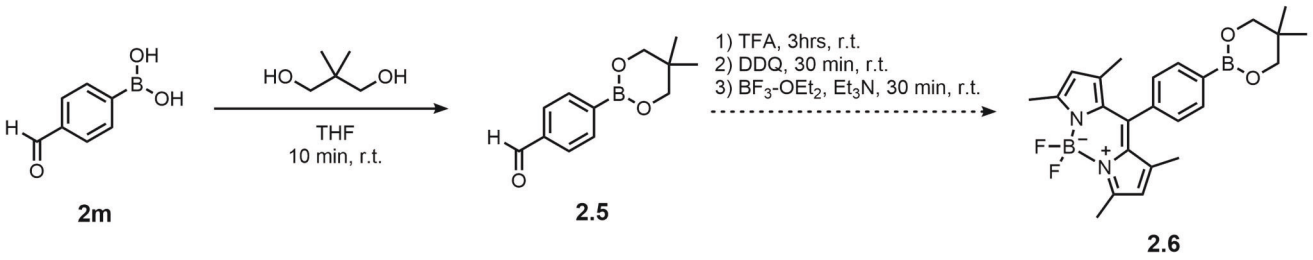

Figure 2.7 Synthesis of a boronic ester BODIPY probe, as proposed by DiCesare et al. [41]

The second idea was to use a commercial dansyl-based boronic acid (**2o**). Dansyl chloride is normally used as a free-amine labeling reagent and has an absorption peak at 340 nm. [42] I measured the UV-vis spectrum of this compound and found that the absorption peak at 337nm was quite low at our working concentration of 0.1 mg/mL. Additionally, this product was prohibitively expensive to purchase on the scale required. Therefore, we decided to synthesize a coumarin probe due to the relatively high cost of the starting materials and purportedly easier synthetic routes.

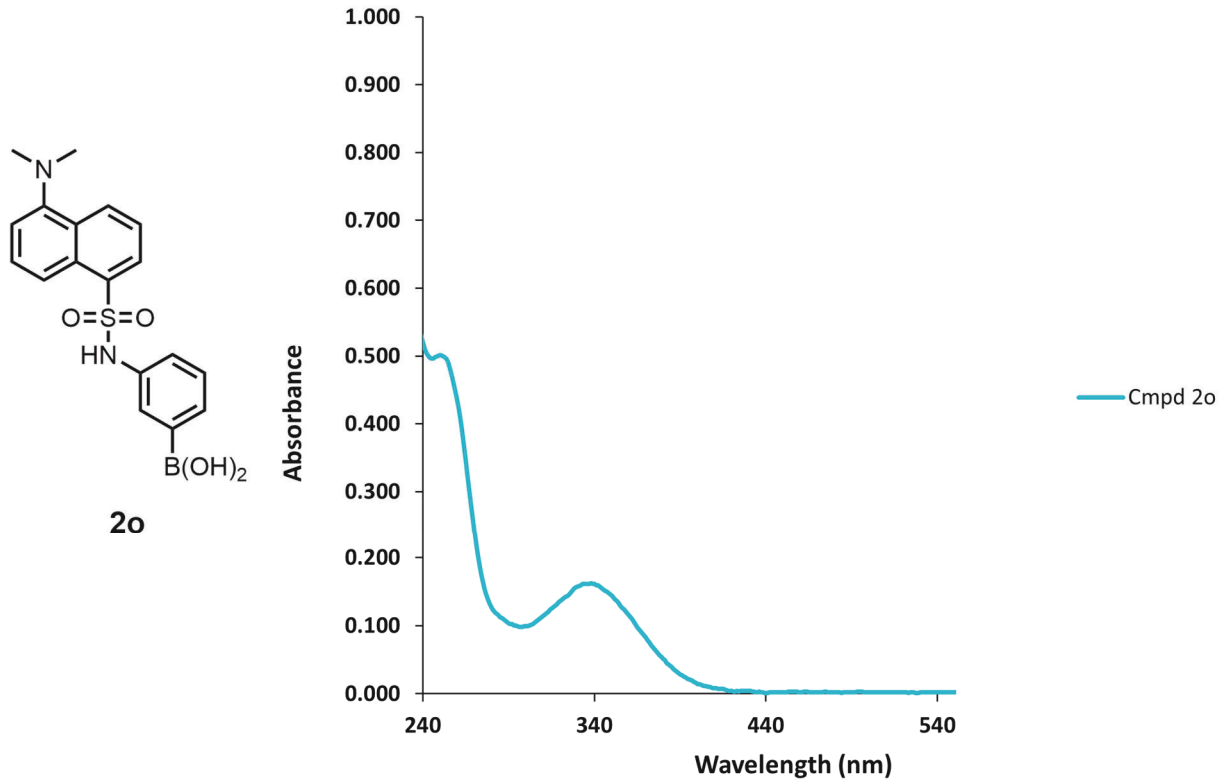

Figure 2.8 Molecular structure of a commercially available dansyl-boronic acid and the corresponding UV-Vis spectrum of the compound in 95% ethanol at 0.1 mg/mL.

2.6 Synthesis of coumarin coupling partner

Starting from 7-hydroxycoumarin (also known as umbelliferone, **2n**), the 8-position was iodinated using elemental iodine and potassium iodide in a 20% aqueous ammonium hydroxide solution.[43] This method allowed for precipitation of the product (**2.7**), removing the necessity of column purification. Additionally, I also protected the free hydroxyl group on the 7-position by methylation with methyliodide (88%, **2.8**). [43]

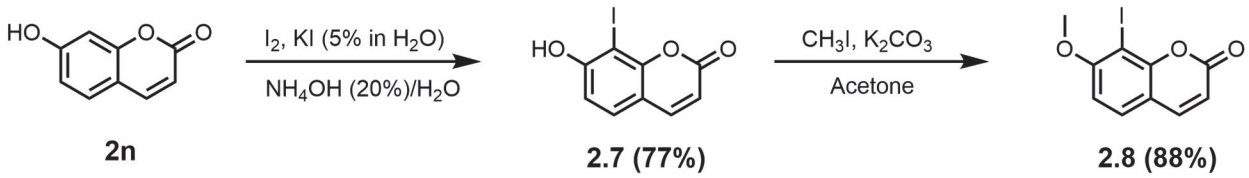

Figure 2.9 Synthesis of a coumarin-based coupling partner.

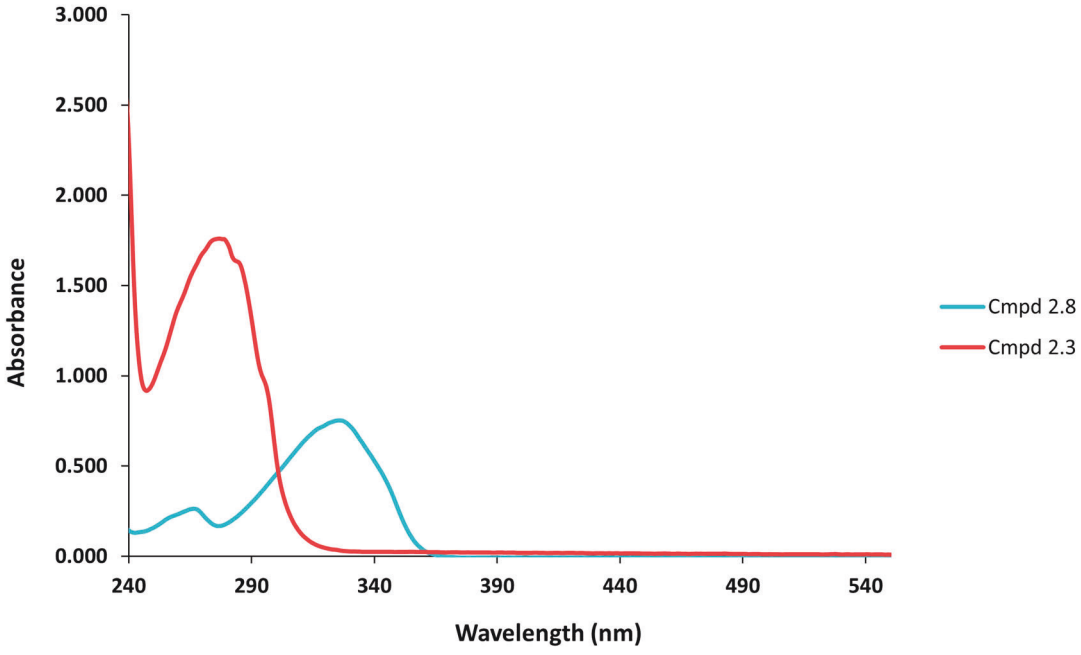

*Figure 2.10 UV-Vis spectral overlay of initially synthesized indole probe **2.3** compared to coumarin probe **2.8**. Both spectra were measured in 95% ethanol, and at 0.1 mg/mL.*

Based on the UV-Vis trace of this coumarin, compared to that of our indole probe, we found there to be a 38 nm difference between absorption maxima. We opted to use a commercially available indole boronic acid (*N*-methylindole-5-boronic acid, **2p**) for further testing in the SMCC reaction with this coumarin probe.

2.7 Coupling indole and coumarin partners via Suzuki-Miyaura coupling

In the literature there was very little precedent for coupling indoles and coumarins together, therefore some testing had to be done to find a reasonable method. Initially, our goal was simply to make a coupled product, and then later establish method conditions that could be transferred to kinetic testing. I did, however, use ethanol or other aqueous solvents so that the method could theoretically be transferred more easily to our kinetics assay.

Initially, a coupling method facilitated by microwave was attempted, due to previous success in the group. However, this proved to be unsuccessful. From there, I evaluated a more traditional method of Suzuki-Miyaura coupling that involved using cesium carbonate as a base and 1,4-dioxanes at reflux for the solvent. Purification by column chromatography proved difficult, therefore coupling product **2.9** was purified by HPLC in a 24% yield.

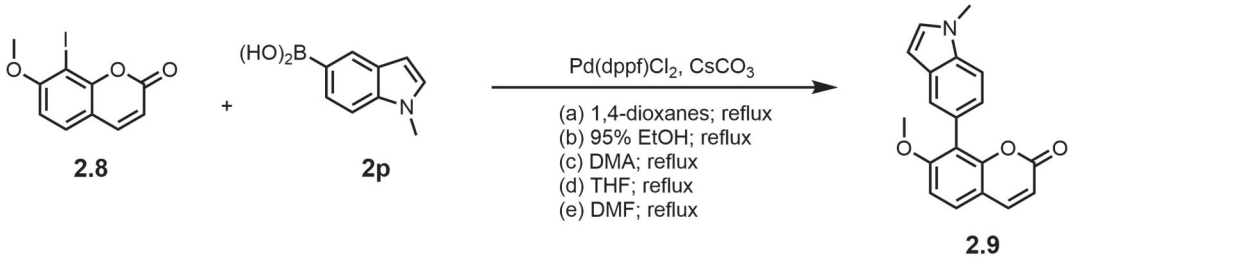

Figure 2.11 Synthesis of an indole-coumarin coupled product via SMCC.

In trying to optimize the reaction to conditions more suitable for our kinetics assay, I repeated the reaction but changed the solvent to 95% ethanol at reflux. This led to a reduction in yield to 18% (calculated by NMR conversion). Dimethylacetamide (DMA) was also used for a trial run of this reaction, but this did not improve the yield (24% conversion by NMR). Lastly, tetrahydrofuran was used. This led to a large improvement in conversion (93% by NMR). While it would not be helpful in trying to investigate this reaction in aqueous conditions, it could be used to evaluate the assay method as well as for comparison of the mechanistic differences between protic/aqueous and organic solvent conditions. We suspected that the reason for the dramatically increased yield in THF was due to all components of the reaction being soluble, leading to a homogenous reaction.

2.8 Testing Kinetics Assay in Organic Solvent

Since THF proved to be an excellent solvent for this coupling reaction, one small scale test was performed to determine if our assay setup would work – i.e., could we obtain meaningful data by tracking the products by UV-Vis spectroscopy over time?

For this assessment, 10 x 1.5mL Eppendorf tubes were prepared to use as blanks by adding 90µL 95% EtOH and 10µL THF. Sample tubes were prepared by taking 10 x 1.5mL Eppendorf tubes and filling with 90µL 95% EtOH; the remaining volume would then consist of 10µL of the reaction sample, taken at hourly and overnight time points. The reaction in THF was performed on a 0.06 mmol scale (4 mg/mL).

Due to difficulties keeping a consistent reaction volume (i.e., due to constant evaporation of the small reaction volume, the concentrations of the reactants could not be kept consistent), proper tracking of this reaction by UV-Vis was unsuccessful. Ideally, there should have been a steady decrease of absorption intensity at 230nm and an increase at 245nm over time. From this trial run of our UV-Vis assay, I found that there would need to be more stringent control methods to properly account for changes in reaction volumes, or to be able to run the reaction at very dilute concentrations and inside the cuvette used to measure the UV-Vis absorption.

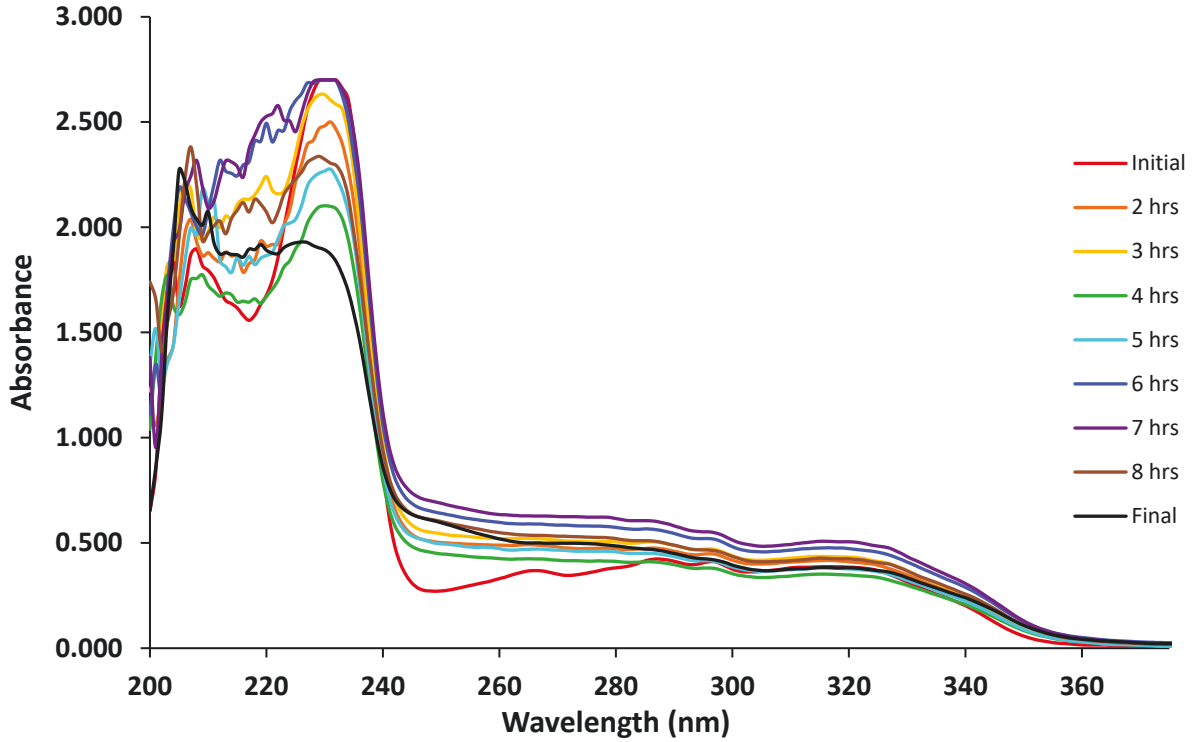

Figure 2.12 Time course experiment of tracking the reaction shown in Figure 2.10 in THF. Time points were taken by removing a 10 µL aliquots and diluting them into 90 µL EtOH, and then taking that combined 100 µL and adding it to 2.9 mL EtOH to take the UV-Vis scan.

When looking at the UV-Vis of coupling product **2.9**, we determined that product **2.9** did not have a substantially different absorption maxima in between the starting materials and the products (5nm between peaks).

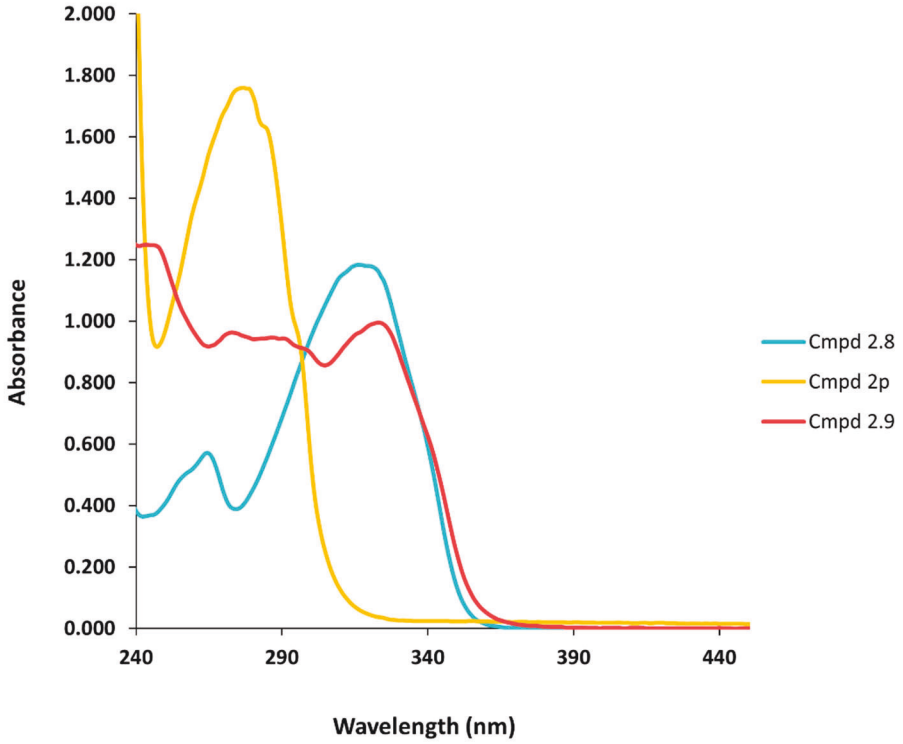

Figure 2.13 UV-Vis spectral overlay of the reactants and product shown in Figure 2.10. Samples were diluted to 0.03 mg/mL in 95% ethanol.

2.9 Fluorescence Testing of Synthesized Probes

In addition to strong UV-Vis profiles, the compounds synthesized in this chapter also displayed fluorescence properties. Indole fluorescence is commonly used in several biological applications [44], whereas coumarin fluorescence is used as inter- and intracellular dyes for fluorescence microscopy.[45] Therefore, we decided to measure the fluorescence excitation and emission of compounds **2.8**, **2p** and **2.9**.

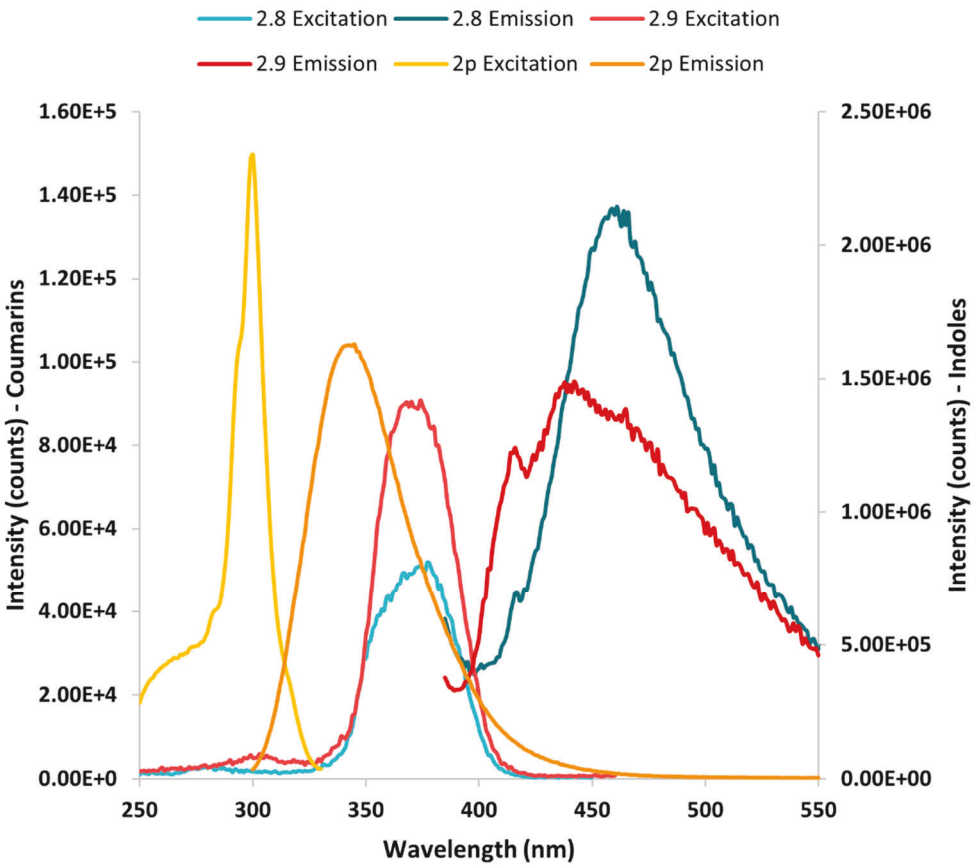

	Excitation (nm)	**Emission (nm)**
Compound **2.8**	377	461
Compound **2p**	300	345
Compound **2.9**	374	442

*Figure 2.14 Fluorescence scans of compounds **2.8**, **2p**, and **2.9** in 95% ethanol at 0.1 mg/mL.*

Based on the early fluorescence data, we assume that fluorescence, rather than UV-Vis would be more suited for tracking of our reaction using the probes synthesized in this chapter. However due to time constraints and an international lab move this project was stopped here.

2.10 Conclusions

After completing the preliminary legwork presented here, I was able to determine some notable considerations for research in this area when moving forward. The first is that fluorescence measurements, rather than UV-Vis, would be more suitable for tracking the components of a biologically inclined Suzuki-Miyaura cross-coupling reaction. This is because the compounds used in my research did not display enough peak separation to distinguish themselves over the course of a coupling reaction. I also found that several in several of my ideal products, the two aromatic rings coupled together would favour lying perpendicular to each other, rather than in the same plane (which would increase the conjugation).

If this work is continued, I would suggest looking at coupling partners that have strong, distinct fluorescent properties, so that tracking of the individual components can be made easier. In addition, I would also suggest looking at a coupling that forces the two aromatic moieties to be in plane with each other. A Suzuki-Miyaura reaction that does force the coupled aromatic rings to be in-plane is discussed further in Chapter 3.

Experimental

General

Reactions were carried out in oven-dried (> 130 °C) or flame-dried glassware under a positive nitrogen atmosphere, unless otherwise stated. Transfer of anhydrous reagents was accomplished with oven-dried syringes or cannulae. Tetrahydrofuran (THF), dichloromethane (DCM), and toluene (PhMe) were dispensed from a solvent system, which dried solvents by passing them through a column of activated molecular sieves (4Å). Any water, or aqueous solutions used in-house generated reverse osmosis water, unless otherwise stated. Thin layer chromatography was performed on glass plates pre-coated with 0.25 mm silica gel with a fluorescent indicator UV254 (EMD Millipore). Flash chromatography columns were packed with 230-400 mesh silica gel (Silacycle). All reagents were purchased from the following commercial suppliers: Millipore-Sigma (Sigma Aldrich), AK Scientific, Acros Organics, Oakwood Chemicals, or Fisher Scientific/VWR, at a purity greater than 95%, and without further purification unless otherwise specifically noted. Proton nuclear magnetic resonance spectra (^{1}H NMR) were recorded at 300, 400 or 500 MHz, and coupling constants (*J*) are reported in Hertz (Hz). Carbon nuclear magnetic

resonance spectra (^{13}C NMR) were recorded at 125 MHz. The chemical shifts were reported on the δ scale (ppm) and referenced to the residual protonated (^{1}H) solvent or to the deuterated solvent (^{13}C) peaks: DMSO-*d*$_6$ (2.50 ppm, 1H), MeOD-*d*$_4$ (3.31 ppm, 1H), $CDCl_3$ (7.26 ppm, ^{1}H; 77.06 ppm, ^{13}C). s = singlet, bs = broad singlet, d = doublet, t = triplet, q = quartet, dd = doublet of doublets, m = multiplet. For chromatography conditions, EtOAc = ethyl acetate, and Hex = hexanes.

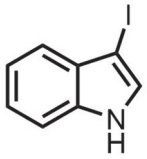

Compound 2.2

1g indole (8.53 mmol, 1.0 eq), 20 mL DMF, and a magnetic stirrer were added to a 100 mL RBF. While stirring, 3 mL Et_3N (2.5 eq) was added to the indole. Separately, 2.73 g elemental iodine (9.38 mmol, 1.1 eq) was dissolved in 20 mL DMF and added to an addition funnel. The iodine solution was slowly added to the reaction solution over a period of 30 minutes, while stirring at room temperature. The solution was stirred for an additional hour at room temperature. The reaction was then quenched by the addition of 150 mL of cold quenching solution (0.5% aqueous NH_3 (v/v), 0.1% metabisulphite (w/v)), causing a precipitate to form. The resulting suspension was filtered by vacuum filtration and washed with cold water (~200 mL). Further solvent removal in vacuo provided crude **2.2** in 52% yield, used without further purification. This compound decomposes readily at room temperature and is sensitive to light exposure. The compound can be stored for several months at -20 °C in a foil-covered glass vial before using in subsequent reactions. Spectrum match reported literature values.[40] ^{1}H NMR (400MHz, DMSO-*d*$_6$): δ 7.53 (d, *J* = 2.5 Hz, 1H), 7.40 (d, *J* = 7.0 Hz, 1H), 7.27 (d, *J* = 7.7 Hz, 1H), 7.13 (m, 2H).

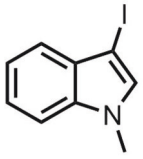

Compound 2.3

4 mL THF was added to a flame-dried 50 mL RBF. 23.9 mg NaH (60% dispersion, 1.8 eq) was suspended in 6 mL dry THF then added to the RBF. The NaH was rinsed with a further 2 mL of THF. This suspension was cooled to 0 °C. Compound **2.2** (100 mg, 0.41 mmol, 1.0 eq) was dissolved in 4 mL dry THF and added to NaH via syringe. The reaction mixture was stirred at 0 °C for 15 minutes before removing the vessel from the ice bath and letting it warm to room temperature. Once at room temperature (~15 minutes), 225 μL CH_3I (4.11 mmol, 10.0 eq) was added and the reaction mixture was left to stir overnight at room temperature. The next morning the solvent was then removed by rotary evaporation, which resulted in a golden yellow oil. This oil was then suspended in cold H_2O, from which it was then extracted 3x with 1:1 EtOAc:Hexanes. The organic layers were combined, washed with cold H_2O, and dried over Na_2SO_4. The solvent was removed in vacuo yielding 96 mg **3.3** as a yellow-brown solid (86% yield). Spectrum matched reported literature values.[46] ^{1}H NMR (500MHz, DMSO-d_6): δ 7.54 (s, 1H), 7.46 (d, J = 8.7 Hz, 1H), 7.27 (d, J = 8.2 Hz, 1H), 7.18 (dt, J = 44.5 Hz, J = 7.5 Hz, 2H), 3.81 (s, 3H).

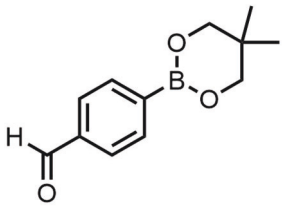

Compound 2.5

4-formylphenyl boronic acid (300 mg, 2.0 mmol, 1.0 eq) was added to 15 mL dry THF in a 50 mL RBF and dissolved. 2,2-dimethylpropane-1,3-diol (2.2 mmol, 1.14 eq) was then added to the boronic acid and THF. Addition of the diol led to a loss of yellow colour. The solution was stirred under N_2 for *exactly* 12 minutes. The solvent was removed by rotary evaporation and the remaining pale-yellow oil was dissolved in 20 mL DCM. The organic layer was washed 5 x 10 mL H_2O, then dried with Na_2SO_4. Evaporation of the solvent lead to a pale-yellow oil. To this oil, hexanes were added, and this mixture was then cooled on ice. After ~30 minutes white crystals precipitated out. The white crystals (product) were collected in an 89% yield (382 mg). Spectrum matched reported literature values.[47] ^{1}H NMR (500MHz, $CDCl_3$): δ 10.01 (s, 1H), 7.95 (d, J = 8.0 Hz, 2H), 7.84 (d, J = 8.2 Hz, 2H), 3.79 (s, 4H), 1.03 (s, 6H). ^{13}C NMR (125MHz, $CDCl_3$): δ 192.80, 137.81, 134.33, 128.65, 72.44, 31.91, 21.88.

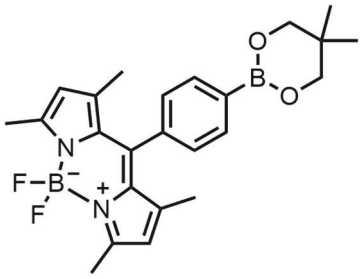

Compound 2.6

3 mL DCM was added to a 25 mL RBF. N_2 was bubbled through the DCM for 5 minutes. 50 mg **2.5** (0.229 mmol, 1.0 eq), followed by 42 μL of 2,4-dimethylpyrrole (0.407 mmol, 2.05 eq), and lastly 0.3 μL trifluoroacetic acid (0.0001%) were then added to the flask in succession. The solution turned dark orange and was stirred at RT. Checking by TLC (neat DCM) at 30 minutes, 2 hours and 3 hours, the orange spot became less strong and a pink spot near the baseline began appearing. After 3 hours, a sample of the reaction was neutralized and extracted with DCM. ^{1}H NMR of this sample in $CDCl_3$ showed a loss of the aldehyde peak from **2.5**. 108 mg DDQ (0.407 mmol, 2.05 eq) was added to the flask and immediately the reaction mixture turned deep red. Continued stirring the reaction mixture for 30 minutes at room temperature. To the same reaction vessel added 9 μL Et_3N and 9 μL BF_3-OEt_2 and stirred for a further 30 minutes. Quenched the reaction by addition of H_2O, which led to formation of a dark red sticky solid. Attempted extraction by DCM led to an insoluble red mass.

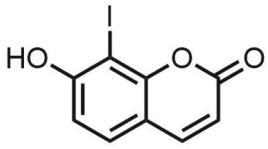

Compound 2.7

Iodine was finely ground with a mortar and pestle. 940 mg of this finely ground iodine (3.70 mmol, 1.0 eq) was added to 50 mL of a solution of 5% KI in dH_2O. Added 600 mg umbelliferone (3.70 mmol, 1.0 eq) and 12 mL 20% NH_4OH in dH_2O to a 250 mL RBF. The I_2 in 5% KI was added dropwise by addition funnel, and the reaction was left to stir at room temperature for 5.5 hours. Quenched the reaction with 2.5N H_2SO_4 until a precipitate formed. The precipitate was collected and dissolved in ethanol. The ethanol was removed by rotary evaporation to give 820 mg of

product (77% yield). ^{1}H NMR (400MHz, MeOD-*d*$_4$): δ 7.79 (d, *J* = 9.4 Hz, 1H), 7.44 (d, *J* = 8.4 Hz, 1H), 6.84 (d, *J* = 8.4 Hz, 1H), 6.20 (d, *J* = 9.4 Hz, 1H).

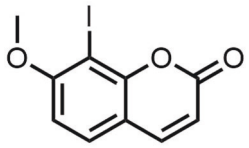

Compound 2.8

100 mL acetone was dried over molecular sieves. To a flame-dried 100 mL RBF was added 820 mg (2.84 mmol, 1.0 eq) **2.7**, 784 mg K_2CO_3 (5.68 mmol, 2.0 eq) and a magnetic stir bar. All components were dissolved in 30 mL dried (over molecular sieves) acetone. Once dissolved, added 265 µL CH_3I, and heated to reflux. The reaction was left to reflux overnight. Acetone was removed by rotary evaporation to leave a residue. 1M HCl was added to the residue, which left a precipitate. This precipitate was filtered by vacuum then washed the precipitate with 1M HCl, then water and last with hexanes. Dried by vacuum to receive the product in an 88% yield (753 mg). ^{1}H NMR (400MHz, $CDCl_3$): δ 7.57 (d, *J* = 9.4 Hz, 1H), 7.43 (d, *J* = 8.5 Hz, 1H), 6.80 (d, *J* = 8.5 Hz, 1H), 6.27 (d, *J* = 9.4 Hz, 1H), 3.99 (s, 3H).

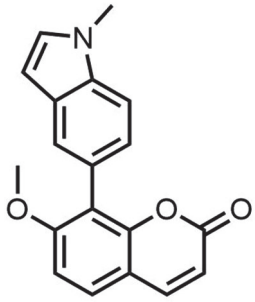

Compound 2.9

Compound **2.8** (60.4 mg, 0.20 mmol, 1.0 eq), **2p** (45.4 mg, 0.26 mmol, 1.3 eq), Cs_2CO_3 (130 mg, 0.40 mmol, 2.0 eq), and $Pd(dppf)Cl_2$ (14.6 mg, 0.02 mmol, 0.1 eq) were added to a 25 mL RBF and dissolved in 10 mL 1,4-dioxanes. The reaction was heated to reflux and left to reflux overnight (~18 hours). The reaction was poured over ~25 mL ice-cold water. The mixture was extracted 3 x 10 mL EtOAc and the organic layers were collected and combined. The organic layer was then washed 5 x 20 mL brine and dried over Na_2SO_4. The remaining solvent was removed by rotary evaporation to yield a yellow oil (108 mg crude material). Some of the crude material was used to

search for the desired mass by LC/MS and to determine HPLC conditions, so the remaining material (54.5 mg) was dissolved in 1 mL and inject onto the preparative HPLC C18 column and eluted using a gradient starting at 2% MeCN/98% H_2O to 95% MeCN/5% H_2O over a period of 13 minutes. The 95% MeCN/5% H_2O gradient was held for an addition 3 minutes. The product was eluted as a single peak at 4.6 minutes. The solvent was evaporated off by rotary evaporation, yielding the product as an off-white solid (14.1 mg, 24% yield). ^{1}H NMR (500 MHz, $CDCl_3$): δ 7.67 (d, J = 9.4 Hz, 1H), 7.63 (s, 1H), 7.43 (d, J = 8.6 Hz, 1H), 7.40 (d, J = 8.4 Hz, 1H), 7.23 (d, J = 8.4 Hz, 1H), 7.06 (d, 2.9 Hz, 1H), 6.97 (d, J = 8.6 Hz, 1H), 6.50 (d, J = 2.8 Hz, 1H), 6.23 (d, J = 9.4 Hz, 1H), 3.83 (s, 3H), 3.81 (s, 3H).

Chapter 3: Towards Designing High Throughput Screening Assays to Test Palladium Catalysts for Suzuki-Miyaura Reactions under Aqueous and Green Conditions

3.1 Introduction

Since florescence proved to be a potential useful avenue to continue studying the aqueous mechanism of the Suzuki-Miyaura reaction, I opted to continue in this vein when looking to design high-throughput screening (HTS) assays to test the Williams Group Pd-complexes. Additionally, since the Williams Group moved to the University of Iowa, we had the opportunity to take advantage of the University's HTS facility located in the Department of Pharmacy. The University of Iowa HTS facility provides a service available to all researchers to aid with assay development, HTS equipment, compound library usage and data analysis. With this facility conveniently available to us, I opted to shift my research focus into optimizing probes (specifically fluorescence reporter molecules to monitor over the course of a Suzuki-Miyaura reaction) for high-throughput screens to rapidly test Pd-complexes being developed in the lab.

Using fluorescence for HTS is not uncommon, in fact, fluorescence assays are one of the most widely used analytical measurements in a high-throughput manner for several reasons.[48] Fluorescence assays are more sensitive than UV-Vis based assays, allow for rapid detection, are less affected by interference and are non-destructive of material.[48] Advances in recent years have allowed for instrumentation that can image multiple fluorescent targets at once, and even measure fluorescence within living cells and organisms.[48]

During the process of working on the assays presented in this chapter, a paper was published in early 2020 from W. Xue et al. in *J. Org. Chem*.[49] These authors had previously successfully synthesized several coumarin probes that exhibited an extended π-system (5 or 6 rings instead of 2). In their latest research, Xue *et al.* sought to further expand the extended π-system to 6 rings and did this via a Suzuki-Miyaura reaction. Additionally, they also reported the synthesis in EtOH/water mixtures, high quantum yields, and the products featured a significant

bathochromic shift from their starting materials.[49] Due to these factors, I felt that applying their probe for use in my HTS assays would be appropriate.

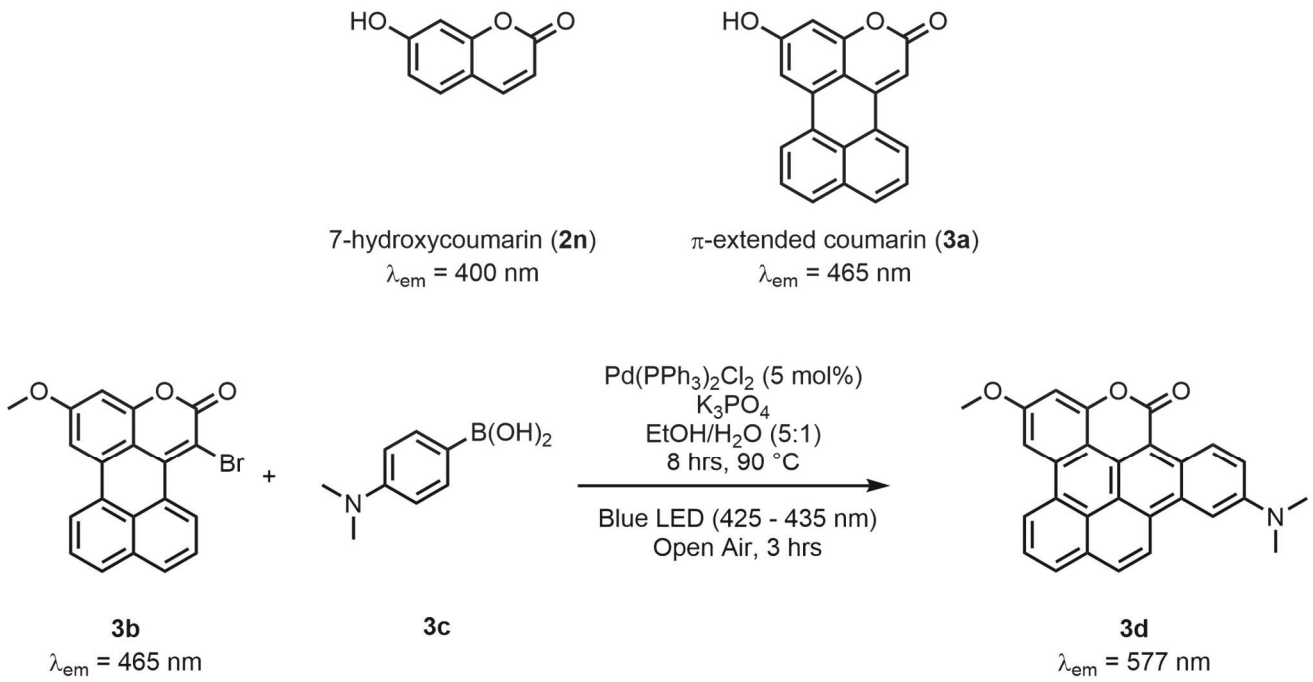

*Figure 3.1. Fluorescence emission maxima for traditional 7-hydroxycoumarin (**2n**), a vertically extended coumarin (**3a**)* [50]*, and an example π-extended coumarin synthesized by Xue et al.* [49]

In this chapter I present a two-pronged approach to designing proof of concept HTS assays and their related fluorescent probes. I felt that the design of the probe could be investigated while developing the HTS assay. Therefore, the first portion of this chapter focuses on the development of proof-of-concept Suzuki-Miyaura HTS assays while the second shows my work synthesizing a mechanistic probe described in Xue et al.'s work.

3.2 Prototype Assay Design to Elucidate Potential Probes

3.2.1 – Compound Storage Testing

I first wanted to determine if I could store boronic acid and/or aryl iodide solutions in a 96-well plate so that when different catalysts were made, I could add them more efficiently to plate

pre-loaded with compounds to be tested. This way the entire library of compounds would always been in the same position on the plate grid between screens. Therefore, to test the stability of compounds sitting in solution I did the following simple experiment:

We made up an unknown concentration of *p*-nitrophenol (PNP) solution in phosphate buffered saline (PBS) and added 1 drop of 4M NaOH to deprotonate the phenol. The *p*-nitrophenolate ion has a strong absorbance at 405 nm and has a known extinction coefficient of 18.4 $mM^{-1}cm^{-1}$.[51] We could therefore calculate the concentration of PNP in the well using Beer's Law. We pipetted 250 µL into each well on a 96-well plate and then took samples from random wells over a three-day period to determine if there was solvent evaporation. The plate was covered with the standard plastic fitted lid, and then sealed with parafilm around the edges. Unfortunately, we found that the concentration of PNP increased over the three-day period, indicating that each time we preformed this assay we would need to pipette a fresh plate.

	Concentration in well (mM)		
Well	Day 1	Day 2	Day 3
A1	3.2	3.8	4.7
A12	3.2	4.0	5.0
B9	3.2	4.1	4.4
C2	3.2	3.8	5.0
D5	3.2	3.6	3.6
E8	3.2	3.6	4.0
F10	3.2	3.8	3.9
G4	3.2	3.9	4.2
H1	3.2	3.8	4.3
H12	3.2	3.7	5.0

Table 3.1. Results from our stability test of PNP in PBS. Over a 3-day period, the absorbance in certain wells (randomly selected) was measured at 405 nm and then the concentration of PNP in the well was determined from Beer's Law. Grey wells indicate the edges of the 96-well plate.

3.2.2 Synthesis of iodophenylalanine

Because the goal of these assays was to test our catalysts on their performance in biologically relevant conditions, I opted to use a biologically relevant aryl iodide as a substrate in these prototype assays. Following a literature procedure [52] that had been optimized an

undergraduate researcher in the Williams Group (Rei Chee), we were able to synthesize *p*-iodophenylalanine in decent quantities (33% yield).

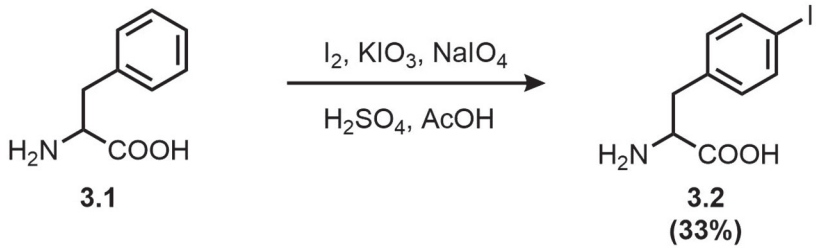

Figure 3.2. Synthesis of p-*iodophenylalanine.*

3.2.3 Solubility testing of boronic acid library and aryl iodide coupling partners

Next, I wanted to determine a solvent that we could run our prototype assays in. The Williams lab had already obtained a wide variety of different boronic acids to use as our library. Taking a spatula tip amount of compound, 0.5 mL solvent and mixing in a test tube I determined the solubility of a variety of coupling agents, as shown in Table 2.

Compound	1:1 EtOH/PBS + 1% DMSO	EtOH + 1% DMSO	PBS + 1% DMSO	DMF	1:1 EtOH:water	Pure water
L-iodophenylalanine (**3.2**)	X	X	X	X	X	X
3-iodoindole (**2.3**)						
3-ethynylphenylboronic acid (**3e**)			X			X
indole-6-boronic acid (**3f**)	PS		X			X
2-fluoropyridine-5-boronic acid (**3g**)	X		PS			X
pyridine-2-boronic acid (**3h**)	X	X		X	X	
pyrimidine-5-boronic acid (**3i**)	X		X	X		
3,5-dimethylisoxazole-4-boronic acid (**3j**)			PS			X
5-formylthiophene-2-boronic acid (**3k**)	PS		X		PS	X
isoquinoline-5-boronic acid (**3l**)	X		X	X	X	X
1-(TIPS)-1*H*-pyrrole-3-boronic acid (**3m**)	X		X		PS	X
3,4,5-trifluorophenylboronic acid (**3n**)			X			X
3-(methoxycarbonyl)-5-nitrophenylboronic acid (**3o**)	X		X		X	PS

Table 3.2. Results from solubility testing of boronic acid library with various protic and aqueous solvents. (Legend: Red = Not soluble, Grey = Not tested, Yellow = Partially soluble, Blue = Soluble)

From these results we also determined that L-iodophenylalanine would not be an ideal screening partner. Therefore, due to our previous success with compound **2.3** (3-iodoindole from previous chapter) we decided to keep going forward with indole **2.3** instead of compound **3.2**.

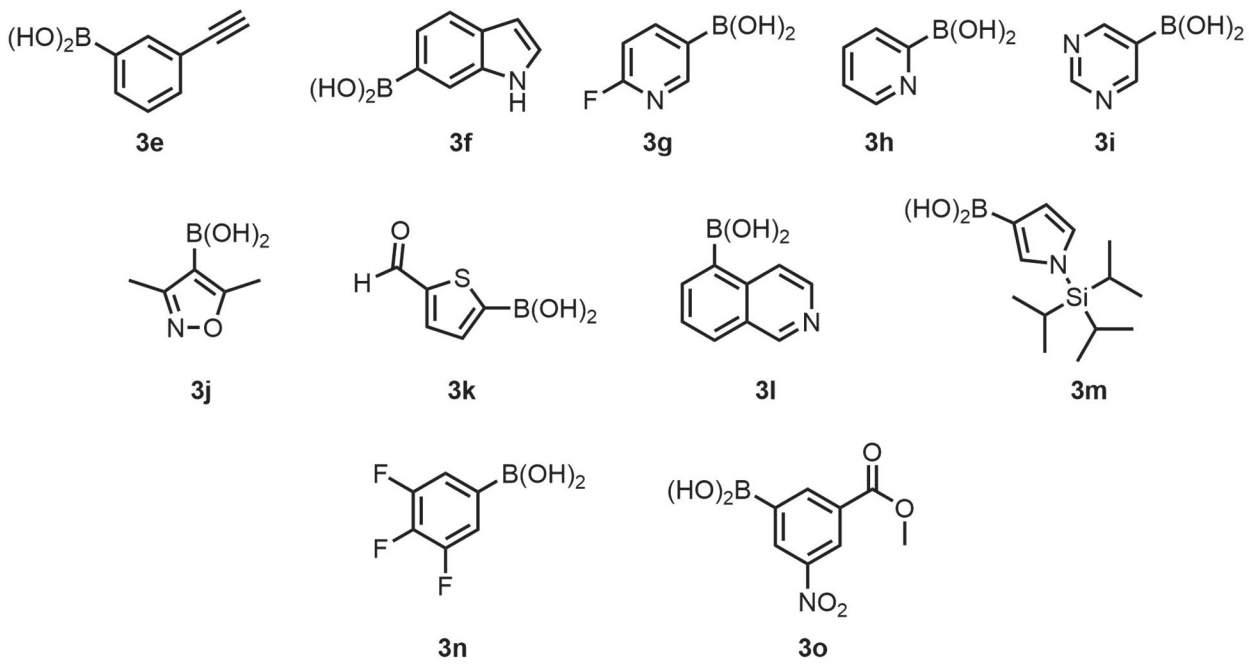

Figure 3.3. Boronic Acid library used from solubility testing and for prototype Suzuki-Miyaura catalyst screening assays.

3.2.4 Prototype Suzuki-Miyaura Assays – Analysis by HPLC

I based concentrations used in our assay on related Suzuki-Miyaura reactions that were successful in our lab. This worked out to approximate final concentrations of 0.03 mM for the aryl iodide (**2.3**), 0.02 mM of the boronic acid, 0.02 mM base (sodium bicarbonate), 0.001 mM catalyst (either $Pd(dppf)Cl_2$ or one of our in-house catalysts, and 0.03 mM tetrabutylammonium fluoride (TBAF). I included TBAF due to one of the Pd-complexes having a -TBDMS group protecting a primary alcohol. All these components were made up as stock solutions and then diluted down and mixed in the wells of a 96-well plate in a total volume of 200 µL.

Our first trial followed the following plate layout (Figure 3.4). Even with testing solubility, I found there to be continued solubility issues (leading to heterogenous reactions within the reaction well) with compounds **3h**, **3l** and **3m** so they were not included in the assay. The first row containing the required components for a Suzuki-Miyaura reaction (an aryl iodide, an aryl boronic acid and base) without catalyst as a control to determine retention times on the HPLC for all

starting materials. The following rows were then different variants of the reaction – either with the gold-standard catalyst ($Pd(dppf)Cl_2$) or catalyst **2a** and then with or without TBAF.

Samples were prepared by mixing the appropriate amount of the stock solutions and diluting into ethanol + 1% DMSO to achieve the concentrations and reaction volumes indicated above. The plate was then sealed with a plate sticker (ThermoFisher Scientific) and put on an orbital shaker (Bellydancer from the Macauley Lab) to gyrate overnight at room temperature. After ~18 hours, the samples were prepared for HPLC by first adding 1.4 mL 1:1 $MeCN:H_2O$ to an Eppendorf tube, then using a cut P200 tip (in case there were particulates, or a non-homogenous sample) 100 µL sample from the reaction well was added to the prepared Eppendorf tube. The entire 1.5 mL was filtered through a makeshift syringe filter (a small wad of cotton put inside the barrel of a 3 mL syringe) into an HPLC vial. The samples were then run on the HPLC using the following conditions: injection volume of 10 µL, flow rate of 0.200 mL/min, runtime of 20 minutes, gradient elution from 100% water to 100% acetonitrile in the first 10 minutes, a hold for 5 minutes at 100% acetonitrile, then a flush back to 100% water over 1 minute and a final hold at 100% water for 4 minutes. Peaks were measured by UV detection at 254 nm and their elution time was recorded. Peaks that were different from the standards where no catalyst added were noted (see Supplemental Data). Following this assay, we felt that Suzuki-Miyaura reactions with boronic acids **3k, 3n,** and **3o** warranted further exploration.

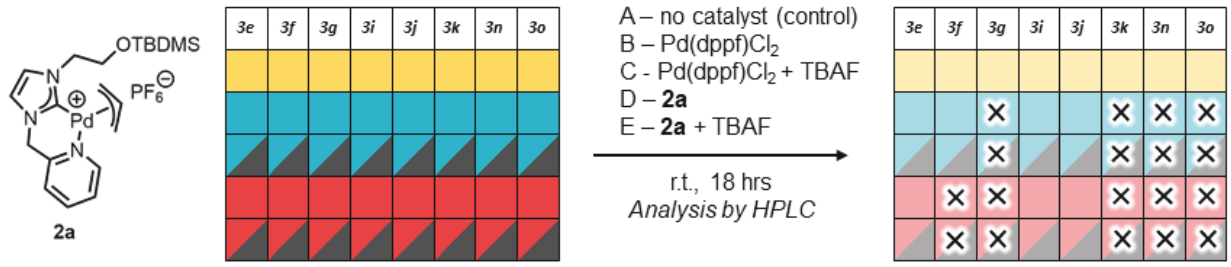

Figure 3.4. Design of prototype Suzuki-Miyaura assay used to test Williams Group catalyst ***2a*** *on a variety of boronic acids (top row of the grid). Every well on the assay grid contained aryl iodide* ***2.3****, boronic acid (noted by the column header) and* $NaHCO_3$ *(base). Conditions used in each row of the assay grid were as follows: Row A (yellow) – control, no catalyst or additives; Row B (blue) –* $Pd(dppf)Cl_2$ *added; Row C (blue/grey split) –* $Pd(dppf)Cl_2$ *and TBAF added; Row D (red) – Williams Group Pd complex* ***2a*** *added; Row E (red/grey split) – Williams Group Pd complex* ***2a*** *+ TBAF added. Components of the reactions were added to the assay grid in sequence of 1) aryl iodide, 2) boronic acid, 3) base, 4) TBAF and 5) catalyst/complex. Plates were sealed with plate seal tape and allowed to shake on an orbital shaker for 18 hours at room temperature. Afterwards, samples from each well were diluted and filtered and then analyzed by HPLC. Wells with a reaction of interest are noted with an "X" in the product grid.*

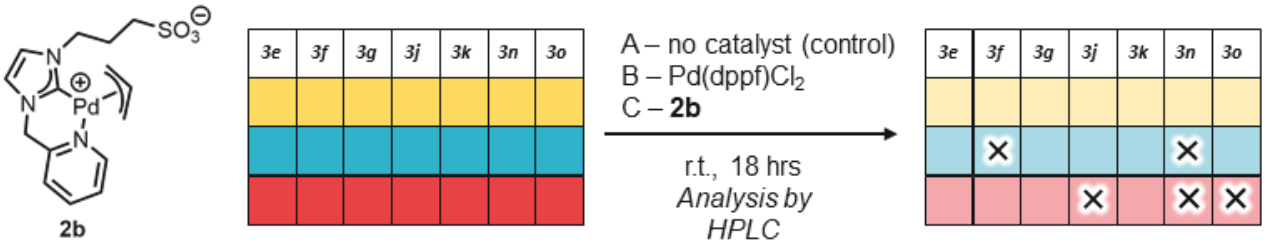

Figure 3.5. Design of prototype Suzuki-Miyaura assay used to test Williams Group catalyst ***2b*** *on a variety of boronic acids (top row of the grid). Every well on the assay grid contained aryl iodide* ***2.3****, boronic acid (noted by the column header) and* $NaHCO_3$ *(base). Conditions used in each row of the assay grid were as follows: Row A (yellow) – control, no catalyst, or additives; Row B (blue) –* $Pd(dppf)Cl_2$ *added; Row C (blue/grey split) – Pd complex* ***2b*** *added; Components of the reactions were added to the assay grid in sequence of 1) aryl iodide, 2) boronic acid, 3) base, and 4) catalyst/complex. Plates were sealed with plate seal tape and allowed to shake on an orbital shaker for 18 hours at room temperature. Afterwards, samples from each well were diluted and filtered and then analyzed by HPLC. Wells with a reaction of interest are noted with an "X" in the product grid.*

Excited that our initial assay showed some promising follow-up reactions, we repeated this assay format with complex **2b**. Since this complex did not have a protected group, TBAF was not needed or included in this assay. (Figure 3.5)

3.3 Synthesis towards a π-extended coumarin probe

While our assays did result in some promising leads, the assays were time consuming (17+ hours per assay on the HPLC) and we believed that adapting our assay for HTS would be more efficient. However, for a HTS screen, we would need a fluorescent probe. We felt inspired, therefore, to pursue a fluorescent probe after viewing a recently published paper in *J. Org. Chem*. Using a synthesis from Taisor et al. [50], these authors have developed a coumarin probe that had significantly shifted wavelengths when coupled to small aromatic molecules via palladium-coupling. We therefore decided to follow their procedure to make their reported π-extended coumarin Suzuki-Miyaura coupling partner.

Starting from 1-acetylnaphthalene (**3p**), an enolate reaction was performed with diethylcarbonate (**3q**) to add an ethylcarbonate group to the existing ketone. This reaction was performed in excellent yields (quant.) and the product (**3.3**) was carried forward without further purification. Next, a Pechmann condensation was performed on **3.3** with resorcinol (**3r**) to form the coumarin ring. A 32% yield was obtained in synthesizing product **3.4**, which was a higher yield than reported in the literature. Compound **3.4** was able to be purified via recrystallization from ethanol in lieu of column chromatography. We stored compound **3.4** under desiccant conditions due to the difficulty of the next step.

To fuse the rings and extend the aromatic system of **3.4**, a Scholl reaction was performed. Scholl reactions are tricky due to their expected low yields and sensitivities to moisture in the air. We therefore opted to spend some time trying several alternative strategies in addition to the Scholl reaction conditions reported. The following table summarizes our attempts to synthesize product **3.5** (Table **3**).

Entry	Scale	Conditions	Result
1	0.080 mmol	DDQ 0 °C / 2 hours DCM/$MeSO_3H$ (9:1)	No reaction
2	0.080 mmol	DDQ Reflux / Overnight DCM/$MeSO_3H$ (9:1)	No reaction
3	0.170 mmol	$FeCl_3$ 0 °C / 1 hour DCM:$MeNO_2$ (9:1)	No reaction
4	0.170 mmol	$FeCl_3$ Reflux / Overnight DCM:$MeNO_2$ (9:1)	No reaction
5	0.350 mmol	$AlCl_3$/NaCl [melt] 140 °C / 4 hours	Crude product present Could not purify
6	0.700 mmol	$AlCl_3$/NaCl [melt] 140 °C / 4 hours	Crude product present Could not purify
7	0.080 mmol	$AlCl_3$/NaCl Reflux / Overnight $CHCl_3$	No reaction
8	0.350 mmol	$AlCl_3$/NaCl [melt] 140 °C / 4 hours	Purified by column chromatography 51% yield

*Table 3.3. Different methods of Scholl reactions attempted to synthesize compound **3.5**, using different Lewis Acids or oxidation agents to close the central aromatic ring.*

After performing the Scholl reaction several times to synthesize compound **3.5**, we found that the original conditions of the paper were necessary, however the purification conditions (the

literature used a technique called dry column vacuum chromatography (DCVC)) proved problematic. When we attempted to use this DCVC technique we could not successfully purify **3.5**. However, traditional column chromatography provided 51% yield of the desired product.

Lastly, we attempted bromination of **3.5** to synthesize the Suzuki-Miyaura coupling partner, again following the literature procedure from Xue *et al*. [49] Upon treatment with *N*-bromosuccinimide and benzoyl peroxide, as per the reported reaction conditions, the expected product (**3s**) was not observed by ^{1}H NMR. Due to time constraints this project concluded at this point.

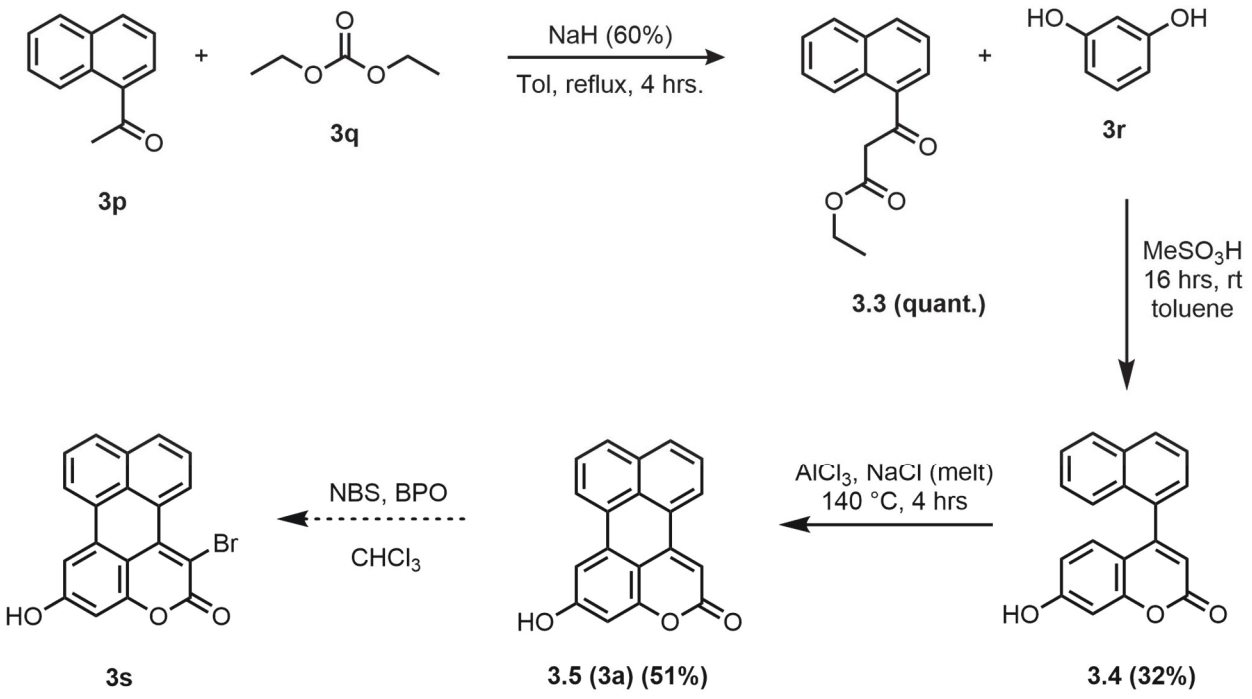

*Figure 3.6. Synthetic steps needed to make probe **3s**.*

3.3.2 Future work

Due to time constraints arising from the COVID-19 pandemic, I could not complete the initial goals of this project. Instead, I would like to present what future work I planned for this project if I had been able to finish.

I only attempted one trial synthesis of **3s**, and similarly to the previous Scholl reaction, it seemed as though this compound was also very sensitive to moisture or impurities in the reagents. In this reaction attempt, I recrystallized the NBS and distilled the chloroform – however I did not use the chloroform immediately after distillation. After letting the reaction stir overnight at room temperature, I came to find an insoluble purple precipitate (instead of a yellow solution) the next morning. In repeating this reaction, I would use freshly distilled chloroform immediately to ensure that there were no impurities or moisture in the reaction.

Following the synthesis of **3s**, still following the literature, I was going to attempt the syntheses of compound **3d** as it reportedly showed fluorescence emissions in the yellow-orange range. These syntheses report using $Pd(PPh_3)_2Cl_2$ as their palladium catalyst. I had also planned to try these syntheses with $Pd(dppf)Cl_2$ and the Williams Group catalysts **2a** and **2b**. I would then follow up with full UV-Vis and fluorescence characterization. The literature (as well as my own observations) is consistent in showing that these π-extended coumarins also exhibit solvatochromism, therefore gaining a full understanding of these compound's UV-Vis and fluorescence properties would be important in determining which excitation and emission wavelengths we could use for reporting and tracking in our Suzuki-Miyaura HTS assay.

Upon concluding that this substrate had sufficient optical properties to facilitate HTS, we would pursue the design of an HTS screen at the HTS facility at University of Iowa. Subsequent "hits" would be followed up with repeated large-scale reactions that would allow for an evaluation of the activity of all new Williams lab palladium complexes. This information would then be used to address current limitations in Suzuki-Miyaura couplings and to design 2nd generation palladium complexes with improved activity.

Of note, while completing this work and preparation of this manuscript, Costa *et al.* [53] reported a HTS for palladium coupling in water/ethanol. This system could also be applied towards the evaluation of Williams lab palladium complexes.

Experimental

General

Reactions were carried out in oven-dried (> 130 °C) or flame-dried glassware under a positive nitrogen atmosphere, unless otherwise stated. Transfer of anhydrous reagents was accomplished with oven-dried syringes or cannulae. Tetrahydrofuran (THF), dichloromethane (DCM), and toluene (PhMe) were dispensed from a solvent system, which dried solvents by passing them through a column of activated molecular sieves (4Å). Any water, or aqueous solutions used in-house generated reverse osmosis water, unless otherwise stated. Thin layer chromatography was performed on glass plates pre-coated with 0.25 mm silica gel with a fluorescent indicator UV254 (EMD Millipore). Flash chromatography columns were packed with 230-400 mesh silica gel (Silacycle). All reagents were purchased from the following commercial suppliers: Millipore-Sigma (Sigma Aldrich), AK Scientific, Acros Organics, Oakwood Chemicals, or Fisher Scientific/VWR, at a purity greater than 95%, and without further purification unless otherwise specifically noted. Proton nuclear magnetic resonance spectra (^{1}H NMR) were recorded at 300, 400 or 500 MHz, and coupling constants (*J*) are reported in Hertz (Hz). Carbon nuclear magnetic resonance spectra (^{13}C NMR) were recorded at 125 MHz. The chemical shifts were reported on the δ scale (ppm) and referenced to the residual protonated (^{1}H) solvent or to the deuterated solvent (^{13}C) peaks: DMSO-d_6 (2.50 ppm, ^{1}H), MeOD-d_4 (3.31 ppm, ^{1}H), $CDCl_3$ (7.26 ppm, ^{1}H; 77.06 ppm, ^{13}C). s = singlet, bs = broad singlet, d = doublet, t = triplet, q = quartet, dd = doublet of doublets, m = multiplet. For chromatography conditions, EtOAc = ethyl acetate, and Hex = hexanes.

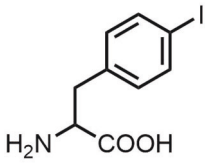

Compound 3.2

To a 300 mL RBF, 8.0 g L-phenylalanine (48.4 mmol, 1.0 eq) and 4.9 g elemental iodine (19.3 mmol, 0.4 eq) were added. Both solids were suspended in 50 mL glacial acetic acid. Next, 2.3 g potassium iodate (10.7 mmol, 0.2 eq) and 6 mL sulphuric acid (conc.) were added to the suspension. The reaction vessel was heated to 80 °C and then held at this temperature to stir for 30 minutes. The reaction was removed from the heat and allowed to cool. Next, 0.5 g sodium periodate was added to the flask. The flask was returned to 80 °C and left to stir until the solution turned light orange. The flask was then removed from the heating bath and left to cool overnight while maintaining stirring. The next morning, the acetic acid was removed by rotovap. The remaining orange residue was dissolved in 100 mL water and transferred to a 500 mL separatory funnel. The aqueous layer was extracted with 1 x 100 mL Et_2O and 1 x 100 mL DCM before collecting the aqueous layer again. The aqueous layer was then stirred with 4 scoops (scoopula) of activated charcoal for approximately 1 hour. The charcoal was then filtered off and the filtrate was neutralized with 4M KOH (aq.) until a pH of 7 was acquired. During the neutralization process a large amount of white solid precipitated out of solution which resulted in a very thick suspension therefore an extra 150 mL of water was added. The white precipitate (crude) was filtered by vacuum filtration, washing first with cold dH_2O (2 x 50 mL) and then once with a minimum amount of absolute ethanol. The crude was then recrystallized by adding the material to a 500 mL beaker and dissolving in 150 mL hot acetic acid. While hot, the solution was gravity filtered and allowed to cool overnight to allow for slow crystallization. The white crystals were filtered from the mother liquor to yield the product in a 33% yield (4.67 g). ^{1}H NMR (500 MHz, DMSO-*d*$_6$): δ 7.62 (d, *J* = 8.2 Hz, 2H), 7.07 (d, *J* = 8.2 Hz, 2H), 4.02 (bs, 2H), 3.06 (dd, *J* = 14.3 Hz, *J* = 6.3 Hz, 1H), 2.81 (dd, *J* = 14.3 Hz, *J* = 7.9 Hz, 1H). Compound matches literature spectrum.[52]

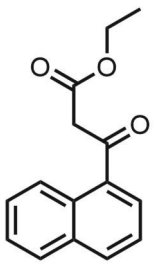

Compound 3.3

To a 2-neck 100 mL RBF was added 1.19 g NaH (60% dispersion in paraffin wax; 29.75 mmol, 2.1 eq) to the flask via the side arm. Washed the NaH 4 x 10 mL with toluene, removing each

aliquot of toluene via cannula filtration. 4 mL toluene and 3.32 g diethylcarbonate (28.0 mmol, 2.0 eq) were added to the RBF. After all the material was added, began heating the reaction to reflux. Once at reflux, 2.38 g 1-acetylnaphthalene (14.0 mmol, 1.0 eq) was dissolved in 5 mL toluene and added slowly to the reaction in the 2-neck flask. The solution turned dark yellow/orange. The reaction was left to reflux overnight. The next day, the reaction was removed from the heat bath and cooled. The reaction has turned very dark orange. This solution was poured over ~100 mL of ice and the pH was checked (pH 10). Using acetic acid, the solution was acidified until it had reached a pH of 6. A white precipitate appeared briefly during this acidification but went away while stirring. 20 mL EtOAc was added. The organic layer was then washed with brine (3 x 10 mL) and dried over Na_2SO_4. The remaining solvent was removed in vacuo and the remaining viscous yellow oil was placed under high vacuum until it was carried forward. The product was collected as a mixture of the enol and keto forms and used without further purification (2.84 g, quant.). ^{1}H NMR (300 MHz, $CDCl_3$): δ 12.74 (s, 1H, minor), 8.76 (d, J = 8.5 Hz, 1H), 8.36 (d, J = 7.5 Hz, 1H, minor), 8.03 (d, J = 8.2 Hz, 1H), 7.93-7.87 (m, 3H), 7.66-7.16 (m, 7H), 5.50 (s, 1H, minor), 4.31 (q, J = 7.1 Hz, 2H, minor), 4.19 (q, J = 7.1 Hz, 2H), 4.11 (s, 2H), 1.36 (t, J = 7.1 Hz, 1H, minor), 1.22 (t, J = 7.1 Hz, 3H). The ^{1}H NMR matched literature values.[49]

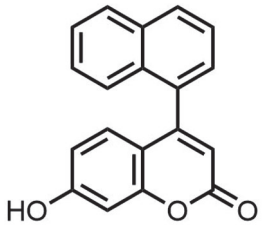

Compound 3.4

To a 50 mL RBF 1.29 g resorcinol was added (11.75 mmol, 1.0 eq), along with 2.84 g of compound **3.3** (11.75 mmol, 1.0 eq) and 15 mL toluene. 3.5 mL $MeSO_3H$ (5.19 g, 54.05 mmol, 4.6 eq) was added dropwise to the suspension (resorcinol did not immediately dissolve). A colour change occurred from orange to dark red. The suspension was stirred at high speed (>800 rpm) overnight at ambient temperature. The next day the suspension had become a viscous dark orange oil suspended in toluene. This oil/toluene mixture was poured into 200 mL H_2O, with a further 200 mL EtOAc added to partition. Using a separatory funnel (recommended to use a large funnel due

to large amounts of solvent needed) the organic and aqueous layers were separated, then the aqueous layer was further extracted with EtOAc (3 x 200 mL). The organic layers were combined and washed with brine (5 x 100 mL). Upon addition of brine to the organic layer the solution turned deep red/pink. The organic layer was separated and dried over Na_2SO_4, and the solvents were removed *in vacuo*. Recrystallization from 100% ethanol yielded the product as a pink-red powder in a 32% yield (1.085 g). ^{1}H NMR (300 MHz, $CDCl_3$): δ 10.62 (s, 1H), 8.07 (dd, J = 14.0 Hz, J = 8.2 Hz, 2H), 7.68-7.44 (m, 5H), 6.83 (d, J = 2.0 Hz, 1H), 6.64 (qd, J = 5.3 Hz, 2H), 6.26 (s, 1H). ^{1}H NMR matched literature values.[49]

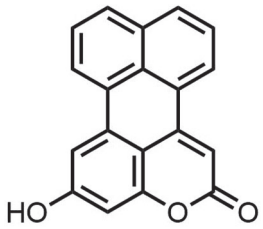

Compound 3.5

To an oven-dried 3-neck flask was added 100 mg **3.4** (0.346 mmol, 1.0 eq), 1.19 g $AlCl_3$ (8.996 mmol, 26.0 eq), and 227 mg NaCl (3.88 mmol, 11.2 eq). N_2 gas was bubbled through the solution using a long 18-gauge needle for 10 minutes. The reaction was heated to 140 °C and the speed was slowly increased. The reaction was allowed to stir for 4 hours at 140 °C. The reaction was then removed from heat and allowed to cool slightly before adding 50 mL of 1:1 EtOAc:H_2O. The reaction was sonicated to solubilize solids in the reaction mixture, then vacuum filtered to remove any remaining black particulates. The organic layer was separated, and the aqueous layer was extracted with EtOAc (3 x 20 mL). All organic layers were combined and washed with brine (3 x 10 mL), then dried over Na_2SO_4. Solvents were removed by rotovap, yielding 88 mg of a yellow powder. Compound **3.5** was purified by column chromatography using a gradient from 15:1 DCM/EtOAc to 5:1 DCM/EtOAc and collected in fractions 71 – 124. Purified yield was 51 mg (51%) as an off-white solid. This compound exhibited strong fluorescence in DMSO-*d*$_6$, therefore it was stored in a vial covered with foil to protect from ambient light. R_f = 0.7 in 2:1 DCM:EtOAc – blue-green spot at 365 nm illumination. ^{1}H NMR (500 MHz, DMSO-*d*$_6$): 10.68 (s, 1H), 8.68 (d, J = 6.6 Hz, 1H), 8.40 (d, J = 7.1 Hz, 1H), 8.20 (d, J = 7.9 Hz, 1H), 8.05 (d, J = 7.9 Hz, 1H), 7.71

(m, J = 7.6 Hz, 2H), 7.65 (d, J = 2.1 Hz, 1H), 7.07 (s, 1H), 6.77 (d, J = 2.1 Hz, 1H). ^{1}H NMR did *not* match literature values.[49]

Supplemental Research (A): Enzymatic digestion studies of BBr_3/BCl_3 treated lignocellulose

Author's note: After submission and defense of this thesis, it was determined through further investigations by the Williams Group that the BBr_3/BCl_3 treated lignocellulose samples did not contain any glucose (as determined by mass spectrometry) after reacting with CTec2 cellulase.

A.1 Introduction

Another area of research occurring in the Williams Lab involves using boron trihalides to cleave asymmetric ethers.[55] We recently applied this reaction to the digestion of one of nature's most abundant polymers: lignocellulose.[55] Recent investigations have focused on understanding how the BBr_3/BCl_3 is degrading the lignocellulose and have included a desire to determine the rate of cellulose digestion by cellulase compared to the digestion of commercially available cellulose blends. Our first objective was to determine if the residual boric acid from the BBr_3/BCl_3 treatment had any effect on the digestion of our collected lignocellulose. Our second objective was to compare the rate of enzymatic digestion of our collected lignocellulose to that of commercial grade cellulose using the commercial enzyme blend CTec2.

A.2 Results and Discussion

A.2.1 Determining enzyme activity of commercial cellulase blend

Since the cellulase enzyme, CTec2, we purchased commercially was a mixture of enzymes (cellulases, hemicellulases) I had to determine the enzyme activity (Units of activity/mL, or U/mL) myself. Using a procedure from Millipore-Sigma, we determined that the enzyme activity of our blend was approximately 32 U/mL (see Experimental for details). We then used this information to test a commercial Glucose HK assay kit, which measures enzyme activity by assessing the increase in NADH over time. In this assay, which uses hexokinase and glucose-6-phosphate dehydrogenase enzymes, the production of NADH is directly proportional to the amount of glucose being released from cellulose over time. The following table (Table A.1) shows our absorbance readings and the calculated enzyme activity.

Time	A_{340nm} (Blank)	A_{340nm} (Test)
0 min	0.000	0.254
1 min	0.002	0.774
2 mins	0.000	1.106
3 mins	0.000	1.405
4 mins	0.001	1.629
5 mins	0.003	1.792
	0.003	1.538
Cellulase Activity (U/mL)	-	32

Table A.1 Absorbance readings for determining enzyme activity of commercial CTec2 using a Glucose-HK assay kit. The absorbance of the samples was taken every minute for five minutes at 340 nm. The change in absorbance at 340 nm was used to further calculated the units of activity per mL.

Time	A_{340nm} (No $B(OH)_3$)	A_{340nm} (with $B(OH)_3$)
0 min	0.095	0.088
1 min	0.130	0.094
2 min	0.152	0.098
3 min	0.175	0.102
4 min	0.205	0.104
5 min	0.233	0.125
ΔA_{340nm} (finial – initial)	0.138	0.037
Cellulase Activity U/mL	2.8	0.71

Table A.2 Absorbance readings for determining enzyme activity of commercial CTec2 using a Glucose-HK assay kit to determine the effects of boric acid on cellulase digestion. The absorbance of the samples was taken every minute for five minutes at 340 nm. The change in absorbance at 340 nm was used to further calculated the units of activity per mL.

A.2.2 Determining the effects of boric acid on the enzyme activity of CTec2

Next, since our process of ether cleavage produces a significant amount of boric acid by-product, we wanted to determine the effect that boric acid would have on cellulose digestion. This would inform our analysis of the digestion of the cellulosic material obtained from the boric acid reaction and would suggest whether boric acid would need to be removed for efficient digestion to monomeric sugars.

Following the procedure used to determine enzyme activity, we repeated the assay adding an additional sample that had been artificially doped with boric acid. Through previous work, we had determined that our boric acid contamination was equal to about 3x the mass of cellulose, therefore we used this calculation for our artificial doping. The results were recorded in Table A.2

From this data, we inferred that boric acid does indeed inhibit the enzyme activity, with a rate decrease of 25% compared to cellulose alone, although we remain unsure by which exact mechanism this occurs. It remains unclear if the boric acid has a direct effect on the cellulase enzyme, perturbs recognition of the cellulose at the catalytic site, or if it interferes with the multicomponent nature of the Glucose-HK assay used for this determination.

A.2.3 Determining conversion rates of BBr_3/BCl_3 treated lignin polymer digested by cellulase compared to Sigmacell cellulose digested by cellulase

When looking to determine the rate of conversion of lignocellulose to glucose by cellulase digestion (and comparison to standardized commercial cellulose), we decided to change our method of analysis for two reasons. The first was that the Glucose HK assay was not very sensitive – requiring several milligram quantities per sample for detection. Since our treated lignocellulose had to be purified by dialysis to remove excess boric acid, this did not leave us with much recovered material. The second reason was discovered when comparing our method to that of Shuai *et al*.'s work.[56] In their digestion studies, they added tetracycline to their reaction as they were digesting their cellulose over a long period of time, which results in a sugary and warm solution that is suitable for microbial growth. When we tested the Glucose HK assay with tetracycline, we found that it also has strong absorbance at 405 nm, making the absorption of the solutions at 340 nm artificially higher and out of the range of the assay, even when subtracting out

the tetracycline absorbance. However, the Glucose GO Assay alternative (GO indicating the assay glucose oxidase enzyme mediated), is a colourimetric assay that would also be complicated by the yellow-colored tetracycline additive. Therefore, the following experiment did not end up using tetracycline as we were hopeful that the lignocellulose could be quickly digested over an hour or two instead of days.

We transitioned to the GO assay because the detection range is more sensitive (micrograms as opposed to milligrams), which was more suited to the quantities of cellulose we would be evaluating. The action of glucose oxidase consumes glucose and produces hydrogen peroxide as a byproduct. Hydrogen peroxide subsequently reacts with *o*-dianisidine (oxidation), producing a colored compound which absorbs at 540 nm. The amount of glucose produced is therefore directly proportional to the absorbance of oxidized *o*-dianisidine and can be back-calculated by standard curve. Briefly (full procedure in Experimental), we reacted our BBr_3/BCl_3 treated lignocellulose with cellulase as well as Sigmacell nanocellulose with cellulase at 50 °C in distilled water. At regular time intervals I would remove an aliquot of the reaction, and begin the GO assay on these aliquots at 37 °C. After 30 minutes of development, the reaction is quenched with sulfuric acid, and then the absorbance is read at 540 nm. Concurrently, I also made a standard curve using a standardized glucose solution so that the mass of glucose in the reaction could be determined. From that we calculated approximately how much of the total mass has been digested to release free glucose.

We determined from this assay that our BBr_3/BCl_3 treated lignocellulose has undergone some sort of transformation that makes it much harder for the cellulase to digest. Follow-up investigations are currently underway in the Williams Lab.

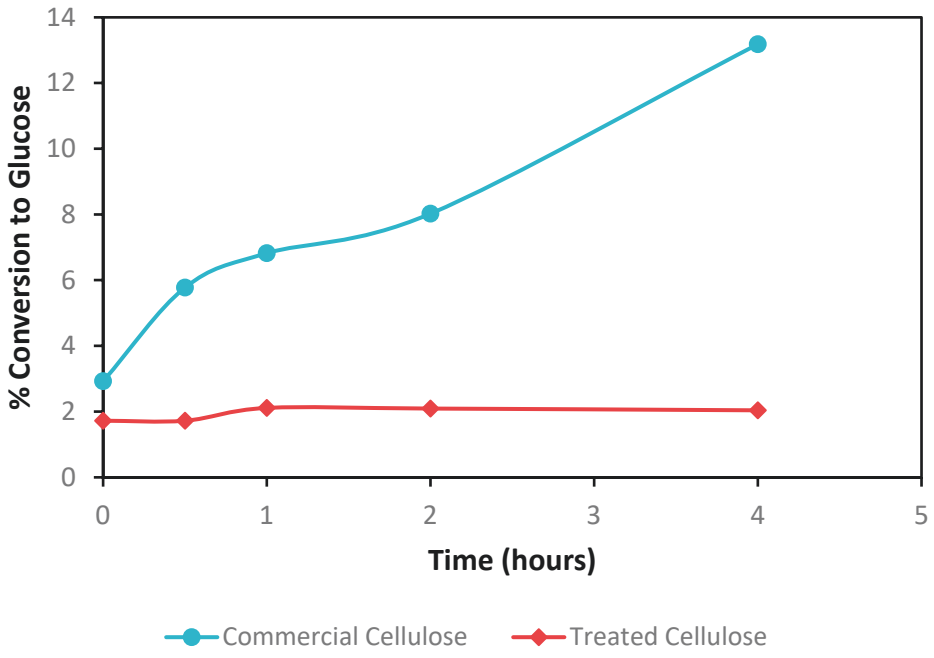

Figure A.1. Comparison of cellulose digestion between standardized commercial Nanocellulose (orange), and BBr3/BCl3 treated lignocellulose (blue).

Experimental

General

Any water or aqueous solutions were made up using in-house generated reverse osmosis water, or NanoPure water generated by a MiliQ water system. Solution pH was checked using an Accumet Basic AB 15 pH meter. Micropipettors and pipette tips used were either Rainin, Gilson, Eppendorf or VWR brands. Test tubes were either plastic Corning™ Falcon tubes (15 or 50 mL), or VWR glass disposable tubes (13 x 10 mm). Cuvettes were disposable plastic cuvettes from Fisher Scientific. All reagents were purchased from Millipore-Sigma (Sigma Aldrich) and used without further purification. Shaking incubators were from New Brunswick Scientific, the water bath incubator was an Isotemp (Fisher Scientific), and absorbance readings were measured on a Beckman Coulter DU 720 General Purpose UV/Vis Spectrophotometer.

i) Determining cellulase enzyme activity

In advance (day before the assay, stored at room temperature on the benchtop), 100 mL 5%(w/v) Sigmacell Cellulose solution in 50mM sodium acetate, pH 5 buffer was prepared. 4 mL Sigmacell solution was added to two separate 15mL Falcon tubes (Blank and Test). The tubes were equilibrated in a 37 °C water bath for 30 minutes. Glucose HK Assay reagent was prepared as per kit instructions. Immediately before use, a solution of cellulase was prepared by removing 40 µL from stock bottle and diluting it into 10 mL cold H_2O. To the Blank tube 1 mL H_2O was added and to the Test tube 1 mL diluted cellulase was added. A stir bar was also added to each tube. These tubes were incubated at 37 °C with stirring for 2 hours. After, both tubes were transferred to an ice bath and allowed to stand until the suspensions had settled. The tubes were centrifuged at 4000 rpm for 2 minutes, then returned to ice bath. To two cuvettes added 3 mL Glucose HK reagent, that had been warmed to room temperature. Testing the Blank first, added 0.1 mL supernatant from Blank tube to the cuvette. Mixed by pipetting up and down, then recorded the absorbance at 340 nm for 5 minutes. To the Test cuvette, added 0.1 mL supernatant from the Test tube. Mixed by pipetting up and down, then recorded the absorbance at 340 nm for 5 minutes. Enzyme activity was then calculated as per the following formula:

$$\frac{(A_{340}[\text{test}] - A_{340}[\text{blank}])}{(V_f) * (V_i) * (DF)} \times \frac{250}{(MEC) * (2) * (1\ mL) * (0.1\ mL)} = \text{Units/mL}$$

V_f = final volume
V_i = initial volume
MEC = molar extinction coefficient
DF = dilution factor

ii) Determining inhibition of cellulase by boric acid

4 mL 5% (w/v) Sigmacell Cellulose was pipetted into three 15 mL Falcon tubes: “Blank”, “Test with $B(OH)_3$”, and “Test without $B(OH)_3$”. To “Test with $B(OH)_3$” 600 mg boric acid (15% (w/v) to cellulose) was added. The tubes were equilibrated in a 37 °C water bath for 30 minutes. Immediately before use, a solution of cellulase was prepared by removing 40 µL from stock bottle

and diluting it into 10 mL fridge-chilled H_2O. To "Blank" tube 1 mL H_2O was added and to "Test" tubes 1 mL diluted cellulase was added. A stir bar was added to each tube. The tubes were incubated in a 37 °C water bath with stirring for 2 hours. After, the tubes were transferred to an ice bath and allowed to stand until suspensions had settled. The tubes were centrifuged at 4000 rpm for 2 minutes, then returned to ice bath. To three cuvettes added 3 mL Glucose HK reagent, that had been warmed to room temperature. Testing the Blank first, 0.1 mL supernatant was transferred from "Blank" tube to the cuvette. The solution was mixed by pipetting up and down, then the absorbance as recorded at 340 nm for 5 minutes. To the Test(s) cuvette(s), 0.1 mL supernatant was transferred from the respective "Test" tube. These solutions were mixed by pipetting up and down, then the absorbance was recorded at 340 nm for 5 minutes. Enzyme activity was calculated using the formula above.

iii) Determining %conversion to glucose of BBr_3/BCl_3 treated lignin polymer digested by cellulase compared to Sigmacell cellulose digested by cellulase

Lyophilized BBr_3/BCl_3 treated lignin polymer that had been dialyzed was dissolved to make a 20 mg/mL solution in H_2O. 20 mg Sigmacell cellulose was suspended into 1 mL dH_2O. Cellulase was prepared by taking 40 µL stock cellulase and diluting it into 10 mL H_2O. Both samples and cellulase were equilibrated to 50 °C in a shaking incubator. Standards were prepared by adding appropriate amounts H_2O and 1 mg/mL glucose standard to 15 mL Falcon tubes. At time = 0, 250 µL warmed cellulase was added to the BBr_3/BCl_3 treated lignin polymer and Sigmacell cellulose (1 mL was used, total reaction volume = 1.25 mL). The tubes were vortexed immediately, then a 45 µL aliquot was removed and added to 955 µL dH_2O. To these tubes and the standards 2 mL Glucose GO Assay reagent was added. The tubes were vortexed, then developed in a 37 °C water bath for exactly 30 minutes. Development was quenched by adding 2 mL 6M H_2SO_4, then the tubes were vortexed again. An aliquot was transferred to a cuvette and the absorbance was read at 540 nm. Continued removing aliquots (aliquot volume may need to be adjusted to fall within range of standard curve) at time points to determine the amount of glucose being converted. The amount of glucose at each time point was then calculated by standard curve, and that calculation was then used to determine the % conversion based on the mass of polymer added (See Supplemental Research Appendix).

Works Cited

(1) Patterson, D. M.; Nazarova, L. A.; Prescher, J. A. Finding the Right (Bioorthogonal) Chemistry. *ACS Chem. Biol.* **2014**, *9*, 592–605.

(2) Van Berkel, S. S.; Van Eldijk, M. B.; Van Hest, J. C. M. Staudinger Ligation as a Method for Bioconjugation. *Angew. Chemie - Int. Ed.* **2011**, *50* (38), 8806–8827.

(3) Saxon, E.; Bertozzi, C. R. Cell Surface Engineering by a Modified Staudinger Reaction. *Science* **2000**, *287* (5460), 2007–2010.

(4) a) Saxon, E.; Armstrong, J. I.; Bertozzi, C. R. A "Traceless" Staudinger Ligation for the Chemoselective Synthesis of Amide Bonds. *Org. Lett.* **2000**, *2* (14), 2141–2143. b) Soellner, M. B.; Nilsson, B. L.; Raines, R. T. Reaction Mechanism and Kinetics of the Traceless Staudinger Ligation. *J. Am. Chem. Soc.* **2006**, *128* (27), 8820–8828. c) Soellner, M. B.; Nilsson, B. L.; Raines, R. T. Reaction Mechanism and Kinetics of the Traceless Staudinger Ligation. *J. Am. Chem. Soc.* **2006**, *128* (27), 8820–8828. d) Lin, F. L.; Hoyt, H. M.; Van Halbeek, H.; Bergman, R. G.; Bertozzi, C. R. Mechanistic Investigation of the Staudinger Ligation. *J. Am. Chem. Soc.* **2005**, *127* (8), 2686–2695.

(5) Tornøe, C. W.; Christensen, C.; Meldal, M. Peptidotriazoles on Solid Phase: [1,2,3]-Triazoles by Regiospecific Copper(I)-Catalyzed 1,3-Dipolar Cycloadditions of Terminal Alkynes to Azides. *J. Org. Chem.* **2002**, *67* (9), 3057–3064.

(6) Rostovtsev, V. V.; Green, L. G.; Fokin, V. V.; Sharpless, K. B. A Stepwise Huisgen Cycloaddition Process: Copper(I)-Catalyzed Regioselective "Ligation" of Azides and Terminal Alkynes. *Angew. Chemie - Int. Ed.* **2002**, *41* (14), 2596–2599.

(7) Breugst, M.; Reissig, H. U. The Huisgen Reaction: Milestones of the 1,3-Dipolar Cycloaddition. *Angew. Chemie - Int. Ed.* **2020**, *59* (30), 12293–12307.

(8) Speers, A. E.; Adam, G. C.; Cravatt, B. F. Activity-Based Protein Profiling in Vivo Using a Copper(I)-Catalyzed Azide-Alkyne [3 + 2] Cycloaddition. *J. Am. Chem. Soc.* **2003**, *125* (16), 4686–4687.

(9) Agard, N. J.; Prescher, J. A.; Bertozzi, C. R. A Strain-Promoted [3 + 2] Azide-Alkyne Cycloaddition for Covalent Modification of Biomolecules in Living Systems. *J. Am. Chem. Soc.* **2004**, *126* (46), 15046–15047.

(10) Devaraj, N. K.; Weissleder, R.; Hilderbrand, S. A. Tetrazine-Based Cycloadditions: Application to Pretargeted Live Cell Imaging. *Bioconjug. Chem.* **2008**, *19* (12), 2297–2299.

(11) Blackman, M. L.; Royzen, M.; Fox, J. M. Tetrazine Ligation: Fast Bioconjugation Based on Inverse-Electron-Demand Diels-Alder Reactivity. *J. Am. Chem. Soc.* **2008**, *130* (41), 13518–13519.

(12) Oliveira, B. L.; Guo, Z.; Bernardes, G. J. L. Inverse Electron Demand Diels-Alder Reactions in Chemical Biology. *Chem. Soc. Rev.* **2017**, *46* (16), 4895–4950.

(13) Boul, P. J.; Reutenauer, P.; Lehn, J. M. Reversible Diels-Alder Reactions for the Generation of Dynamic Combinatorial Libraries. *Org. Lett.* **2005**, *7* (1), 15–18.

(14) Fox, J. “Re: Tetrazine Ligation Inspiration”. Message to Krystyn Dubicki. 12 April 2021. E-mail communication.

(15) Huisgen, R. 1,3-Dipolar Cycloadditions. *Proc. Chem. Soc.* **1961**, 357–369.

(16) Stöckigt, J.; Antonchick, A. P.; Wu, F.; Waldmann, H. The Pictet-Spengler Reaction in Nature and in Organic Chemistry. *Angew. Chemie - Int. Ed.* **2011**, *50* (37), 8538–8564.

(17) Agarwal, P.; Van Der Weijden, J.; Sletten, E. M.; Rabuka, D.; Bertozzi, C. R. A Pictet-Spengler Ligation for Protein Chemical Modification. *Proc. Natl. Acad. Sci. U. S. A.* **2013**, *110* (1), 46–51.

(18) Gray, M. A.; Stanczak, M. A.; Mantuano, N. R.; Xiao, H.; Pijnenborg, J. F. A.; Malaker, S. A.; Miller, C. L.; Weidenbacher, P. A.; Tanzo, J. T.; Ahn, G.; Woods, E. C.; Läubli, H.; Bertozzi, C. R. Targeted Glycan Degradation Potentiates the Anticancer Immune Response in Vivo. *Nat. Chem. Biol.* **2020**, *16* (12), 1376–1384.

(19) Dehnert, K. W.; Baskin, J. M.; Laughlin, S. T.; Beahm, B. J.; Naidu, N. N.; Amacher, S. L.; Bertozzi, C. R. Imaging the Sialome during Zebrafish Development with Copper-Free Click Chemistry. *ChemBioChem* **2012**, *13* (3), 353–357.

(20) Fonovic, M.; Bogyo, M. Activity Based Probes as a Tool for Functional Proteomic Analysis of Proteases. *Expert Rev Proteomics* **2008**, *5* (5), 721–730.

(21) Williams, F. Personal communication. 25 April 2021.

(22) Willems, L. I.; Li, N.; Florea, B. I.; Ruben, M.; van der Marel, G. A.; Overkleeft, H. S. Triple Bioorthogonal Ligation Strategy for Simultaneous Labeling of Multiple Enzymatic Activities. *Angew. Chemie* **2012**, *124* (18), 4507–4510.

(23) Toste Rêgo, A.; da Fonseca, P. C. A. Characterization of Fully Recombinant Human 20S and 20S-PA200 Proteasome Complexes. *Mol. Cell* **2019**, *76* (1), 138-147.e5.

(24) Kurti, L.; Czako, B. Strategic Applications of Named Reactions in Organic Synthesis. 1st Edition. Academic Press, 2005. ISBN: 9780080575414

(25) Li, N.; Lim, R. K. V.; Edwardraja, S.; Lin, Q. Copper-Free Sonogashira Cross-Coupling for Functionalization of Alkyne-Encoded Proteins in Aqueous Medium and in Bacterial Cells. *J.*

Am. Chem. Soc. **2011**, *133* (39), 15316–15319.

(26) Yusop, R. M.; Unciti-Broceta, A.; Johansson, E. M. V.; Sánchez-Martín, R. M.; Bradley, M. Palladium-Mediated Intracellular Chemistry. *Nat. Chem.* **2011**, *3* (3), 239–243.

(27) Godoy, F.; Segarra, C.; Poyatos, M.; Peris, E. Palladium Catalysts with Sulfonate-Functionalized-NHC Ligands for Suzuki-Miyaura Cross-Coupling Reactions in Water. *Organometallics* **2011**, *30* (4), 684–688.

(28) Barder, T. E.; Walker, S. D.; Martinelli, J. R.; Buchwald, S. L. Catalysts for Suzuki-Miyaura Coupling Processes: Scope and Studies of the Effect of Ligand Structure. *J. Am. Chem. Soc.* **2005**, *127* (13), 4685–4696.

(29) Thomas, A. A.; Denmark, S. E. Pre-Transmetalation Intermediates in the Suzuki-Miyaura Reaction Revealed: The Missing Link. *Science (80).* **2016**, *352* (6283), 329 LP – 332.

(30) Ortuño, M. A.; Lledós, A.; Maseras, F.; Ujaque, G. The Transmetalation Process in Suzuki-Miyaura Reactions: Calculations Indicate Lower Barrier via Boronate Intermediate. *ChemCatChem* **2014**, *6* (11), 3132–3138.

(31) Lennox, A. J. J.; Lloyd-Jones, G. C. Transmetalation in the Suzuki-Miyaura Coupling: The Fork in the Trail. *Angew. Chemie - Int. Ed.* **2013**, *52* (29), 7362–7370.

(32) Miyaura, N.; Yamada, K.; Suginome, H.; Suzuki, A. Novel and Convenient Method for the Stereo-and Regiospecific Synthesis of Conjugated Alkadienes and Alkenynes via the Palladium-Catalyzed Cross-Coupling Reaction of 1-Alkenylboranes with Bromoalkenes and Bromoalkynes. *J. Am. Chem. Soc.* **1985**, *107* (4), 972–980.

(33) Carrow, B. P.; Hartwig, J. F. Distinguishing between Pathways for Transmetalation in Suzuki-Miyaura Reactions. *J. Am. Chem. Soc.* **2011**, *133* (7), 2116–2119.

(34) Amatore, C.; Jutand, A.; Le Duc, G. Kinetic Data for the Transmetalation/Reductive Elimination in Palladium-Catalyzed Suzuki–Miyaura Reactions: Unexpected Triple Role of Hydroxide Ions Used as Base. *Chem. – A Eur. J.* **2011**, *17* (8), 2492–2503.

(35) Schmidt, A. F.; Kurokhtina, A. A.; Larina, E. V. Role of a Base in Suzuki-Miyaura Reaction. *Russ. J. Gen. Chem.* **2011**, *81* (7), 1573.

(36) Matos, K.; Soderquist, J. A. Alkylboranes in the Suzuki−Miyaura Coupling: Stereochemical and Mechanistic Studies. *J. Org. Chem.* **1998**, *63* (3), 461–470.

(37) Braga, A. A. C.; Morgon, N. H.; Ujaque, G.; Lledós, A.; Maseras, F. Computational Study of the Transmetalation Process in the Suzuki-Miyaura Cross-Coupling of Aryls. *J. Organomet. Chem.* **2006**, *691* (21), 4459–4466.

(38) Fortman, G. C.; Nolan, S. P. N-Heterocyclic Carbene (NHC) Ligands and Palladium in Homogeneous Cross-Coupling Catalysis: A Perfect Union. *Chem. Soc. Rev.* **2011**, *40* (10), 5151–5169.

(39) Predy, A. Personal communication. 28 May 2019.

(40) D'Attoma, J.; Cozien, G.; Brun, P. L.; Robin, Y.; Bostyn, S.; Buron, F.; Routier, S. Fast Functionalization of (7-Aza)Indoles Using Continuous Flow Processes. *ChemistrySelect* **2016**, *1* (3), 338–342.

(41) DiCesare, N.; Lakowicz, J. R. Fluorescent Probe for Monosaccharides Based on a Functionalized Boron-Dipyrromethene with a Boronic Acid Group. *Tetrahedron Lett.* **2001**, *42* (52), 9105–9108.

(42) Lohani, C.; Lee, K. The Effect of Absorbance of Fe3+ on the Detection of Fe3+ by Fluorescent Chemical Sensors. *Sensors Actuators B Chem.* **2010**, *143*, 649–654.

(43) Gillmore, A.; Lauret, C.; Roberts, S. M. A Route to the Structure Proposed for Puetuberosanol and Approaches to the Natural Products Marshrin and Phebalosin. *Tetrahedron* **2003**, *59* (24), 4363–4375.

(44) Rattanopas, S.; Piyanuch, P.; Wisansin, K.; Charoenpanich, A.; Sririrak, J.; Phutdhawong, W.; Wanichacheva, N. Indole-Based Fluorescent Sensors for Selective Sensing of Fe2+ and Fe3+ in Aqueous Buffer Systems and Their Applications in Living Cells. *J. Photochem. Photobiol. A Chem.* **2019**, *377*, 138–148.

(45) Liao, Y.-C.; Venkatesan, P.; Wei, L.-F.; Wu, S.-P. A Coumarin-Based Fluorescent Probe for Thiols and Its Application in Cell Imaging. *Sensors Actuators B Chem.* **2016**, *232*, 732–737.

(46) Sundberg, R. J.; Cherney, R. J. Synthesis of Analogs of Iboga Alkaloids. Investigation of Electrophilic, Palladium-Catalyzed and Radical Cyclizations for Preparation of 5,6-Homoiboga Derivatives. *J. Org. Chem.* **1990**, *55* (24), 6028–6037.

(47) Pietrzyk, A.; Suriyanarayanan, S.; Kutner, W.; Chitta, R.; D'Souza, F. Selective Histamine Piezoelectric Chemosensor Using a Recognition Film of the Molecularly Imprinted Polymer of Bis(Bithiophene) Derivatives. *Anal. Chem.* **2009**, *81* (7), 2633–2643.

(48) Fang, X.; Zheng, Y.; Duan, Y.; Liu, Y.; Zhong, W. Recent Advances in Design of Fluorescence-Based Assays for High-Throughput Screening. *Anal. Chem.* **2019**, *91* (1), 482–504.

(49) Xue, W.; Wang, D.; Li, C.; Zhai, Z.; Wang, T.; Liang, Y.; Zhang, Z. π-Expanded Coumarins: One-Pot Photo Synthesis of 5 H-Benzo[12,1]Tetrapheno[7,6,5- Cde]Chromen-5-Ones and Photophysical Properties. *J. Org. Chem.* **2020**, *85* (5), 3689–3698.

(50) Tasior, M.; Deperasińska, I.; Morawska, K.; Banasiewicz, M.; Vakuliuk, O.; Kozankiewicz, B.; Gryko, D. T. Vertically π-Expanded Coumarin - Synthesis via the Scholl Reaction and Photophysical Properties. *Phys. Chem. Chem. Phys.* **2014**, *16* (34), 18268–18275.

(51) Bowers Jr, G. N.; McComb, R. B.; Christensen, R. G.; Schaffer, R. High-Purity 4-Nitrophenol: Purification, Characterization, and Specifications for Use as a Spectrophotometric Reference Material. *Clin. Chem.* **1980**, *26* (6), 724–729.

(52) Koch, S.; Schollmeyer, D.; Löwe, H.; Kunz, H. C-Glycosyl Amino Acids through Hydroboration–Cross-Coupling of Exo-Glycals and Their Application in Automated Solid-Phase Synthesis. *Chem. – A Eur. J.* **2013**, *19* (22), 7020–7041.

(53) Costa, P.; Sandrin, D.; Scaiano, J.C. Real-time fluorescence imaging of a heterogeneously catalysed Suski-Miyaura reaction. *Nat Catal*. **2020**, *3*, 427-437.

(54) Atienza, B. J. P.; Truong, N.; Williams, F. J. Reliably Regioselective Dialkyl Ether Cleavage with Mixed Boron Trihalides. *Org. Lett.* **2018**, *20* (20), 6332–6335.

(55) Kazmi, M. Z. H.; Karmakar, A.; Michaelis, V. K.; Williams, F. J. Separation of Cellulose/Hemicellulose from Lignin in White Pine Sawdust Using Boron Trihalide Reagents. *Tetrahedron* **2019**, *75* (11), 1465–1470.

(56) Shuai, L.; Talebi Amiri, M.; M. Questell-Santiago, Y.; Heroguel, F.; Li, Y.; Kim, H.; Meilan, R.; Chapple, C.; Ralph, J.; S. Luterbacher, J. Formaldehyde Stabilization Facilitates Lignin Monomer Production during Biomass Depolymerization. *Science* **2016**, *354* (6310), 329–333.

Appendix A: Supplemental Research Data

(1) Standard curve for determining the amount of glucose converted in the BBr_3/BCl_3 treated lignin cellulase reaction by Glucose-GO Assay

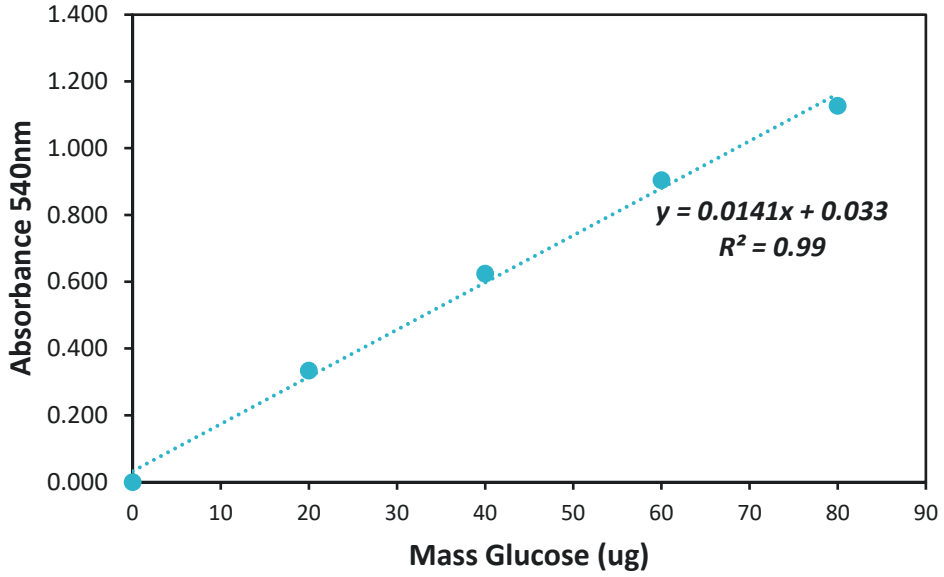

(2) Standard curve for determining the amount of glucose converted in the commercial lignin cellulase reaction by Glucose-GO Assay

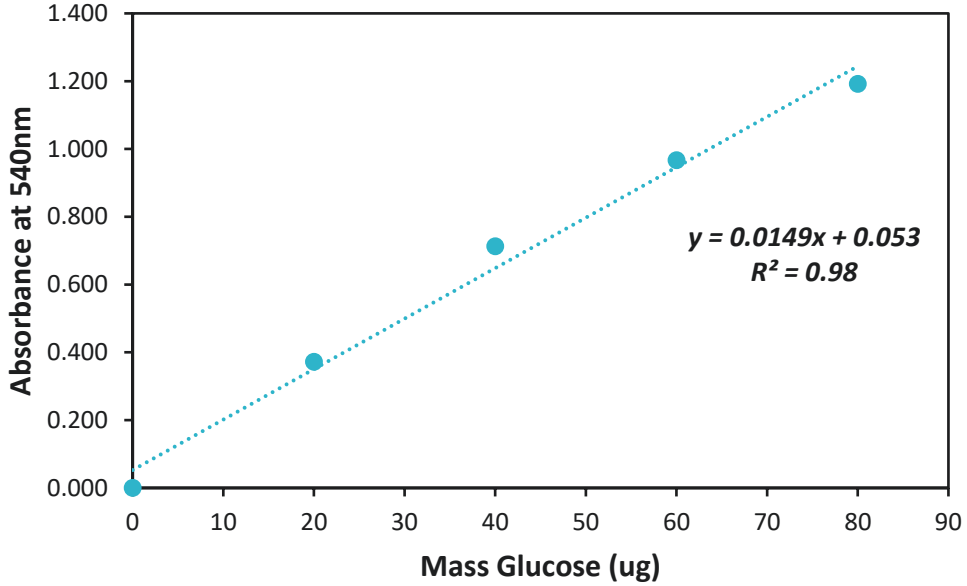

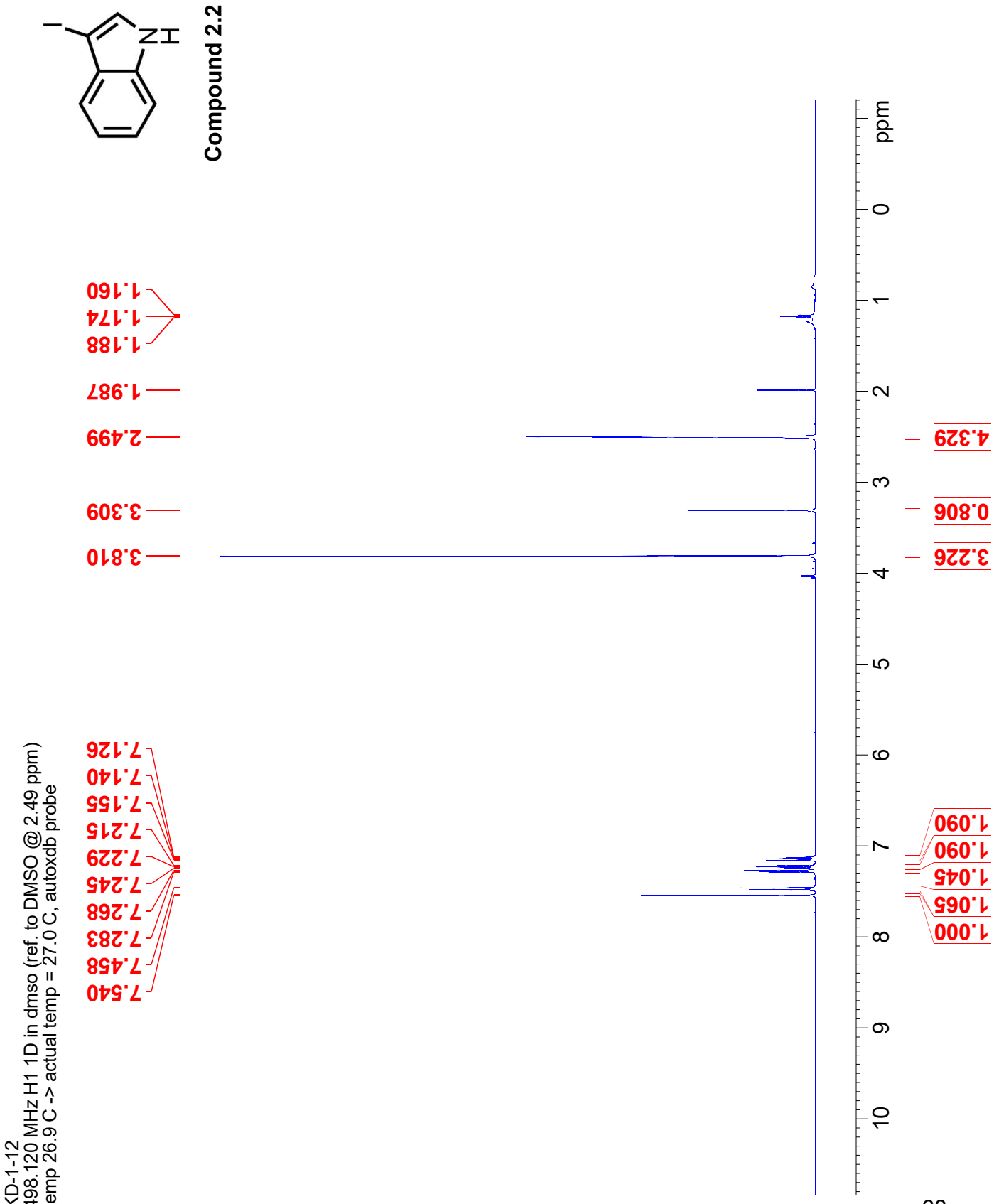
Compound 2.2
KD-1-12
498.120 MHz H1 1D in dmso (ref. to DMSO @ 2.49 ppm)
temp 26.9 C -> actual temp = 27.0 C, autoxdb probe
ppm
1.160
1.174
1.188
1.987
2.499
3.309
3.810
7.126
7.140
7.155
7.215
7.229
7.245
7.268
7.283
7.458
7.540
4.329
0.806
3.226
1.090
1.090
1.045
1.065
1.000

498.120 MHz H1 1D in dmso (ref. to DMSO @ 2.49 ppm)
temp 26.9 C -> actual temp = 27.0 C, autoxdb probe

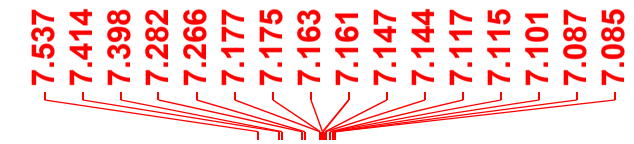

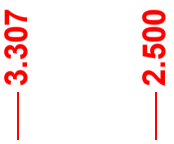

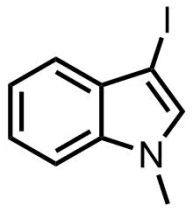

Compound 2.3

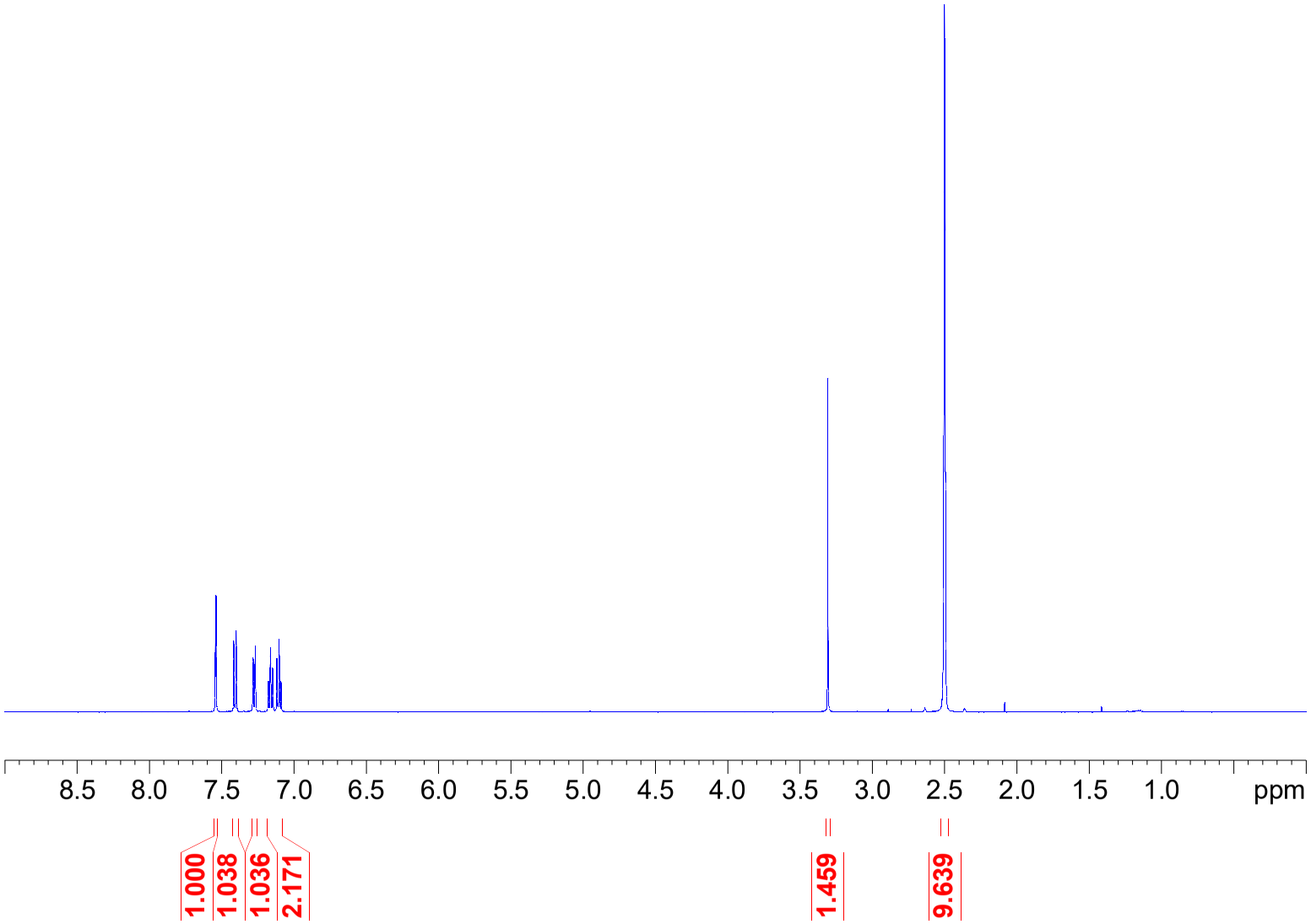

KD-1-27_crude (BODIPY starting material)
498.118 MHz H1 1D in cdcl3 (ref. to CDCl3 @ 7.26 ppm)
temp 26.9 C -> actual temp = 27.0 C, autoxdb probe

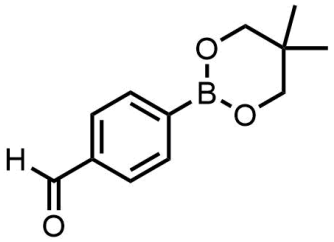

Compound 2.5

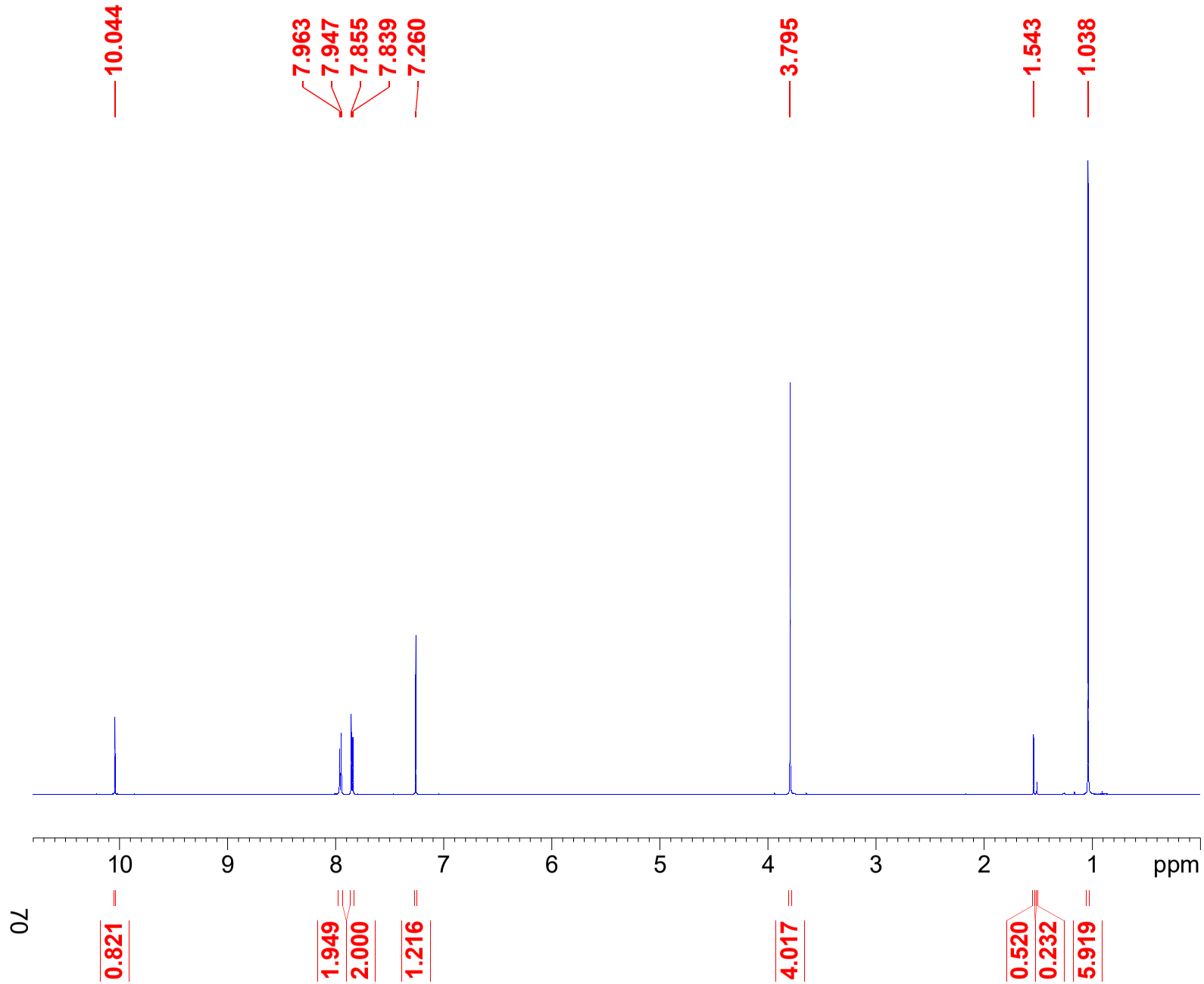

KD-1-27
125.266 MHz C13{H1} 1D in cdcl3 (ref. to CDCl3 @ 77.06 ppm)
temp 26.9 C -> actual temp = 27.0 C, autoxdb probe

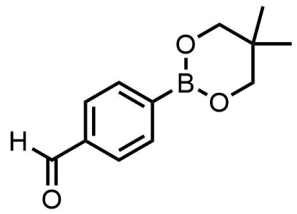

Compound 2.5

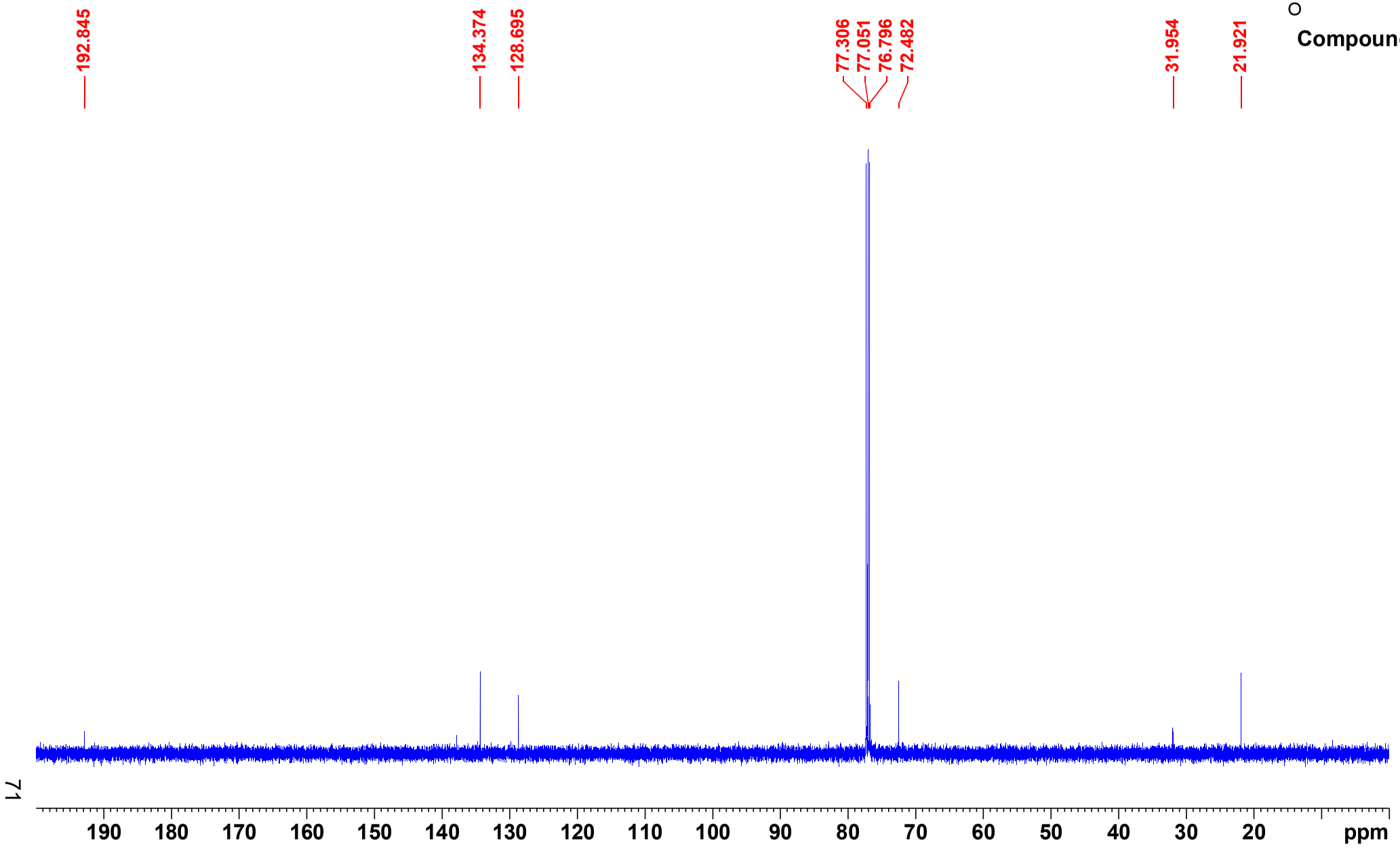

399.980 MHz H1 1D in cd3od (ref. to CD3OD @ 3.30 ppm)
temp 25.9 C -> actual temp = 27.0 C, onenmr probe

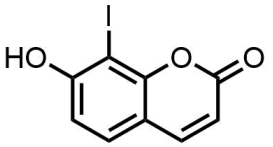

Compound 2.7

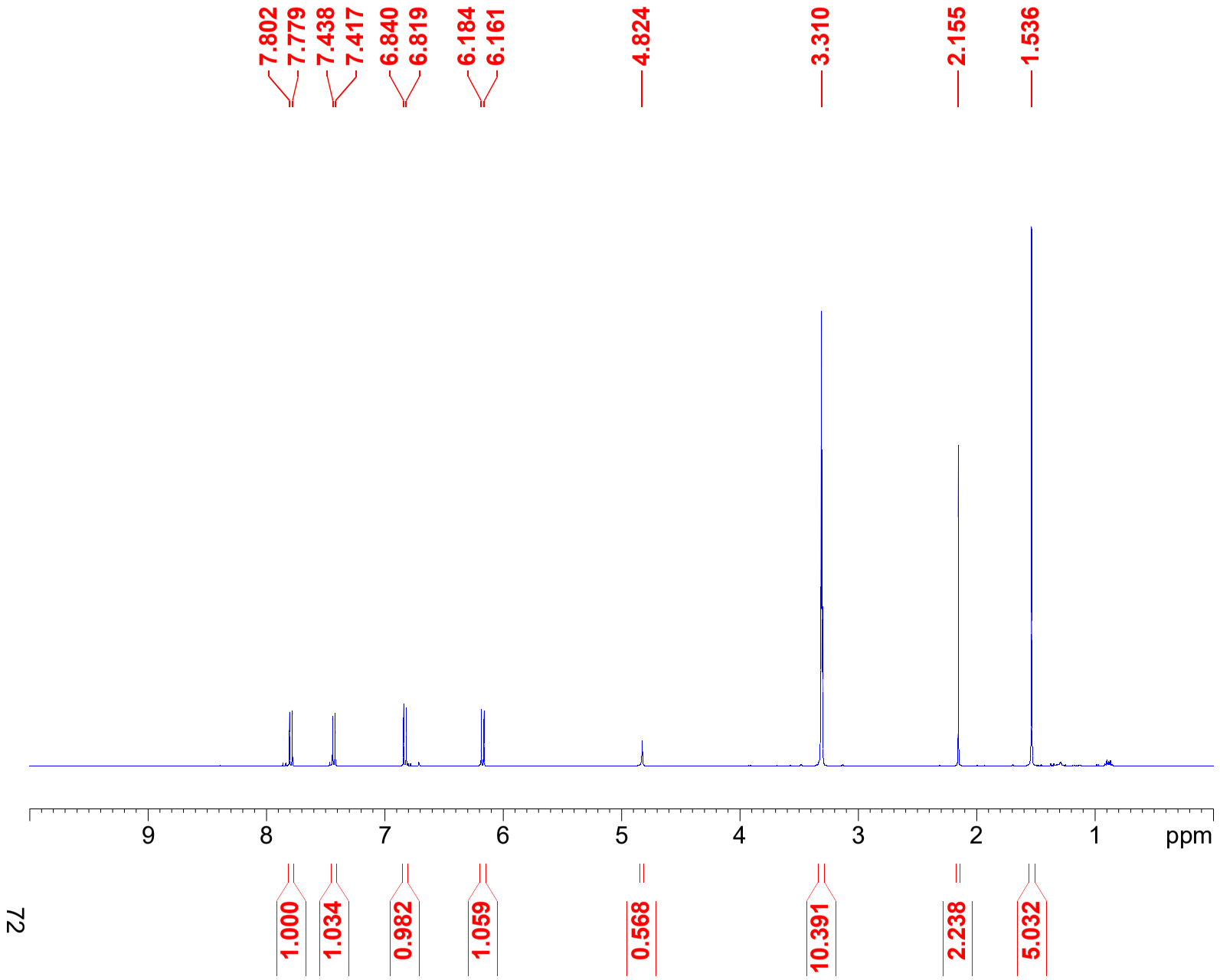

KD-1-41
399.978 MHz H1 1D in cdcl3 (ref. to CDCl3 @ 7.26 ppm)
temp 25.9 C -> actual temp = 27.0 C, onenmr probe

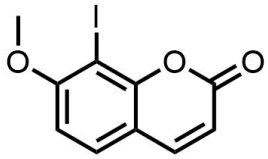

Compound 2.8

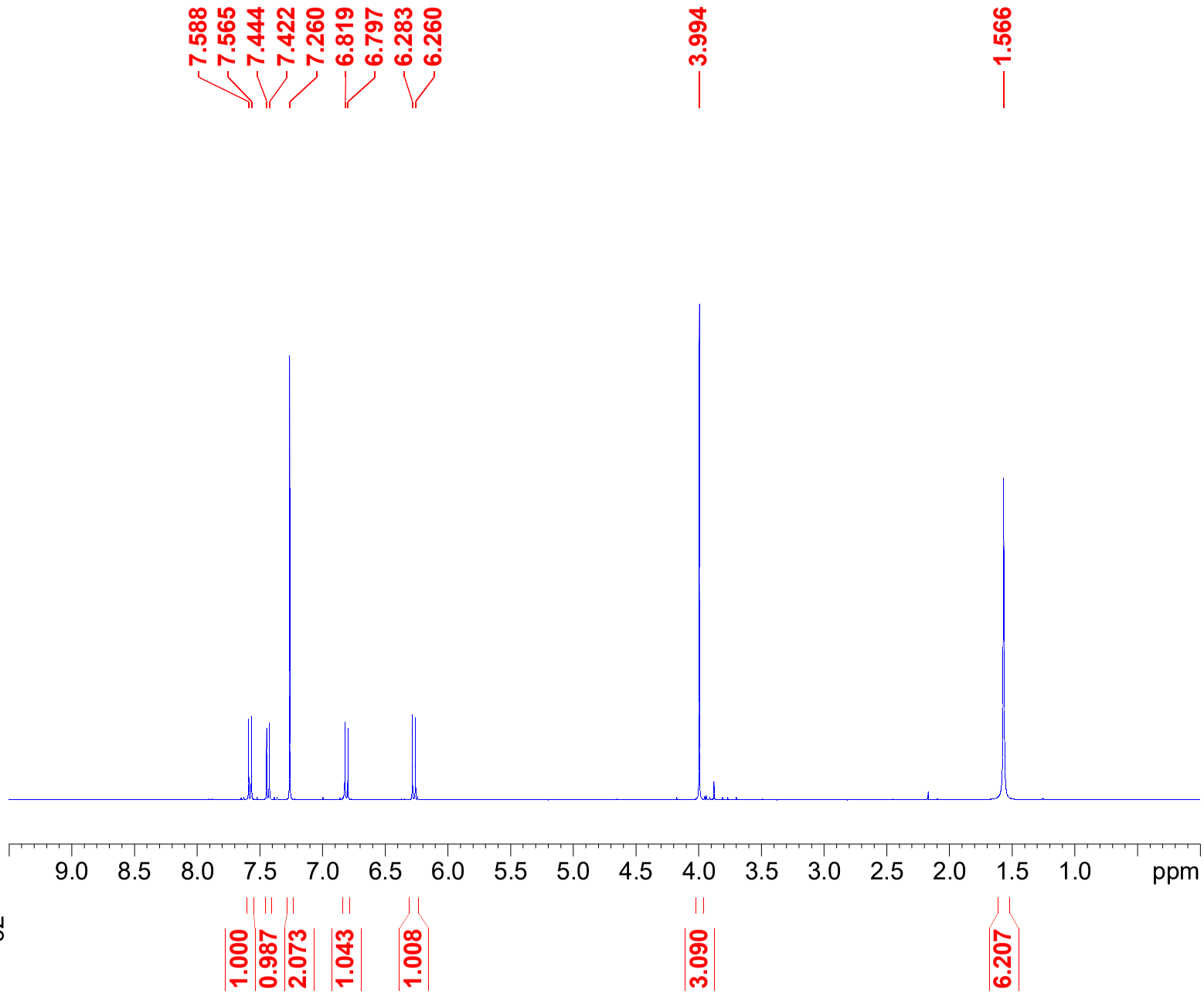

KD-1-47; final product after HPLC purification
498.118 MHz H1 1D in cdcl3 (ref. to CDCl3 @ 7.26 ppm)
temp 26.9 C -> actual temp = 27.0 C, autoxdb probe

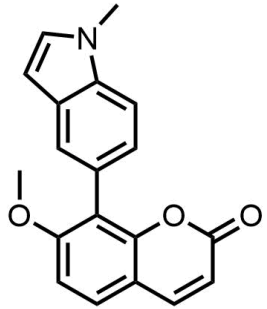

Compound 2.9

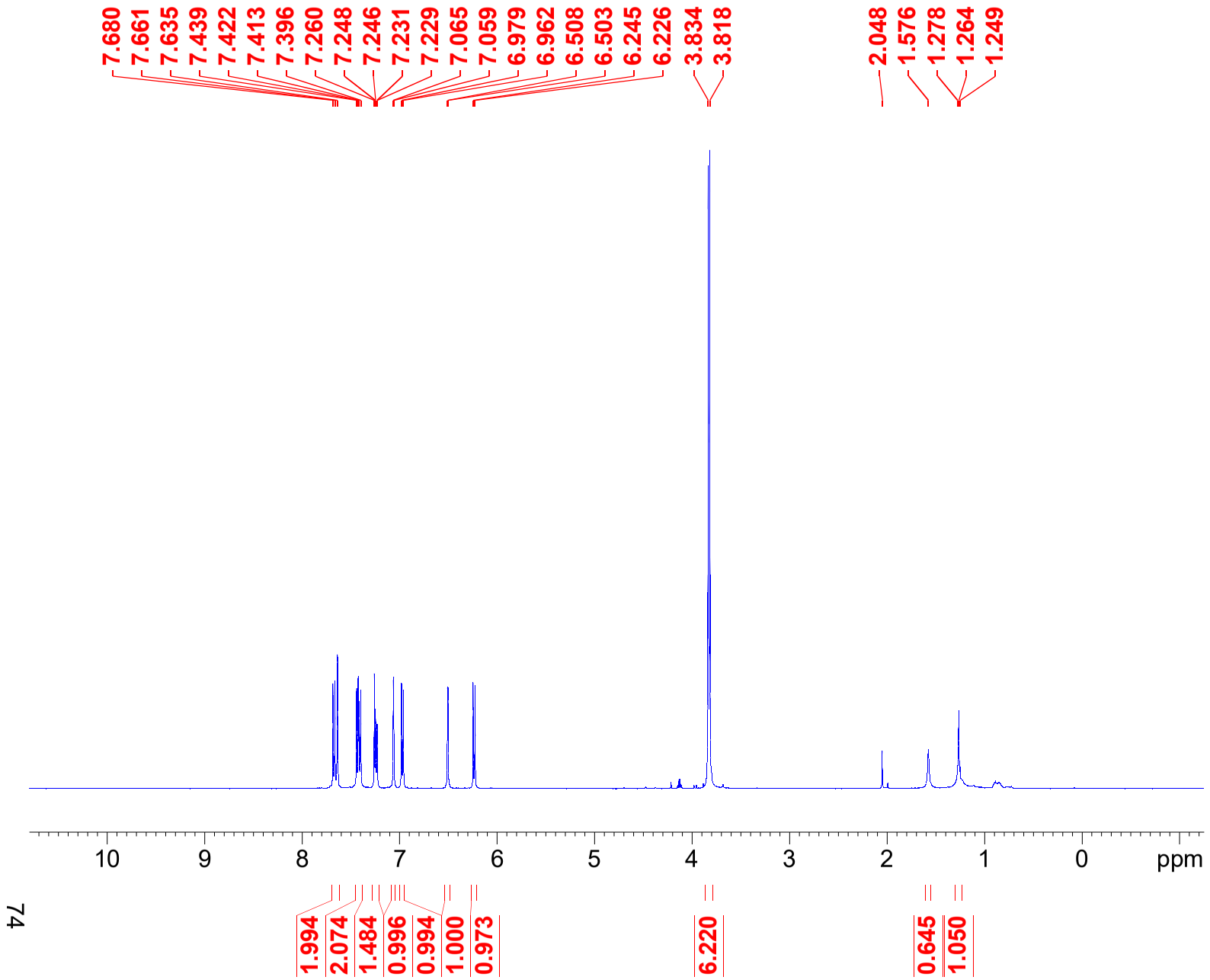

KD-1-81; recrys from AcOH; DMSO
498.120 MHz H1 1D in dmso (ref. to DMSO @ 2.49 ppm)
temp 26.9 C -> actual temp = 27.0 C, autoxdb probe

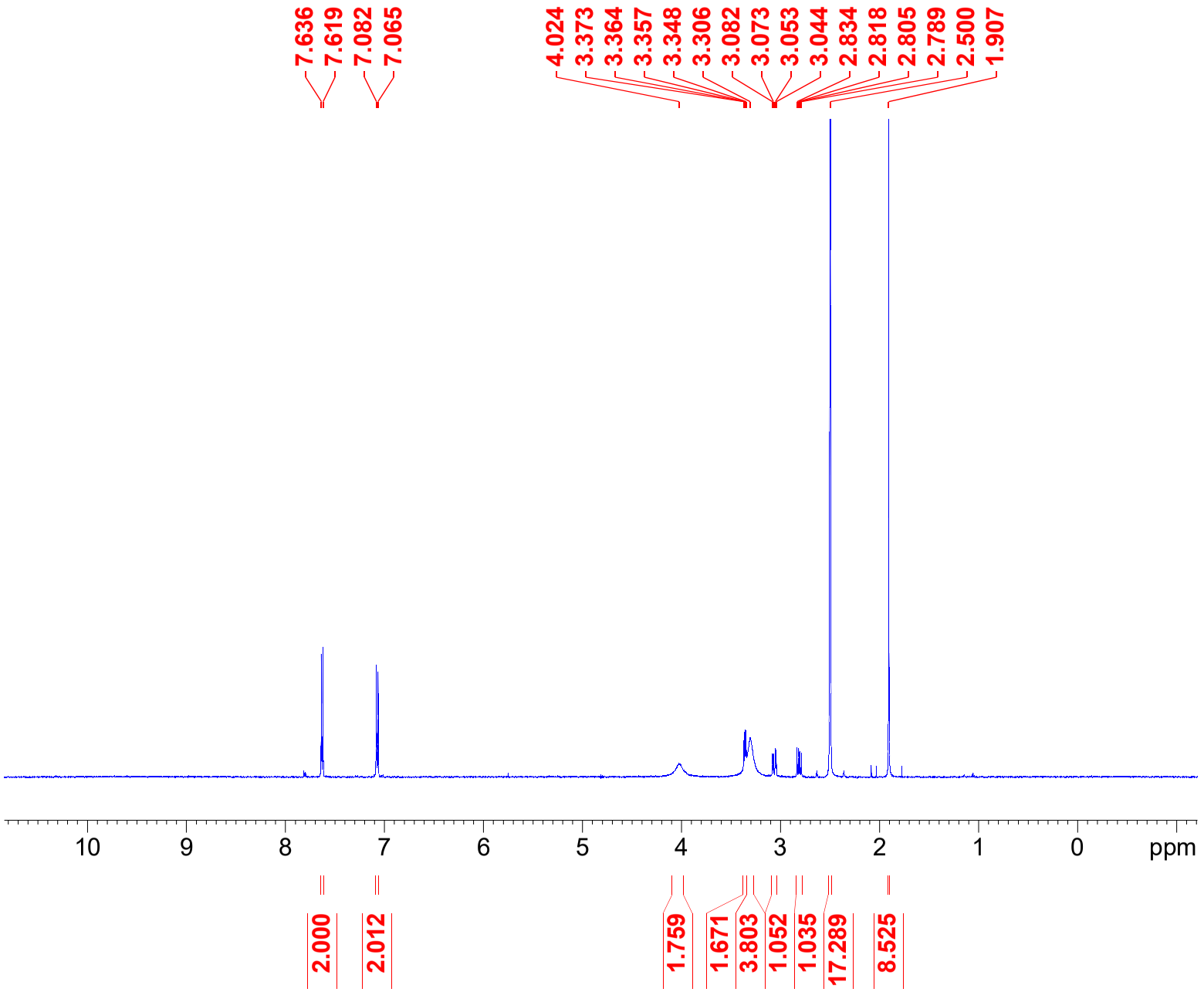

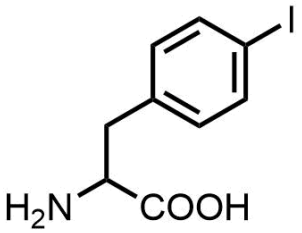

Compound 3.2

KD-1-138; crude yellow oil from extraction, 3 hours on high vac; CDCl3

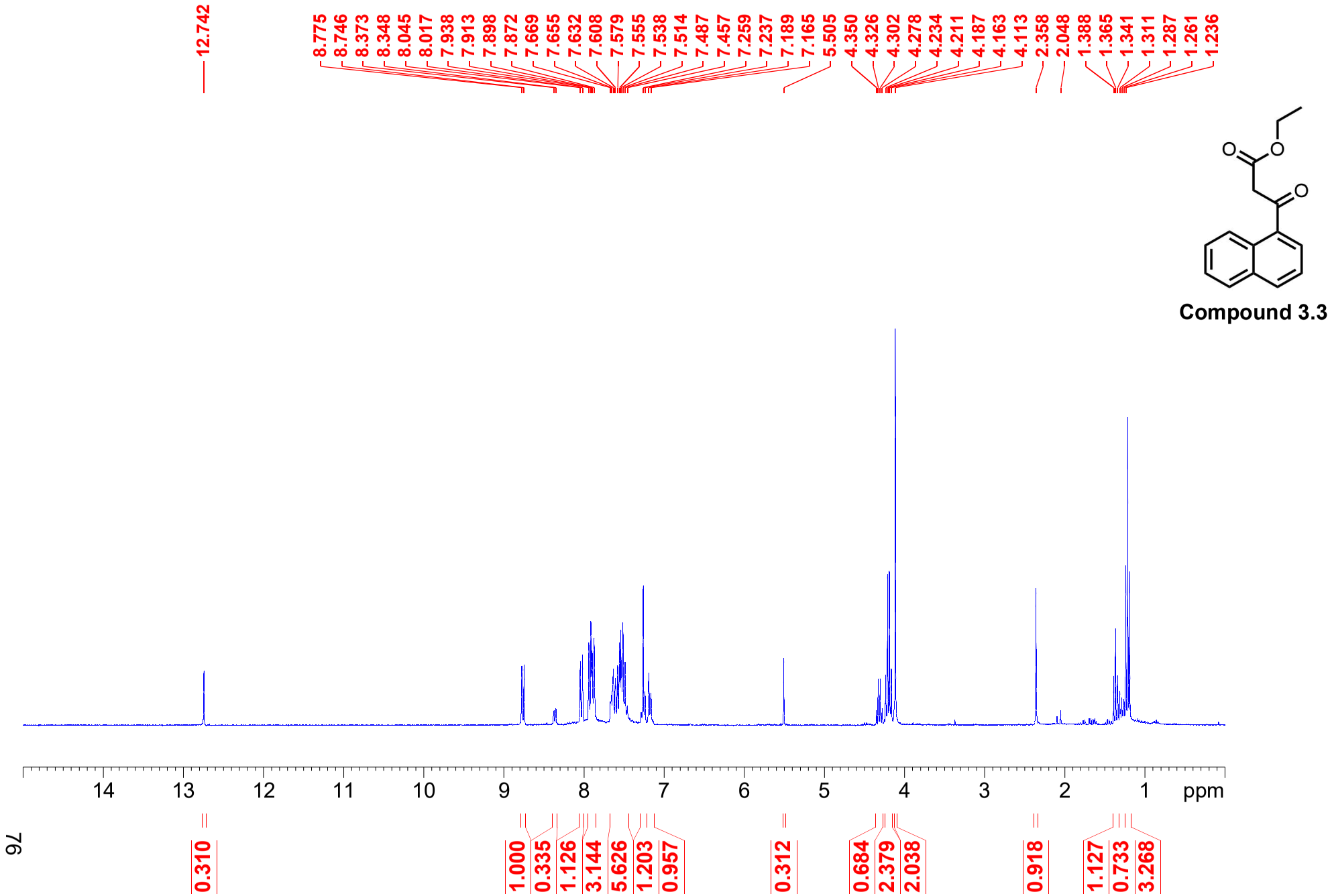

Compound 3.3

KD-1-140; red solid crashed out with cold EtOH after wrkp; DMSO

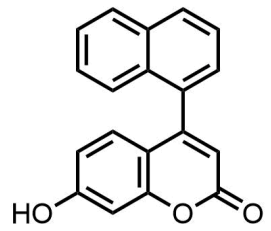

Compound 3.4

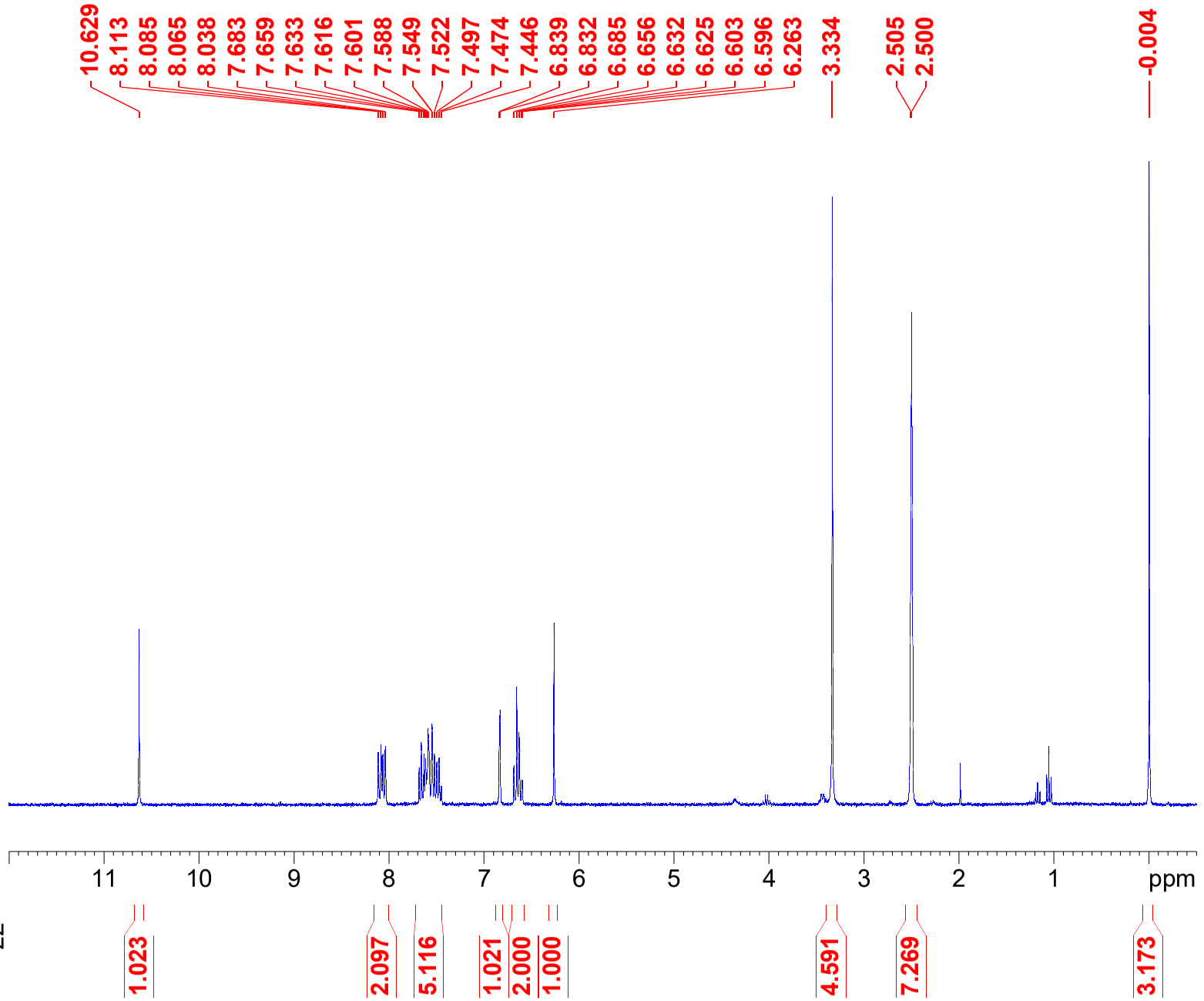

77

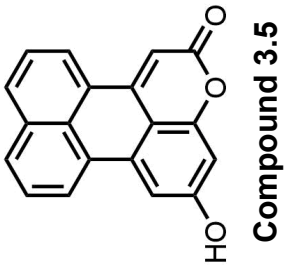
O
O
HO

Compound 3.5

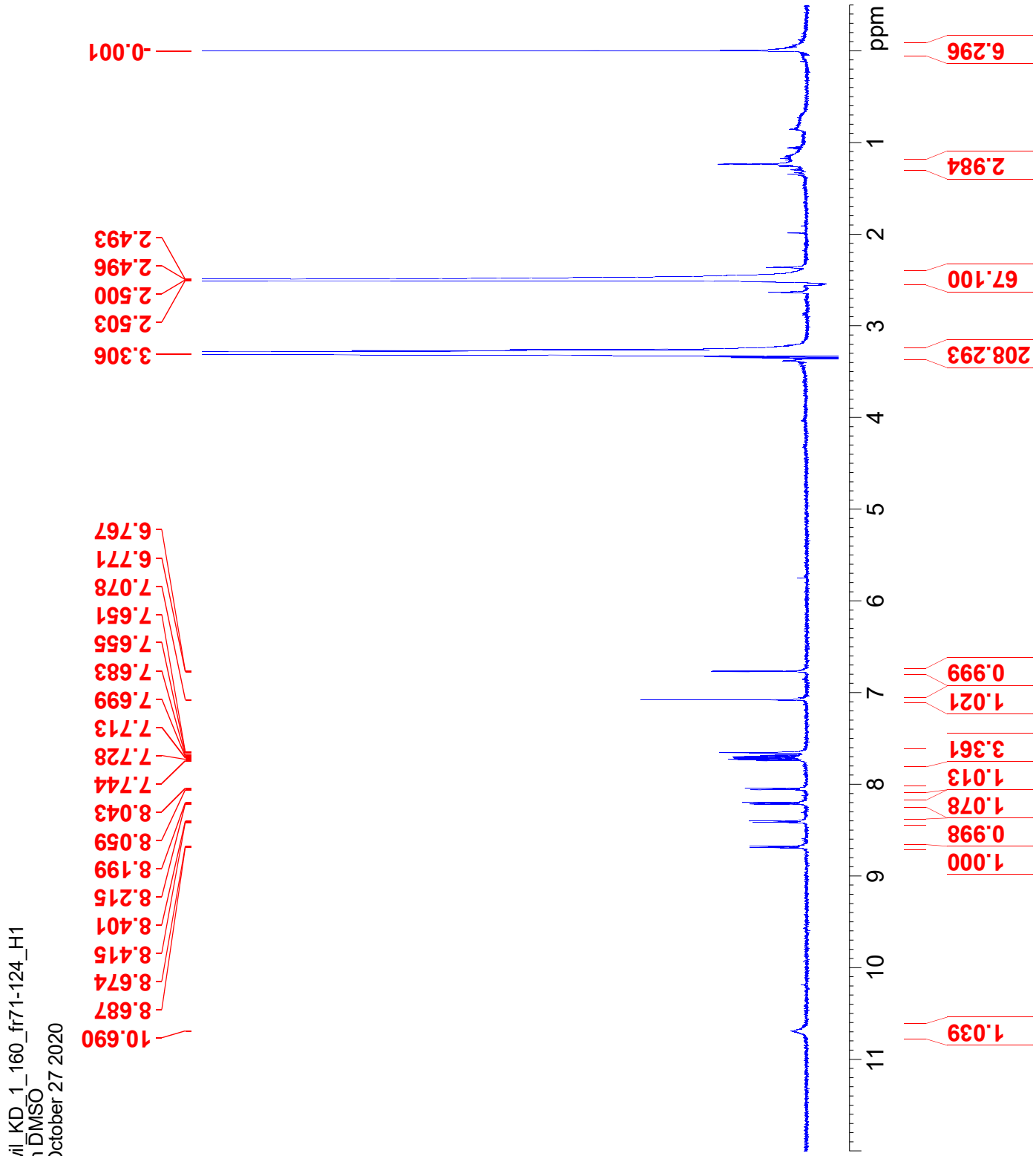
wil_KD_1_160_fr71-124_H1
in DMSO
October 27 2020
-0.001
3.306
2.503
2.500
2.496
2.493
10.690
8.687
8.674
8.415
8.401
8.215
8.199
8.059
8.043
7.744
7.728
7.713
7.699
7.683
7.655
7.651
7.078
6.771
6.767
ppm
1
2
3
4
5
6
7
8
9
10
11
6.296
2.984
67.100
208.293
0.999
1.021
3.361
1.013
1.078
0.998
1.000
1.039

B1: 3-ethynylphenyl boronic acid

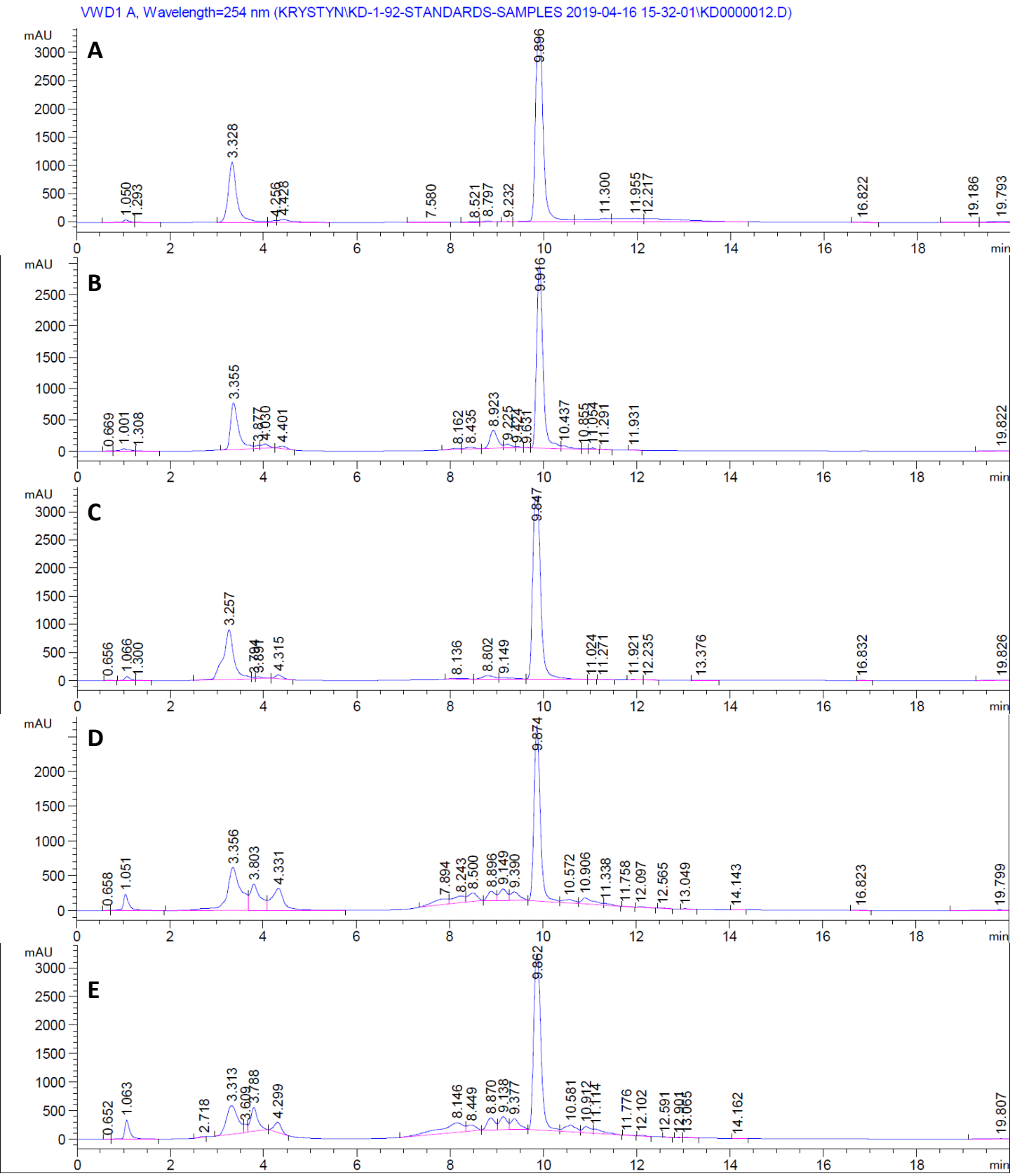

B2: indole-6-boronic acid

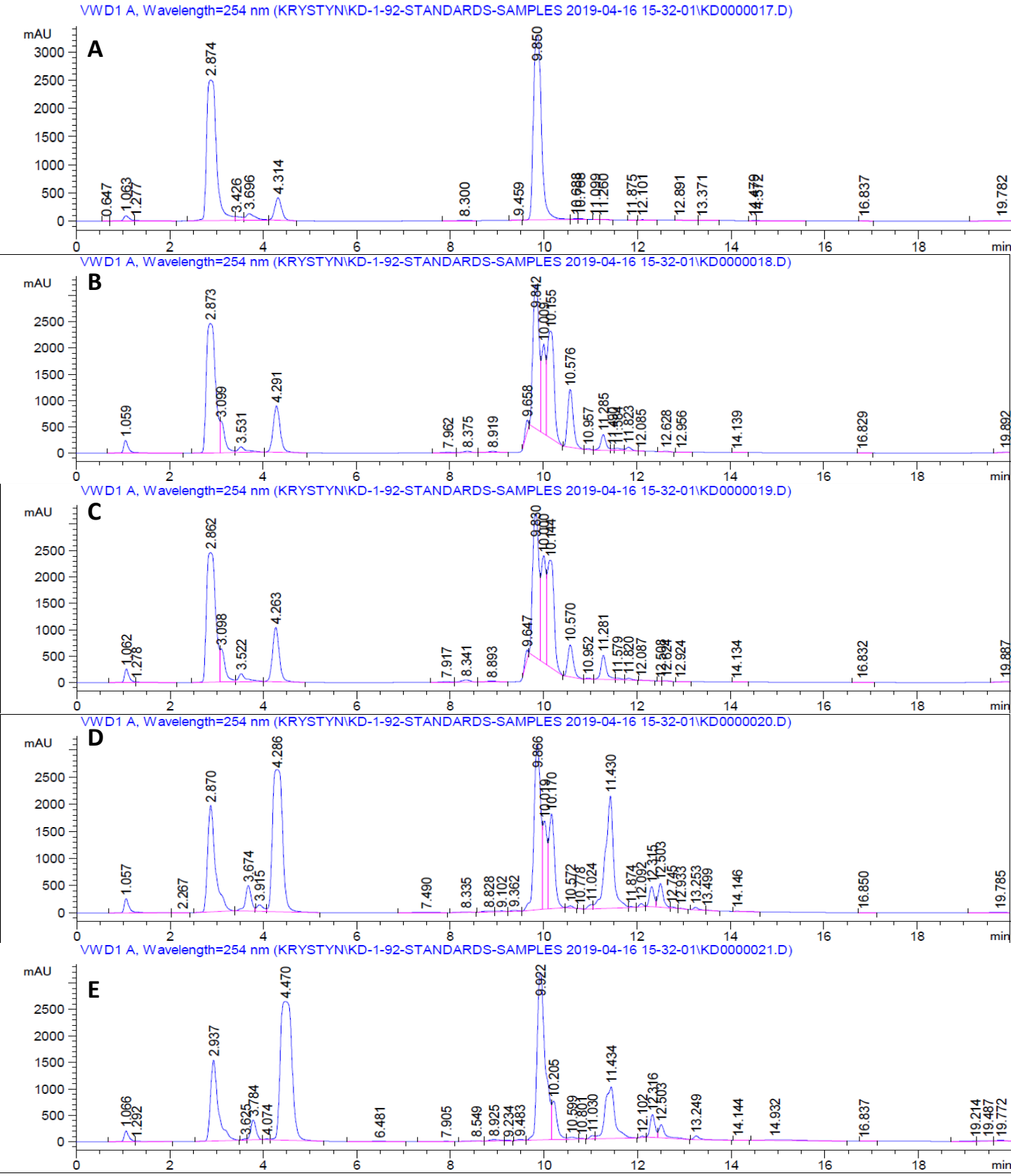

B3: 2-fluoropyridine-5-boronic acid

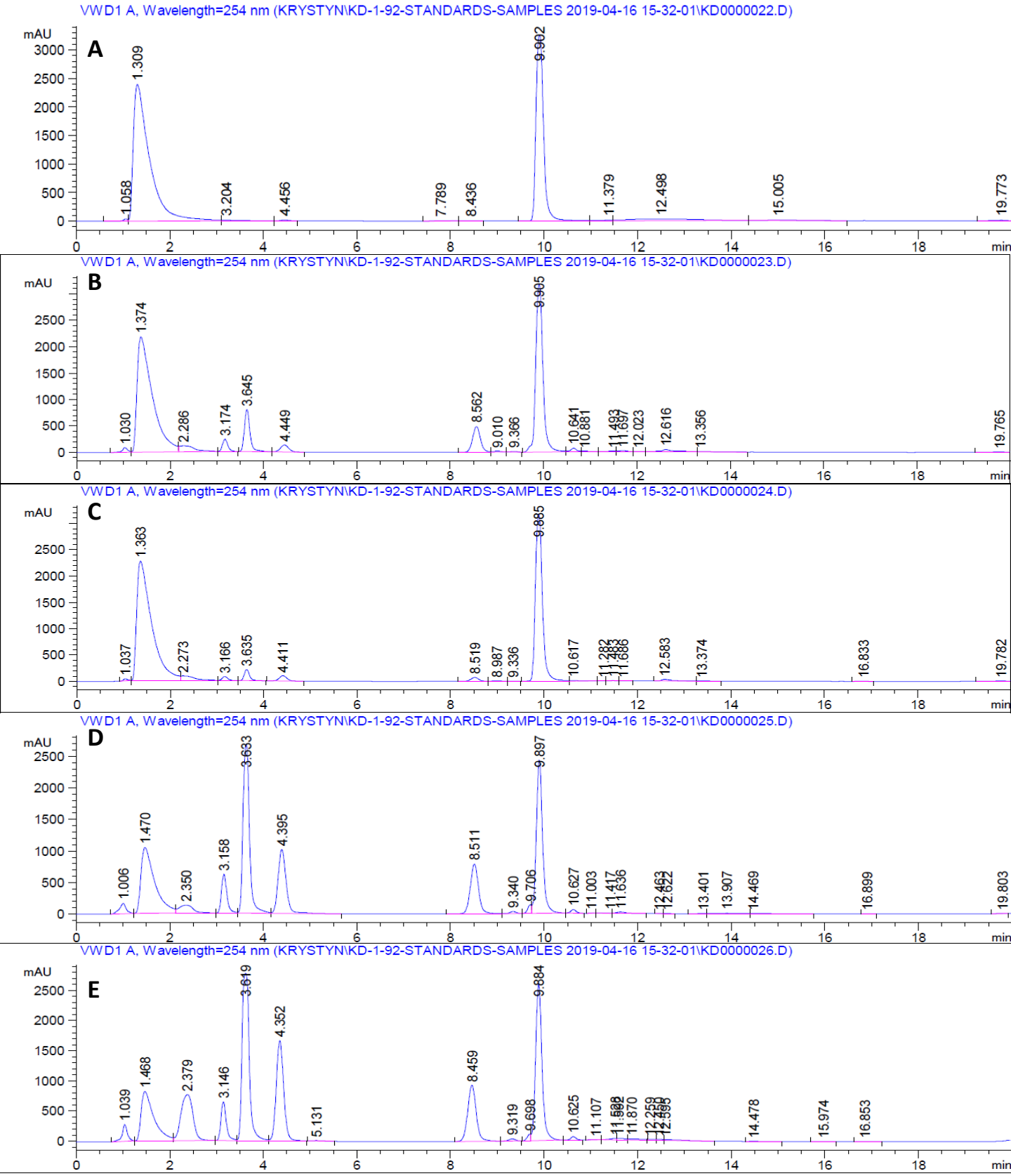

B4: pyrimidine-5-boronic acid

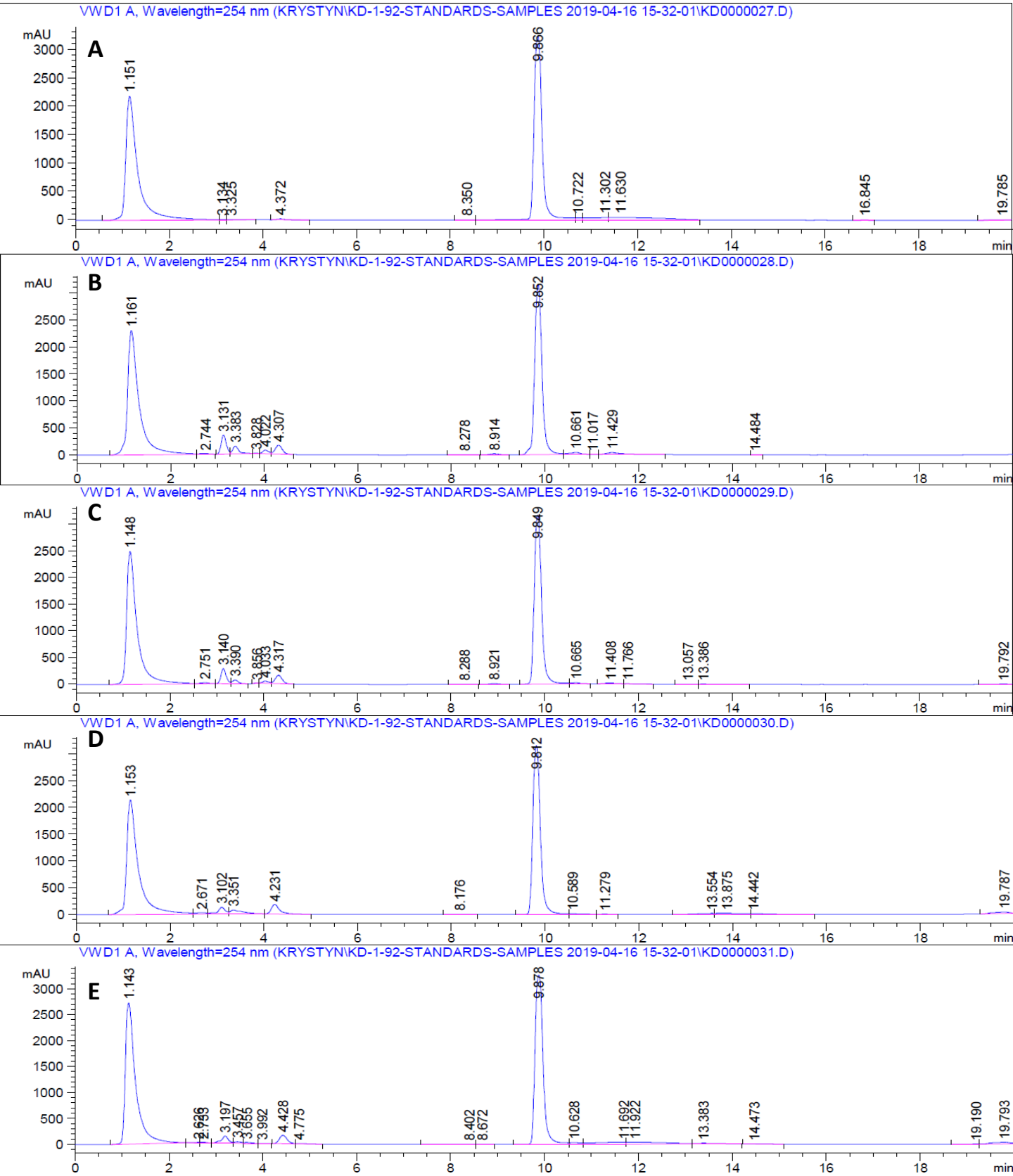

B5: 3,5-dimethylisoxazole-4-boronic acid

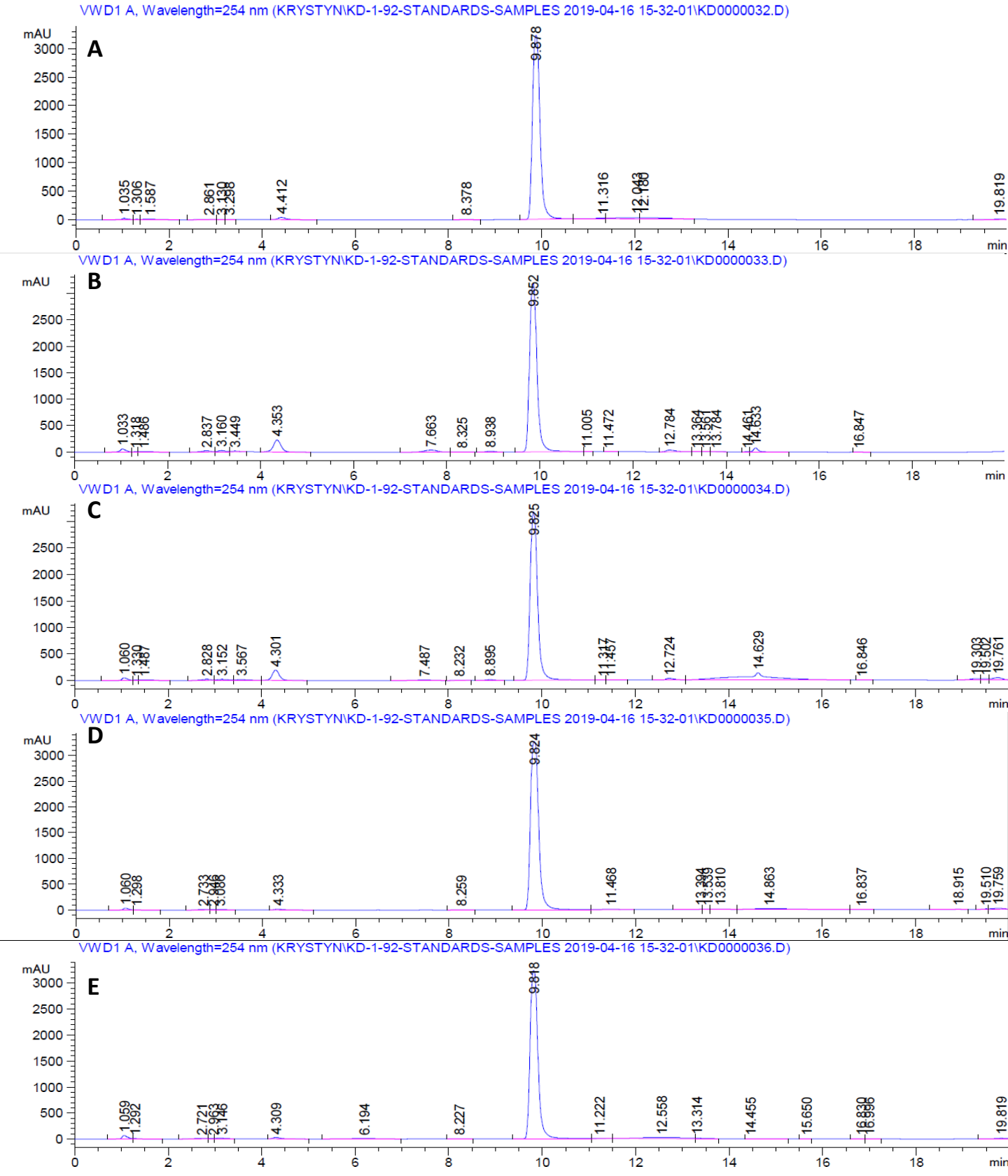

B6: 5-formylthiophene-2-boronic acid

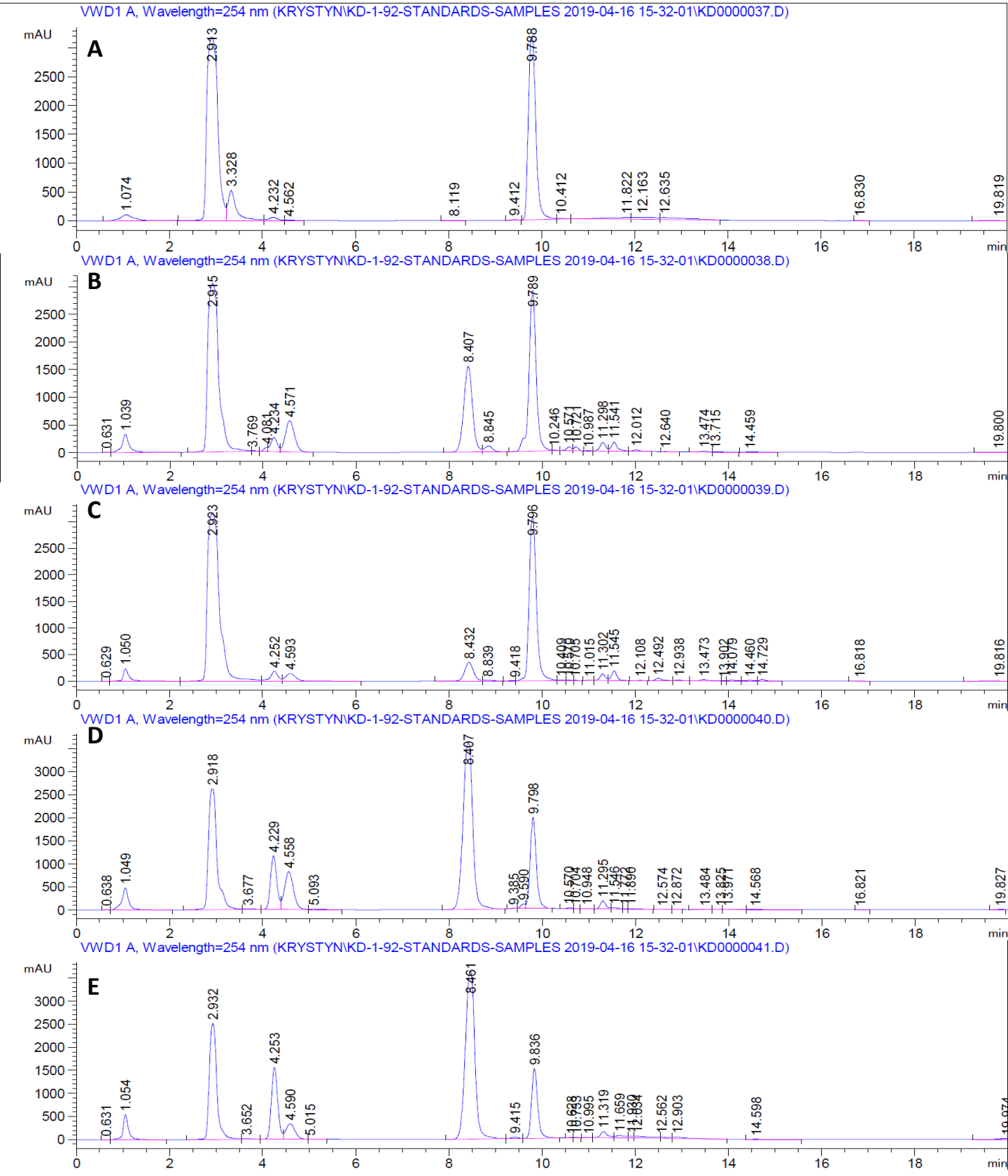

B9: 3,4,5-trifluorophenylboronic acid

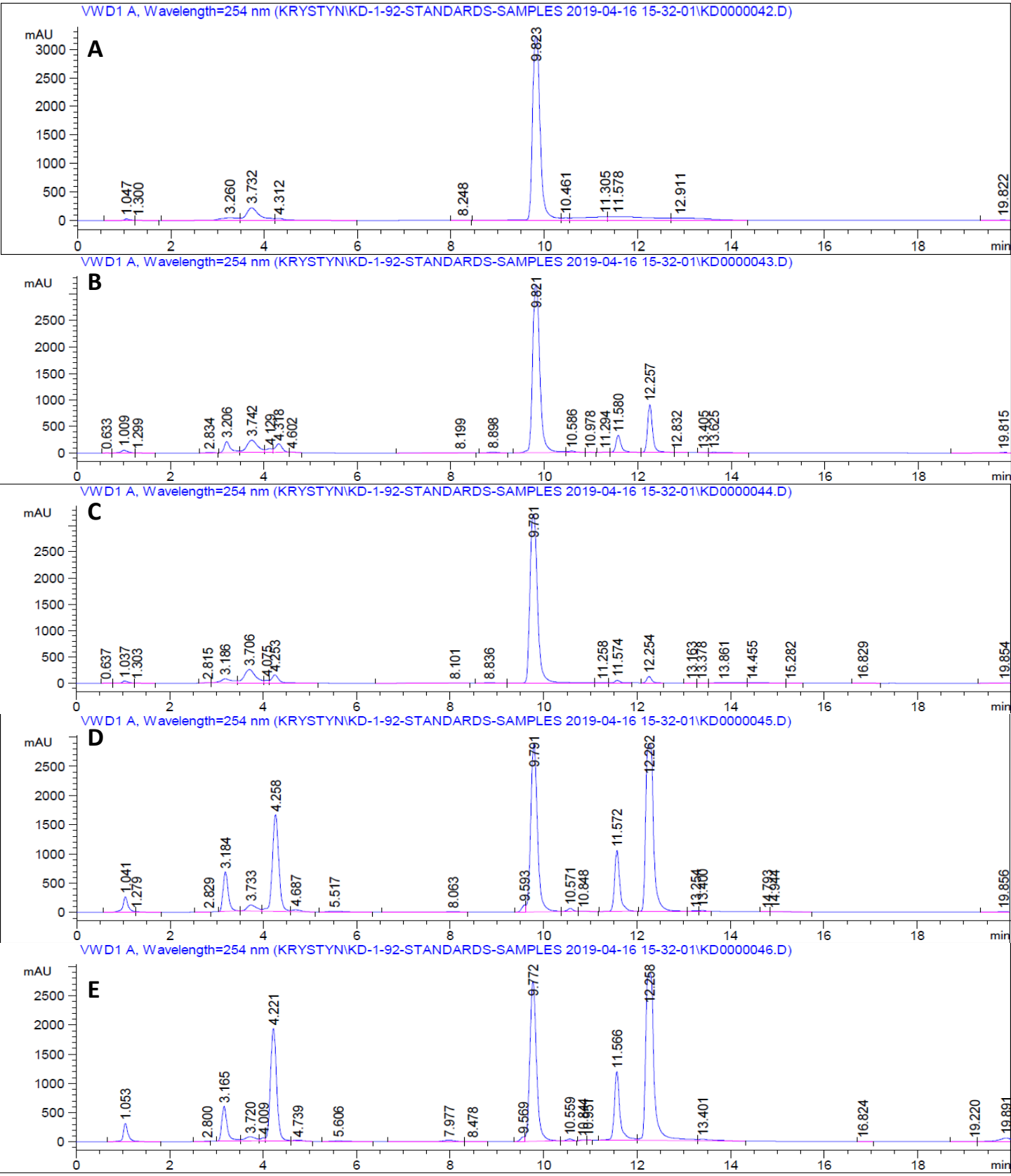

B10: 3-(methoxycarbonyl)-5-nitrophenylboronic acid

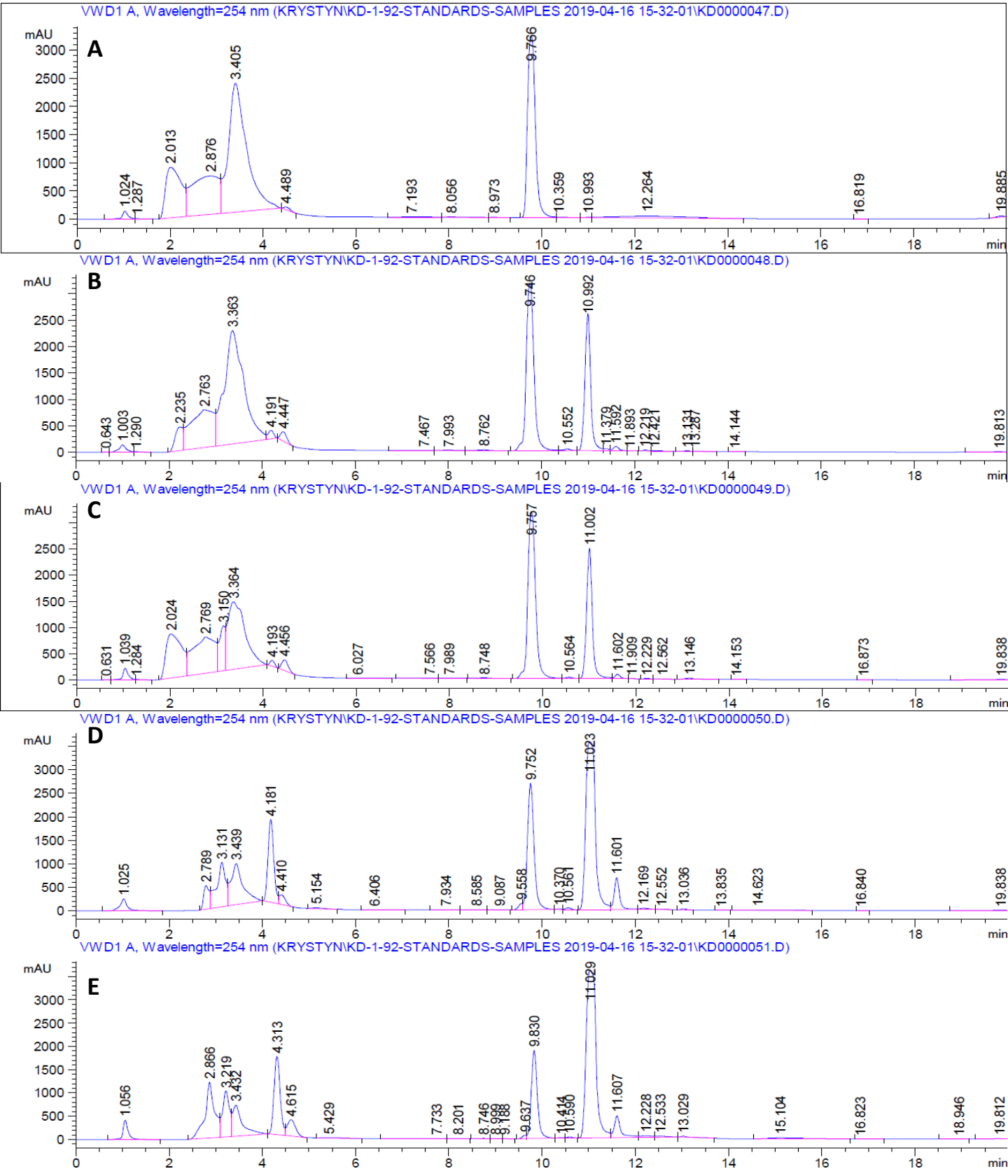

B1: 3-ethynylphenylboronic acid

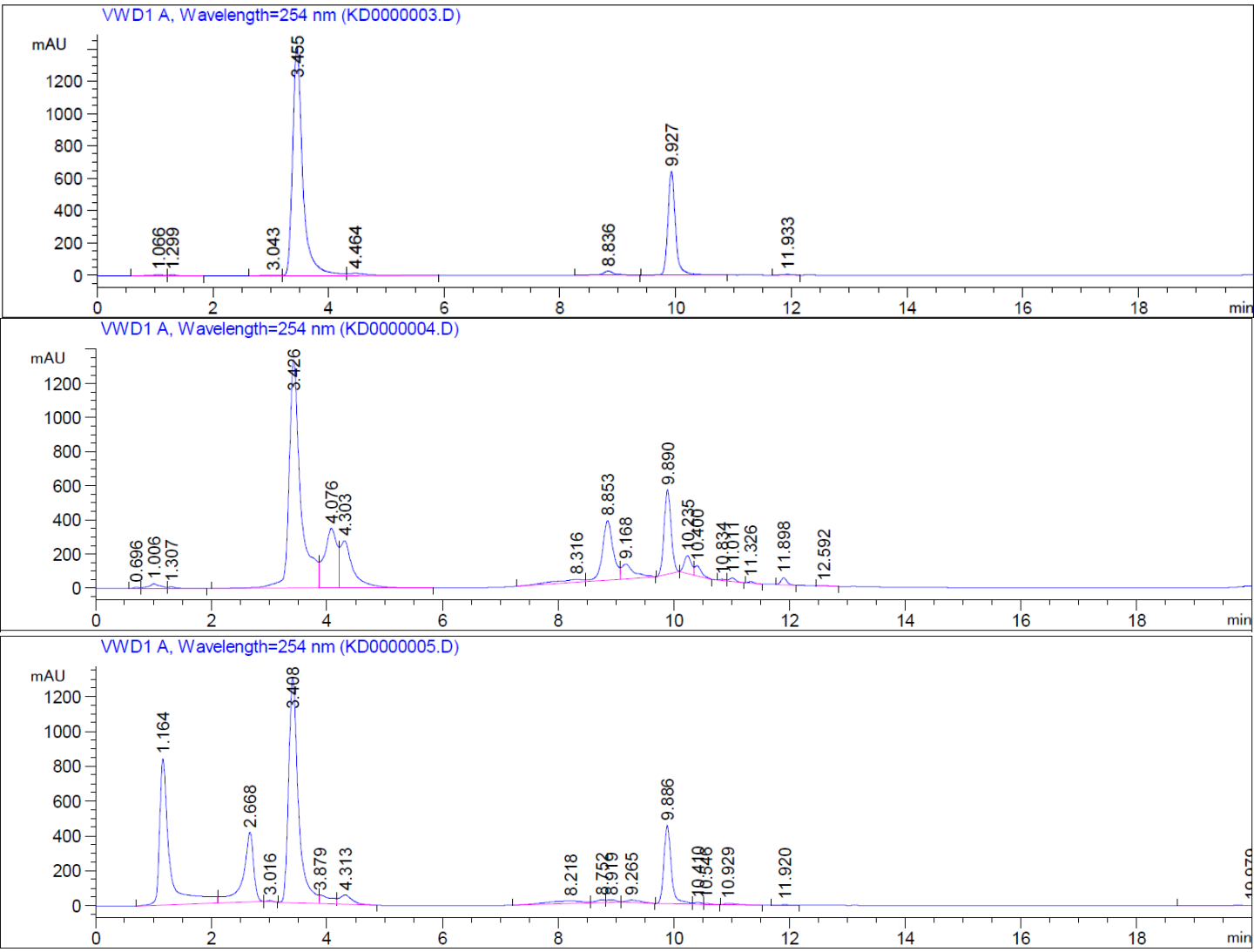

B2: indole-6-boronic acid

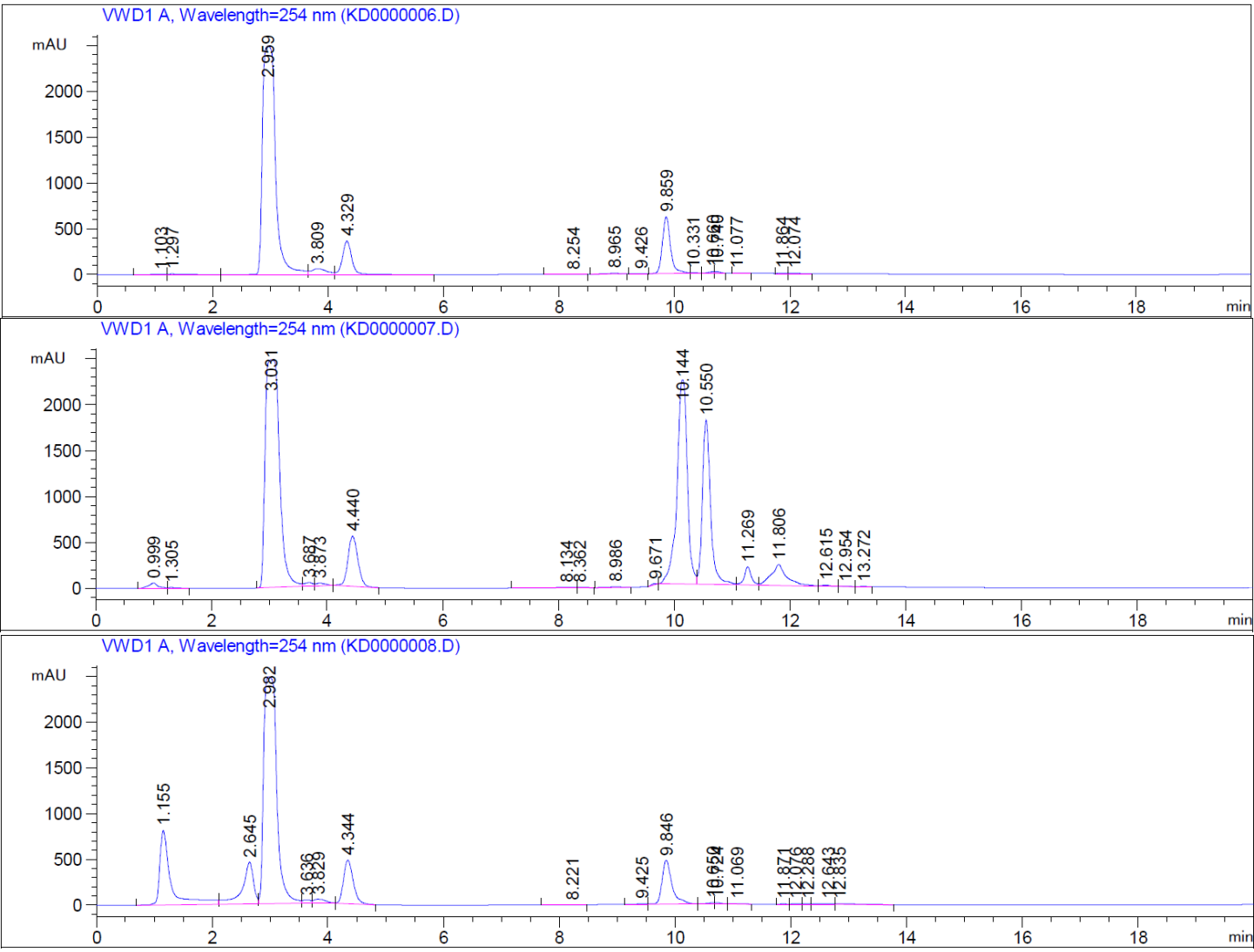

B3: 2-fluoropyridine-5-boronic acid

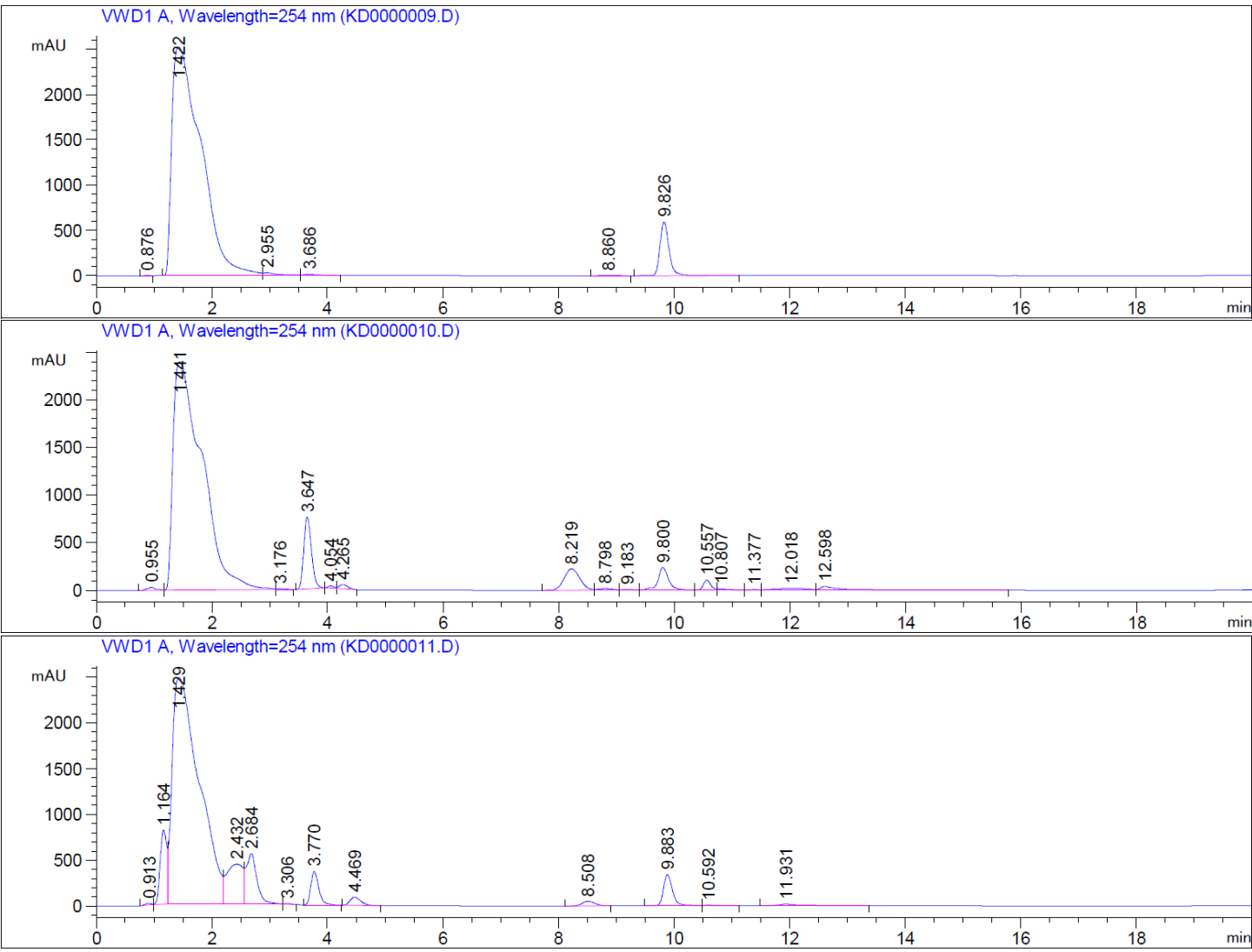

B4: 3,5-dimethylisoxazole-4-boronic acid

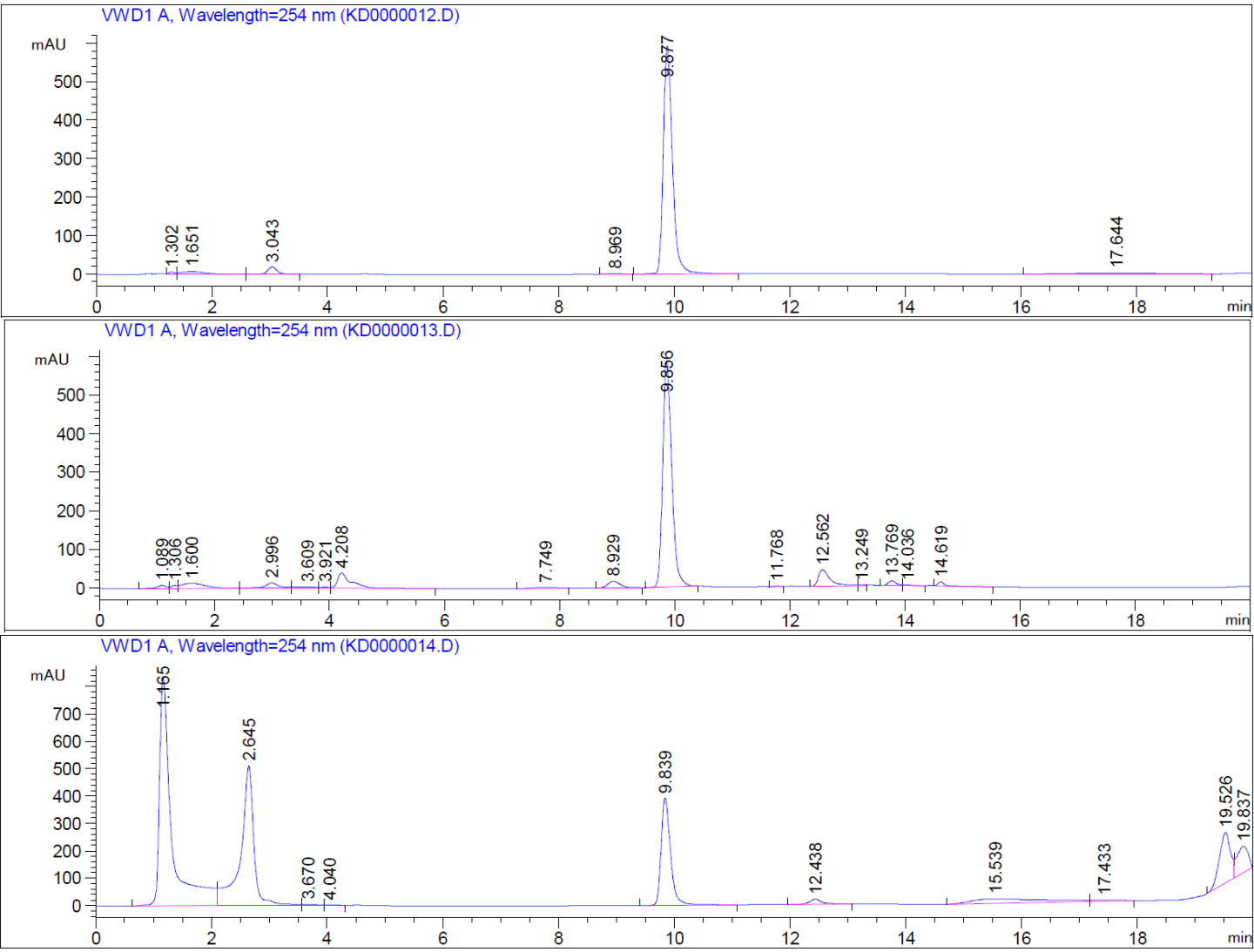

B5: 5-formylthiophene-2-boronic acid

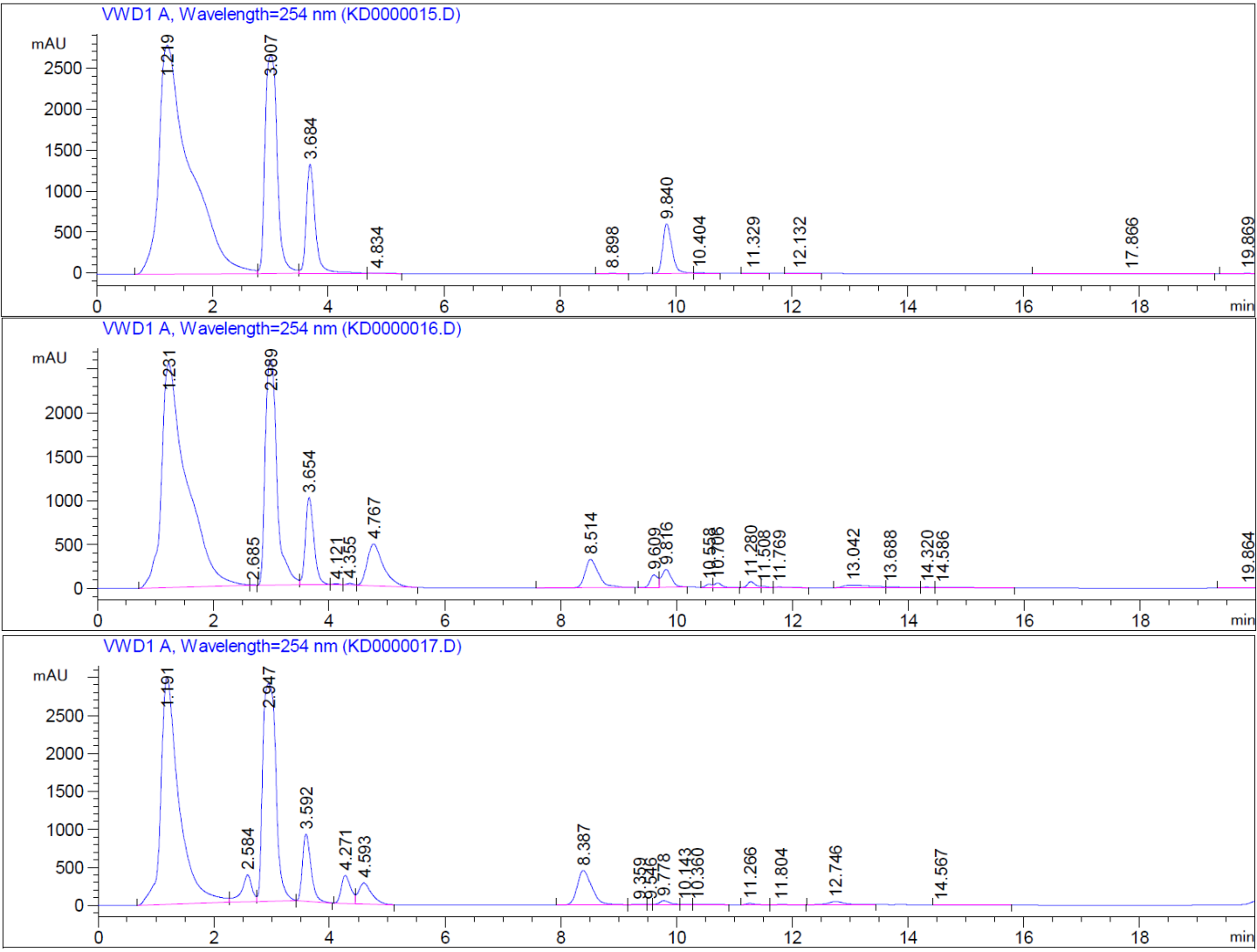

B6: 3,4,5-trifluorophenylboronic acid

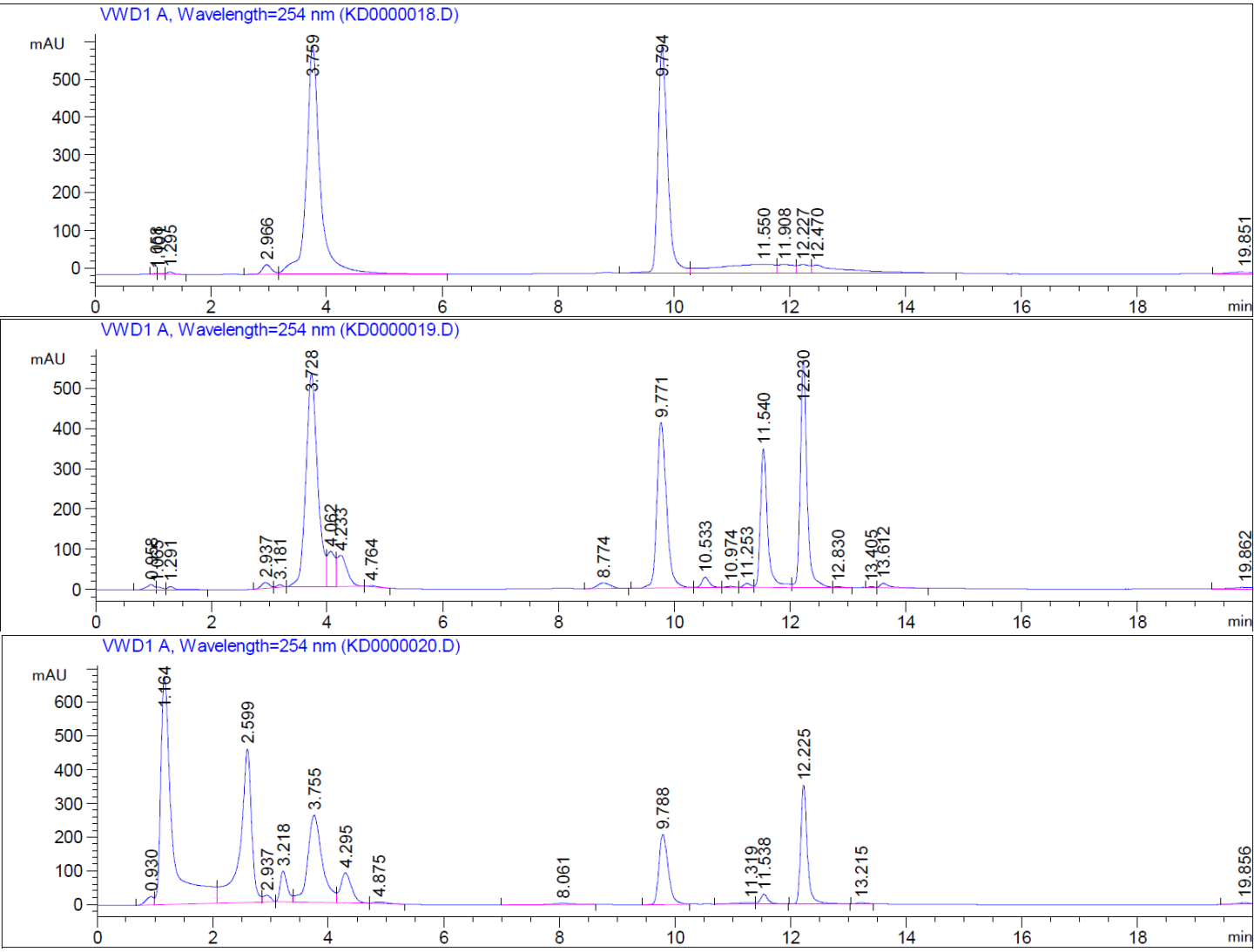

B7: 3-(methoxycarbonyl)-5-boronic acid